

NEUTRINO REACTIONS AT ACCELERATOR ENERGIES

C. H. Llewellyn Smith

ErratumPage 90: line 7 should read:

"... can be fitted by $C_4^V = C_5^V = 0$ or $C_5^V = 0, C_4^V = -\frac{MC_3^V}{M+M^*}$

which implies that "

Page 149: in line 3 of the table

$$\frac{-C_3^V}{2M^2} - \frac{C_4^V}{2M^2} \text{ should read } \frac{-C_5^V}{2M^2} - \frac{C_4^V}{2M^2}$$

SLAC-PUB-958
(TH) and (EXP)
May 1971

NEUTRINO REACTIONS AT ACCELERATOR ENERGIES*

C. H. Llewellyn Smith

Stanford Linear Accelerator Center
Stanford University, Stanford, California 94305

(To be published in Physics Reports)

* Work supported in part by the U. S. Atomic Energy Commission.

TABLE OF CONTENTS

	<u>Page</u>
Historical Introduction	1
Plan of this Review	2
 <u>Chapter 1 — Theories of Weak Interactions</u>	
1.1 The Phenomenological Theory	4
A. The effective Lagrangian for leptonic and semileptonic processes	4
B. Properties of the lepton current	5
C. Properties of the hadron current in semileptonic processes .	9
D. The complete effective Lagrangian	19
1.2 CP Violation	21
1.3 The Intermediate Vector Boson	22
1.4 Limitations of the Phenomenological Theory	22
1.5 Some Alternative Theories of Weak Interactions	24
A. Models with strongly interacting IVBs	24
B. The model of Gell-Mann, Goldberger, Kroll and Low	26
C. The Model of Lee and Wick	27
D. The model of Tanikawa and Watanabe	28
E. The models of Kummer, Segrè, Shabalin and Christ	29
 <u>Chapter 2 — General Properties of Neutrino Reactions</u>	
2.1 Tests of the Current-Current Interaction and Properties of the Lepton Current	31
2.2 Tests of Properties of the Hadron Current	37
A. Selection rules	37
B. CVC and PCAC (Adler's theorem)	40
C. Current algebra	43

	<u>Page</u>
2.3 T Violation	45
Chapter 3 — Phenomenological Descriptions of Neutrino Reactions	
3.1 Neutrino Beams	48
3.2 Neutrino Lepton Interactions	52
A. Interactions with electron targets	53
B. Interactions in the electromagnetic field of a nucleus	55
3.3 Quasi-Elastic Neutrino Scattering ($\Delta Y = 0$)	57
A. General remarks	57
B. Cross sections in the conventional theory and theoretical ideas about the axial form factors	61
C. Polarization measurements	64
D. T violating effects	69
E. Nuclear effects	70
F. Experimental results	74
3.4 Quasi-Elastic Neutrino Scattering ($\Delta Y = \pm 1$)	75
3.5 $N^*(1238)$ Production	81
A. General remarks	81
B. Dynamical calculations	83
C. Isobar models	89
D. Higher symmetries and quark models	92
E. Comparison between models	93
F. Experimental results	95
3.6 Highly Inelastic Reactions	97
A. Kinematics	97
B. Scale invariance	100

	<u>Page</u>
C. Models and sum rules	103
D. Experimental results	119
3.7 Detailed Descriptions of Highly Inelastic Reactions	124
A. The diffraction region	124
B. The large Q^2 region	126
3.8 Tests of PCAC	130
A. The shadow effect	130
B. Experimental results	134
3.9 W Production	135
A. Production cross section	135
B. Branching ratios and the detection of W's	138
C. Other means of establishing the existence of W's	140
3.10 Miscellaneous Topics	142
A. Experimental anomalies	142
B. Y^* production by neutrinos	143
C. Neutrino production of higher resonances	143
D. Nuclear effects in inelastic reactions	143
E. Event rates expected at NAL	145
Acknowledgements	146
Appendix	147
References	151
Tables	165
Figures	181

Historical Introduction

Neutrino cross sections were first calculated in 1934^(B19) soon after Pauli postulated the existence of neutrinos (1930) and Fermi laid the foundations of our present description of weak interactions (1933). * It was not until 1953, however, that the existence of the neutrino was directly demonstrated by the observation of neutrino induced reactions.^(R5) During the following years several people pointed out that neutrino experiments would be possible at large accelerators^(A20, C26, F1, M2, P17, S3) and cross sections were calculated for accelerator energies.^(C3, L12, Y1) The first accelerator experiment established the difference between electron and muon neutrinos in 1962.^(D2) Since then several experiments have been performed but no spectacular new discoveries were made; because of the small statistics these experiments may, perhaps, be fairly described as exploratory.

The second generation of neutrino experiments is now about to begin. Enormous new bubble chambers are coming into operation at existing laboratories (ANL, BNL and CERN) which will greatly increase the event rates and also allow the study of neutrino reactions on hydrogen and deuterium targets. The possible neutrino energy range will soon be vastly extended by the new 500 GeV accelerator (NAL). The anticipated experimental progress in neutrino physics may be judged from Fig. 1.

* We shall use the word neutrino as a generic term for muon and electron neutrinos and antineutrinos. When a distinction is necessary, we will write ν_μ , $\bar{\nu}_\mu$ or $\bar{\nu}_e$.

Plan of this Review

Our present knowledge of weak interactions has mainly been derived from studies of weak decays and muon capture. A phenomenological description of these processes has been developed which is rather successful for leptonic and semileptonic processes. It is well known, however, that this description cannot be correct at very high energies where neutrino scattering experiments are the only practical way to study weak interactions.

We can therefore distinguish three goals for neutrino experiments:

1. To establish the domain of validity of the present phenomenological theory.
2. To provide clues for the construction of alternative theories.
3. Given a theory of weak interactions, to probe the structure of hadrons.

Clearly the first step in the analysis of neutrino experiments is to confront the results with the predictions of the phenomenological theory. Therefore we begin in Chapter 1 with a brief review of this theory and the evidence for its various ingredients. Next we discuss its inadequacies. Then we review various alternative theories of weak interactions, which suggest where we might look for failures of the phenomenological theory.

In Chapter 2 we discuss tests of the basic assumptions of the phenomenological theory which are possible in neutrino experiments. This chapter echoes Chapter 1; we start with tests of the current-current interaction hypothesis and then discuss tests of successively stronger hypotheses about the currents.

Chapter 3 is devoted to a detailed discussion of some specific neutrino reactions. We begin with a brief review of the nature of neutrino beams since

a qualitative idea of the spectra available is essential for an appreciation of experimental results and possibilities. Although we elaborate on the details of the tests of general assumptions discussed already in Chapter 2, the main emphasis is on a phenomenological description in the framework of the usual theory and the use of neutrinos to probe hadron structure. Comparisons with experiment are made whenever possible.

Theoretical discussion of neutrino physics has far outstripped experimental progress because of the inevitably slow progress of the latter up to now (the situation will probably be reversed in a few years). The reviewer is faced with many papers on the same subject espousing different hypotheses (and very different notations). Hardly one of these papers can be said to have been disproved or verified by experiment, yet all may turn out to be irrelevant if the behavior of weak interactions at high energy contains surprises. It has therefore been necessary to apply subjective criteria in many cases in order to decide which subjects are too "well known" to warrant detailed discussion, which points should be emphasized and, in controversial cases, which models merit exposition. At this point it is appropriate to apologize to those whose work has been overlooked; this is as likely to be due to the author's ignorance as to subjective discrimination.

CHAPTER 1

THEORIES OF WEAK INTERACTIONS

Several excellent reviews of weak interactions are available (see, e.g., L10 and M4) and the brief summary presented here is not intended to compete with them (more detailed references to the literature may be found in the reviews cited). It is intended to establish notation for later analysis, to define various hypotheses about the weak interactions which can be tested in neutrino experiments and to summarize the evidence for them. (Unless otherwise stated experimental results cited below are taken from P11.)

1.1 The Phenomenological Theory

A. The effective Lagrangian for leptonic and semileptonic processes

All leptonic and semileptonic interactions directly observed up to now can be described by the phenomenological Lagrangian:

$$\mathcal{L}_{\text{eff}} = \frac{G}{\sqrt{2}} \left[\left(j_{\lambda}^{(e)} + j_{\lambda}^{(\mu)} \right)^{\dagger} J^{(h)\lambda} + j_{\lambda}^{(e)\dagger} j_{\lambda}^{(\mu)} + \text{hermitian conjugate} \right] \quad (1.1)$$

where G is Fermi's constant

$$G = \frac{(1.023 \pm 0.001) \times 10^{-5}}{M_p^2}$$

$J_{\lambda}^{(h)}(x)$ is a current constructed from the hadronic fields and the muon and electron currents are given by

$$j_{\lambda}^{(\mu), (e)} = \bar{\psi}_{\mu, e}(x) \gamma_{\lambda} (1 - \gamma_5) \psi_{\nu_{\mu}, \nu_e}(x) \quad (1.2)$$

where the notation is defined in the appendix. The matrix elements of \mathcal{L}_{eff} are supposed to give transition amplitudes directly (if \mathcal{L}_{eff} is used in perturbation theory many of the higher order contributions are infinite).

B. Properties of the lepton current

In writing (1.1) and (1.2) many assumptions have been made (beyond those which we take for granted here such as Lorentz invariance, CPT invariance, etc.):

1. Two component neutrino theory. All experiments are in agreement with the hypothesis that ν_{μ} and ν_e have helicity -1 and $\bar{\nu}_{\mu}$ and $\bar{\nu}_e$ have helicity $+1$ (by definition: $\pi^+ \rightarrow \mu^+ \nu_{\mu}$, $\pi^- \rightarrow \mu^- \bar{\nu}_{\mu}$, $(A, Z) \rightarrow (A, Z-1) e^+ \nu_e$, $(A, Z) \rightarrow (A, Z+1) e^- \bar{\nu}_e$).

2. Lepton conservation. Two lepton numbers can be assigned to all particles:

$$\begin{aligned}
 L_e &= +1 && \text{for } e^-, \nu_e \\
 &= -1 && \text{for } e^+, \bar{\nu}_e \\
 &= 0 && \text{for all other particles.} \\
 \\
 L_{\mu} &= +1 && \text{for } \mu^-, \nu_{\mu} \\
 &= -1 && \text{for } \mu^+, \bar{\nu}_{\mu} \\
 &= 0 && \text{for all other particles.}
 \end{aligned}$$

The conservation law usually assumed (implicit in Eqs. (1.1) and (1.2)) is that L_e and L_{μ} are separately conserved. The evidence for this is the absence of processes such as:

$$Z \rightarrow (Z+2) + 2e^-, \quad \frac{|A(Z \rightarrow (Z+2) + 2e^-)|}{|A(Z \rightarrow (Z+2) + 2e^- + 2\nu_e)|} \leq 10^{-3} \quad \text{B2}$$

$\mu^\pm \rightarrow e^\pm + \gamma$	Branching ratio $< 2 \times 10^{-8}$
$\rightarrow e^\pm + 2\gamma$	Branching ratio $< 1.6 \times 10^{-5}$
$\rightarrow 2e^\pm + e$	Branching ratio $< 1.3 \times 10^{-7}$
$K^+ \rightarrow \pi^+ + \mu^+ + e^-$	Branching ratio $< 3 \times 10^{-5}$ (C22)
$K_L^0 \rightarrow \mu^\pm + e^\mp$	Branching ratio $< 1.57 \times 10^{-9}$ (C21)
$\nu_\mu + N \rightarrow e^- + \dots$	$\frac{\sigma(\nu_\mu \rightarrow e^-)}{\sigma(\nu_\mu \rightarrow \mu^-)} < 1\%$ (F10)
$\nu_\mu + N \rightarrow \mu^+ + \dots$	$\frac{\sigma(\nu_\mu \rightarrow \mu^+)}{\sigma(\nu_\mu \rightarrow \mu^-)} < 4.6 \times 10^{-3}$ (B39)

(If we accept the two component theory, then the evidence concerning the lepton helicity in β , π and K decay constitutes excellent support for lepton conservation (see, e.g., L10).) All the evidence is also consistent with the weaker hypothesis^(F5) that $L_e + L_\mu$ and the sign of $(-)^{L_e}$ are conserved. This would allow certain processes forbidden by the usual scheme:

$\mu^+ \rightarrow e^+ + \bar{\nu}_e + \nu_\mu$	
$e^- e^- \rightarrow \mu^- \mu^-$	(Coupling < 610 G, assuming V-A interaction ^(B1))
muonium \rightarrow antimuonium	(Coupling < 5800 G, assuming V-A interaction ^(A18))
$\nu_\mu + \text{hadrons} \rightarrow e^- + \mu^+ + \nu_e + \text{hadrons}'$	(Coupling < 5 G, assuming V-A interaction ^(C12))
$\bar{\nu}_\mu + \text{hadrons} \rightarrow e^+ + \mu^- + \bar{\nu}_e + \text{hadrons}'$	

It might be possible to observe the last two processes ($\sim Z\alpha^2 G^2$). It may also be possible to observe the decay $\mu^+ \rightarrow e^+ \bar{\nu}_e \nu_\mu$, if it occurs. Kalbfleisch has pointed out^(K4) that it would introduce a $\bar{\nu}_e(\nu_e)$ component in $\nu_\mu + \nu_e$ ($\bar{\nu}_\mu + \bar{\nu}_e$) beams. The energy dependence of this component would be sufficiently different from the small $\bar{\nu}_e(\nu_e)$ background present anyway that even a small $r = \Gamma(\mu^+ \rightarrow e^+ \bar{\nu}_e \nu_\mu) / \Gamma(\mu^+ \rightarrow e^+ \nu_e \bar{\nu}_\mu)$ could be detected. Kalbfleisch estimates that if $r = 0.5$ it would certainly be detected in the experiment now underway at CERN and that r should be known to $\pm 5\%$ by the end of the decade.

Henceforth we assume the additive conservation law in this paper.

Lepton conservation and the two component theory together imply that the neutrino has zero rest mass.^(L10) The present limits are:

$$m_{\nu_e} < 60 \text{ eV}$$

$$m_{\nu_\mu} < 1.6 \text{ MeV}$$

We shall assume that the neutrino mass is zero. A scheme has been proposed in which e^- and μ^- have opposite lepton number.^(K11) This is equivalent to the usual scheme if the neutrino mass is zero.

A scheme has also been proposed (the "neutrino flip" hypothesis^(F3)) in which the hypercharge conserving hadron current couples to $(\bar{\nu}_e e)$ and $(\bar{\nu}_\mu \mu)$ and the $\Delta Y = 1$ current couples to $(\bar{\nu}_\mu e)$ and $(\bar{\nu}_e \mu)$. Experimentally the neutrino flip coupling must be less than 20% of the usual coupling.^(Y4)

3. Absence of neutral currents. Present limits on the branching ratios

are:

$$\begin{aligned} K_S^0 \rightarrow \mu^+ \mu^- &< 0.7 \times 10^{-5} \\ &\rightarrow e^+ e^- \end{aligned}$$

$$\begin{aligned} K_L^0 \rightarrow \mu^+ \mu^- &< 1.82 \times 10^{-9} \text{ (C21)} \\ &\rightarrow e^+ e^- &< 1.82 \times 10^{-9} \text{ (C21)} \end{aligned}$$

$$\begin{aligned} K^+ \rightarrow \pi^+ e^+ e^- &< 0.4 \times 10^{-6} \\ &\rightarrow \pi^+ \mu^+ \mu^- &< 2.4 \times 10^{-6} \\ &\rightarrow \pi^+ \nu \bar{\nu} &< 1.4 \times 10^{-6} \text{ (K10)} \end{aligned}$$

$$K^+ \rightarrow \pi^+ \pi^0 e^+ e^- < 8 \times 10^{-6} \text{ (C22)}$$

$$\frac{\sigma(\nu_\mu p \rightarrow \nu_\mu p)}{\sigma(\nu_\mu n \rightarrow \mu^- p)} \leq 0.12 \pm 0.06 \text{ (C27)}$$

$$\frac{\sigma(\nu_\mu p \rightarrow \nu_\mu \pi^+ n)}{\sigma(\nu_\mu p \rightarrow \mu^- \pi^+ p)} \leq 0.08 \pm 0.04 \text{ (C27)}$$

$$\frac{\sigma(\nu_\mu e^- \rightarrow \nu_\mu e^-)}{\sigma(\nu_e e^- \rightarrow e^- \nu_e) \text{ V-A theory}} < 0.4 \text{ (A10)}$$

For a theoretical analysis of interactions involving neutral currents we refer to A14 and references therein. We note that even in the absence of a neutral weak current the neutrino can undergo "contact" electromagnetic interactions by virtue of its charge form factor. (B18, L8)

4. Universality of electron and muon interactions. Except for a possible discrepancy in e/μ scattering (C8, E4, T2) all evidence is at present in agreement

with the hypothesis that muons and electrons are identical, apart from their masses.

In $\Delta S = 0$ weak interactions, the best evidence is the agreement of theory and experiment for the $\pi_{\mu 2}$ to $\pi_{e 2}$ branching ratio (assuming the V-A lepton current):

$$\frac{\Gamma(\pi^+ \rightarrow e^+ \nu_e)}{\Gamma(\pi^+ \rightarrow \mu^+ \nu_\mu)} = \left(\frac{m_e}{m_\mu}\right)^2 \left(\frac{M_\pi^2 - m_e^2}{M_\pi^2 - m_\mu^2}\right)^2 = 1.23 \times 10^{-4} \quad (\text{theory})$$

$$= (1.24 \pm 0.03) \times 10^{-4} \quad (\text{expt.})$$

C. Properties of the Hadron Current in Semileptonic Processes

Assuming (1.2) for the lepton current, the hadron current $J_\lambda^{(h)+}$ must carry charge +1 (and $J_\lambda^{(h)}$ charge -1). Many other properties of $J_\lambda^{(h)}$ have been established or proposed:

(1) $\Delta Y = 0, \pm 1$ (where Y is the hypercharge). In semileptonic decays, the evidence for this selection rule is based on:

$$\frac{\Gamma(\Xi^0 \rightarrow p e^- \bar{\nu}_e)}{\Gamma(\Xi^0 \rightarrow \Lambda \pi^0)} < 1.3 \times 10^{-3}$$

$$\frac{\Gamma(\Xi^0 \rightarrow p \mu^- \bar{\nu}_\mu)}{\Gamma(\Xi^0 \rightarrow \Lambda \pi^0)} < 1.3 \times 10^{-3}$$

$$\frac{\Gamma(\Xi^0 \rightarrow p e^- \bar{\nu}_e)}{\Gamma(\Xi^- \rightarrow \Lambda e^- \bar{\nu}_e)} < 1.8$$

The first two limits are not very useful, since leptonic decays are generally suppressed by a factor $\gtrsim 10^{-3}$ relative to nonleptonic decays. The last limit is better than it might appear, since the phase space is about 25 times larger

for the upper decay so that

$$\frac{|\Lambda(\Xi^0 \rightarrow p e^- \bar{\nu})|}{|\Lambda(\Xi^- \rightarrow \Lambda e^- \bar{\nu})|} < 0.27$$

(2) In $\Delta Y = \pm 1$ transitions, the change of charge of the hadrons satisfies $\Delta Q = \Delta Y$. Limits on processes which would violate this rule are:

$$\frac{\Gamma(K^+ \rightarrow \pi^+ \pi^+ e^- \bar{\nu}_e)}{\Gamma(K^+ \rightarrow \pi^+ \pi^- e^+ \nu_e)} < 0.023$$

$$\frac{\Gamma(K^+ \rightarrow \pi^+ \pi^+ \mu^- \bar{\nu}_\mu)}{\Gamma(K^+ \rightarrow \pi^+ \pi^- \mu^+ \nu_\mu)} < 0.6$$

$$\frac{\Gamma(\Sigma^+ \rightarrow e^+ n \nu)}{\Gamma(\Sigma^- \rightarrow e^- n \nu)} < 0.037$$

$$\frac{\Gamma(\Xi^0 \rightarrow \Sigma^- e^+ \nu)}{\Gamma(\Xi^0 \rightarrow \Lambda \pi^0)} < 1.5 \times 10^{-3}$$

$$x' = \frac{A(K_{\mu 3}^0, \Delta S = -\Delta Q)^*}{A(K_{\mu 3}^0, \Delta S = \Delta Q)} = 0.04 \pm 0.10 - 0.13 + i(0.12 \pm 0.17) \quad (G17)$$

$$x = \frac{A(K_{e 3}^0, \Delta S = -\Delta Q)^*}{A(K_{e 3}^0, \Delta S = \Delta Q)} = -0.13 \pm 0.11 + i(-0.04 \pm 0.16) \quad (M1)$$

(3) The $|\Delta I| = \frac{1}{2}$ rule for $\Delta Y = \pm 1$ transitions (in which the $\Delta Y = \Delta Q$ rule gives $|\Delta I_3| = \frac{1}{2}$, and, therefore, $|\Delta I| \geq \frac{1}{2}$).^(G6) This relation has been tested in K_{e3} and $K_{\mu 3}$ decays:

*See (G17) and (M1) for the precise definition of x' and x . (Im x , $x' \neq 0$ would imply that T is not conserved.) We have quoted the results of one recent experiment for illustration. K. Winter has reviewed the present experimental situation at the Amsterdam conference.

$$\frac{\Gamma_{K_{e3}^0}}{2\Gamma_{K_{e3}^+}} = 1.012 \quad (\text{theory})$$

$$= 0.94 \pm 0.04 \quad (\text{experiment})$$

$$\frac{\Gamma_{K_{\mu 3}^0}}{\Gamma_{K_{e3}^0}} \left[\frac{\Gamma_{K_{\mu 3}^+}}{\Gamma_{K_{e3}^+}} \right]^{-1} = 1 \quad (\text{theory})$$

$$= 1.05 \pm 0.6 \quad (\text{experiment})$$

There is an indication that the rule fails, but the compilers of the data quoted^(P11) urge caution in view of disagreements among the data.

(4) $|\Delta I| = 1$ rule for $\Delta Y = 0$ transitions. This holds automatically for the decays of all presently known stable particles; it can be tested in neutrino reactions.

(5) Charge symmetry of the $\Delta Y = 0$ part of $J_{\lambda}^{(h)}$.^(L13) This is the hypothesis that

$$J_{\lambda}^{0+} = -e^{-i\pi I_2} J_{\lambda}^0 e^{+i\pi I_2} \quad \left(J_{\lambda}^{(h)} = J_{\lambda}^{Y=0} + J_{\lambda}^{Y=\pm 1} \right) \quad (1.3)$$

where I_i are the components of the isospin operator. It implies the equality of the hadronic parts of the matrix elements for $\Sigma^+ \rightarrow \Lambda e^+ \nu_e$ and $\Sigma^- \rightarrow \Lambda e^- \bar{\nu}_e$ and hence:*

$$\frac{\Gamma(\Sigma^- \rightarrow \Lambda e^- \bar{\nu}_e)}{\Gamma(\Sigma^+ \rightarrow \Lambda e^+ \nu_e)} = 1.64 \quad (\text{theory})$$

$$= 1.60 \pm 0.56 \quad (\text{experiment})$$

*The $e^- \bar{\nu}_e / e^+ \nu_e$ tensors (Eq. 2.3 below) differ only in the V-A interference term which does not contribute to decay rates (as is easily seen by considering the $e-\nu$ tensor after integration over the relative $e-\nu$ momentum). The predicted difference of the Σ^{\mp} decay rates is due to the mass difference.

It also implies mirror symmetry for ft values in nuclear β decay. Wilkinson and Alburger^(W7, A15) have recently presented evidence against this hypothesis in many cases. In the decays ${}^8\text{B}/{}^8\text{Li} \rightarrow {}^8\text{Be}$, for example,^(A15) they found

$$\delta = \frac{(ft)^+}{(ft)^-} - 1 = 0.107 \pm 0.011.$$

${}^8\text{Be}$ is a broad state which decays rapidly to 2α so that the energy release can be varied without changing the nuclear physics very much. The asymmetry appears to be independent of the energy release which implies that a one-body operator is not responsible.* It is not clear at present whether the asymmetry is really due to a failure of the charge symmetry condition or to an electromagnetic violation of isospin invariance. Tests of CVC in nuclear β decay suggest that nuclear wave functions are highly isosymmetric, but it is possible to imagine isospin violating terms which would contribute directly to axial decays but not to vector decays (e.g., the $\omega - \rho$ mixing effect suggested by Lipkin^(L16)).

If we accept the charge symmetry condition and the $\Delta I = 1$ rule, then J_λ^0 and J_λ^{0+} must belong to the same isotriplet; the SU(3) generalization of this is that J_λ^h and J_λ^{h+} belong to the same octet.

*It has been asserted^(L16) that a one-body operator cannot cause an asymmetry in ft values. The argument is only true, however, if n and p are degenerate. If one-body operators are used, the nucleons must be given effective masses (or energies), depending on the nucleus in question, in order for the decays to proceed. This (ambiguous) procedure gives rise to an asymmetry δ proportional to the energy release in the decay if the charge symmetry condition is violated.

(6) Absence of "second-class currents." It is useful to split the vector and axial vector parts of the $\Delta Y = 0$ current J_μ^0 into two parts following a classification due to Weinberg^(W2):

$$J_\mu^0 = V_\mu^0 - A_\mu^0$$

$$V_\mu^0 = V_\mu^0(1) + V_\mu^0(2)$$

$$A_\mu^0 = A_\mu^0(1) + A_\mu^0(2)$$

$$\left. \begin{aligned} GV_\mu^0(1)G^{-1} &= V_\mu^0(1) \\ GA_\mu^0(1)G^{-1} &= -A_\mu^0(1) \end{aligned} \right\} \text{"first-class currents"}$$

$$\left. \begin{aligned} GV_\mu^0(2)G^{-1} &= -V_\mu^0(2) \\ GA_\mu^0(2)G^{-1} &= A_\mu^0(2) \end{aligned} \right\} \text{"second-class currents"}$$

where the G parity operator is defined in terms of the charge conjugation operator C and the isospin I by $G = C e^{i\pi I_2}$. The proposal that second-class currents are absent is equivalent to assuming the charge symmetry of J_λ^0 if time reversal invariance holds to lowest order in G in $\Delta Y = 0$ reactions. In this case,

$T J_\lambda^0(0) T^{-1} = J_\lambda^{0\lambda}(0)$ (given the behavior of the lepton current under T). Necessarily, we have $(CPT) J_\lambda^h(0) (CPT)^{-1} = -J_\lambda^h(0)^+$ and, therefore,

$$C V_\lambda^0(0) C^{-1} = -V_\lambda^{0+}(0)$$

$$C A_\lambda^0(0) C^{-1} = A_\lambda^{+0}(0) \quad (\text{if T is a good symmetry.})$$

The equivalence of the charge symmetry condition and the absence of second-class currents follows immediately.

The hypothesis that second-class currents are absent is very badly tested, because their effects vanish at zero momentum transfer and momentum transfers are small in semileptonic decays. (Generally the consequences of assuming the charge symmetry condition and the absence of second-class currents are different--see, e. g., page 58 of this paper; however, the absence of second-class currents, together with CPT invariance, would imply mirror symmetry for ft values so that the Wilkinson-Alburger results discussed above are presumably relevant to the second-class current question.)

(7) Conserved vector current hypothesis (CVC)^(F7, G9). The hypothesis that V_λ^0 is conserved was introduced in order to explain the near equality of the vector coupling constants in μ decay and β decay; the conservation is broken by electromagnetic corrections in the usual scheme--hypothesis 8. Assuming that the bare coupling constants are equal, CVC implies $g_\beta^V = g_\mu^V + O(\alpha)$; experimentally $(g_\mu^V - g_\beta^V) / g_\mu^V \approx 2.2\%$ (taking into account radiative corrections)--the discrepancy is accounted for in the Cabibbo theory in which the bare coupling constants are different (see below).

(8) The isotriplet current hypothesis (frequently referred to as the CVC hypothesis; we will sometimes employ this useful but regrettable nomenclature) states that V_λ^0 and V_λ^{0+} are the $I_3 = \mp 1$ components, respectively, of the isovector part of the electromagnetic current.^(F7) This hypothesis subsumes the hypotheses 4, 5, 6, and 7 for V_λ^0 . Predictions of the hypothesis which have been tested are

$$\begin{aligned} \text{(a)} \quad \Gamma(\pi^+ \rightarrow \pi^0 e^+ \nu_e) &= 0.411 \text{ sec}^{-1} \quad (\text{theory}) \\ &= 0.392 \pm 0.027 \text{ sec}^{-1} \quad (\text{experiment}) \end{aligned}$$

$$\text{(b)} \quad \lim_{q_\mu \rightarrow 0} \langle \Lambda^0 | V_\mu^0 | \Sigma^+ \rangle = 0 \quad \text{in agreement with experiment}$$

(c) The magnitude of the "weak magnetism" term $\sim \bar{u}_p \sigma_{\lambda\nu} q_\nu u_n$ in $\langle p | V_\lambda^{0+} | n \rangle$ is successfully predicted^(G3) in terms of $\mu_p - \mu_n$ to within the experimental accuracy of 20%.

(9) Octet hypothesis for $J_\lambda^{(h)}$ and Cabibbo's formulation of universality. Following Gell-Mann's hypothesis^(G4) that the vector and axial vector currents transform as members of octets under the group SU(3) (which is supposed to be an approximate symmetry of strong interactions), Cabibbo^(C1) (see also G7) formulated the hypothesis of universality of the weak interactions in a way which is conveniently stated by saying that the currents transform as if they were built from quark fields, thus*:

$$\begin{aligned}
 J_\lambda^{(h)+} &= V_\lambda^+ - A_\lambda^+ \\
 V_\lambda^+ &= \bar{p} \gamma_\lambda (n \cos \theta_V + \lambda \sin \theta_V) \\
 A_\lambda^+ &= \bar{p} \gamma_\lambda \gamma_5 (n \cos \theta_A + \lambda \sin \theta_A)
 \end{aligned}
 \tag{1.4}$$

In Gell-Mann's notation^(G4) in which the octet states are labelled with an index $i = 1 \dots 8$ (the labels $i = 1, 2, 3$ refer to the isovector states):

*We recall that three quark states (G5, Z3) have the quantum numbers:

	<u>B</u>	<u>Q</u>	<u>Y</u>	<u>I₃</u>	
p	1/3	2/3	1/3	+ 1/2	} I = 1/2
n	1/3	-1/3	1/3	-1/2	
λ	1/3	-1/3	-2/3	0	I = 0

The quark states can be represented by a vector $q = \begin{pmatrix} p \\ n \\ \lambda \end{pmatrix}$. Under an SU(3) transformation, $q' = Uq$, while for antiquarks $\bar{q}' = U^* \bar{q}$, where U is a 3×3 unitary unimodular matrix. The use of quark states here in no way implies that quarks exist.

$$\begin{aligned}
V_{\lambda}^{+} &= \left(\mathcal{F}_{\lambda}^1 + i \mathcal{F}_{\lambda}^2 \right) \cos \theta_V + \left(\mathcal{F}_{\lambda}^4 + i \mathcal{F}_{\lambda}^5 \right) \sin \theta_V \\
A_{\lambda}^{+} &= \left(\mathcal{F}_{\lambda}^{(5)1} + i \mathcal{F}_{\lambda}^{(5)2} \right) \cos \theta_A + \left(\mathcal{F}_{\lambda}^{(5)4} + i \mathcal{F}_{\lambda}^{(5)5} \right) \sin \theta_A.
\end{aligned} \tag{1.5}$$

θ_V and θ_A are often assumed to be the same.

The octet hypothesis incorporates the hypotheses 1 - 8 already discussed. If SU(3) symmetry breaking is neglected, the parameters θ_V and θ_A can be determined in several ways^(B41, E1):

$$(a) \quad g_{\beta}^V / g_{\mu}^V \rightarrow \sin \theta_V = 0.209 \pm 0.008$$

$$(b) \quad \frac{\Gamma(K^+ \rightarrow \pi^0 e \nu)}{\Gamma(\pi^+ \rightarrow \pi^0 e \nu)} \rightarrow \sin \theta_V = 0.220 \pm 0.003$$

$$(c) \quad \frac{\Gamma(K^+ \rightarrow \mu \nu)}{\Gamma(\pi^+ \rightarrow \mu \nu)} \rightarrow \sin \theta_A = 0.265$$

(d) Ten leptonic baryon decays can be described in terms of four parameters: θ_V , θ_A , and the reduced matrix elements D and F for the two possible SU(3) couplings. A fit gives:

$$\sin \theta_V = 0.250 \pm 0.009$$

$$\sin \theta_A = 0.236 \pm 0.011$$

These results suggest that $\theta_V = \theta_A$; in the following, we assume that this is so and write $\theta_C = \theta_V = \theta_A$.

(10) Current Algebra. Gell-Mann has proposed^(G4) that if we define

$$F^i(x_0) = \int \mathcal{F}_0^i(x) d^3x$$

$$F^{(5)i}(x_0) = \int \mathcal{F}_0^{(5)i}(x) d^3x,$$

then these operators satisfy the algebra:

$$[F^k, F^\ell] = if^{k\ell m} F^m \quad (1.6)$$

$$[F^k, F^{(5)\ell}] = if^{k\ell m} F^{(5)m} \quad (1.7)$$

$$[F^{(5)k}, F^{(5)\ell}] = if^{k\ell m} F^m \quad (1.8)$$

where $f^{k\ell m}$ are the SU(3) structure functions. These equations are supposed to be true although SU(3) symmetry is broken (as in the quark model, for example). Equation (1.6) states that the vector charges satisfy the algebra of the generators of SU(3), and Eq. (1.7) that the axial charges transform as an octet (these assumptions are tested by the success of the Cabibbo theory which incorporates an additional universality hypothesis). Equation (1.8) closes the algebra and sets the scale of the axial current relative to the vector current.

Unfortunately all the tests of the current algebra hypothesis which have been carried out so far rely on additional assumptions (PCAC, smallness of σ terms, commutation relations for the currents themselves, etc.). The successful calculation of g_A/g_V (A4, W3) using Eq. (1.8) is the most impressive test. Other calculations have met with mixed success (e.g., scattering length and $K \rightarrow n\pi$ calculations seem to work, but $K_{\ell 3}$ and $\eta \rightarrow 3\pi$ calculations fail; for a review, see A8).

(11) PCAC. (B17, C18, G7) The hypothesis of "partial conservation of the axial current"--PCAC--(or "pion dominance of the divergence of the axial current"--PDDAC--as it should perhaps more correctly be called) can be stated in many nearly equivalent ways (for reviews, see A8 and C24). Two statements are:

- (a) An unsubtracted dispersion relation can be written for the matrix elements of $\partial_\mu A_\mu^0$ in the variable q^2 (where q_μ is the four momentum carried by A_μ^0 --the $\Delta Y = 0$ axial current) and it is dominated by the pion pole term near $q^2 = 0$.

(b) If the interpolating field of the pion is defined to be $\phi_\pi = c \partial_\mu A_\mu^0(\mathbf{x})$, where $c = M_\pi^2 f_\pi \cos \theta$ is a normalization constant ($f_\pi \approx 0.96 M_\pi$ is the pion decay constant), then the matrix elements of the corresponding source current $(\square + m_\pi^2) \phi_\pi$ do not vary much in the interval $0 \lesssim q^2 \lesssim m_\pi^2$.

(Brandt and Preparata^(B40) have recently advocated a "weak" version of PCAC, defined by replacing the words "matrix elements" by "matrix elements between physical states" in the definitions a and b of "strong" PCAC given here.)

The only direct test of the PCAC hypothesis is the Goldberger-Treiman relation^(G12) which motivated the PCAC postulate and is satisfied with an error of 10%. Many indirect tests of PCAC have been made (Adler and Weisberger's calculation of g_A/g_V is perhaps the best), but they usually involve current algebra, and often other additional assumptions; their mixed success cannot truly be said to confirm the PCAC hypothesis.

D. The Complete Effective Lagrangian

It is usually assumed that the Lagrangian (1.1) is only part of the complete effective Lagrangian for weak interactions:

$$\mathcal{L}_{\text{eff}} = \frac{G}{\sqrt{2}} J_\lambda^+ J_\lambda \quad (1.9)$$

where J_λ is the sum of the currents previously defined:

$$J_\lambda = J_\lambda^{(h)} + J_\lambda^{(\mu)} + J_\lambda^{(e)} \quad (1.10)$$

This form of \mathcal{L}_{eff} arises naturally at low momentum transfer if it is assumed that the weak interactions are mediated by an intermediate vector boson (see below). The Lagrangian (1.9) implies the existence of additional processes not

given by (1.1):

- (1) Additional leptonic processes, such as $\nu_e e^- \rightarrow \nu_e e^-$ with a definite probability. Astrophysical evidence has been used to deduce:

$$g_{\nu-e}^2 = 10^{0 \pm 2} G^2 \quad (\text{S14})$$

in a somewhat indirect way. Neutrino experiments have so far only given limits

$$\frac{\sigma(\bar{\nu}_e + e \rightarrow \bar{\nu}_e + e)}{\sigma_{\text{theory}}} < 2.5 \quad (\text{reactor experiment (R7)})$$

$$\frac{\sigma(\nu_e + e \rightarrow \nu_e + e)}{\sigma_{\text{theory}}} < 324 \quad (\text{CERN bubble chamber experiment (C27)})$$

$$< 40 \quad (\text{CERN spark chamber experiment (C14)})$$

The reactor experiment cited is still under way and should eventually be able to confirm or disprove the theory.

Chen has pointed out^(C14) that these experiments give stronger limits if the coupling is not of the conventional V-A form.* If, for example, the coupling has the form:

$$g_{V+A} \bar{e} \gamma_\lambda (1 + \gamma_5) e \bar{\nu}_e \gamma_\lambda (1 + \gamma_5) \nu_e$$

(the analogous form for μ decay gives the same results as the V-A theory as long as the ν 's are not observed--see section 3.2.), then

*We note that there exist theories which predict values other than the V-A theory result, e. g., in the "isospin-symmetric" coupling model^(A14) $4\sigma(\bar{\nu}_e e \rightarrow \bar{\nu}_e e) = \sigma(\text{V-A theory})$.

the reactor experiment gives:

$$g_{V+A}^2 < 0.13 G^2$$

The limits for other couplings are also given by Chen.

- (2) Nonleptonic interactions with $\Delta Y = 0$. While they are almost impossible to observe directly, the existence of these interactions can be inferred from the parity violating admixtures they induce in nuclear states. Such admixtures have been established by the observation of apparent parity violations in γ transitions; they have the expected order of magnitude and (despite the errors and the uncertainties of nuclear physics) attempts have already been made to use them to make qualitative tests of models of the hadron current (for a review see B30).
- (3) Nonleptonic interactions with $\Delta Y = 1$. These transitions are well known. Empirically, they seem to satisfy the selection rules $\Delta Y < 2$ and $\Delta I = 1/2$.^(G6) No exception is known to the $\Delta Y < 2$ rule, which follows from (1.6) and the usually accepted properties of $J_\lambda^{(h)}$ discussed above (the small value of $m_{K^0} - m_{\bar{K}^0}$ strongly supports the idea that $\Delta Y = 2$ transitions are strictly forbidden to order G). The $\Delta I = 1/2$ rule does not follow from (1.9) and the properties of $J_\lambda^{(h)}$; generally $J_\lambda^{(h)+} J_\lambda^{(h)}$ contains an $I = 3/2$ part, as well as an $I = 1/2$ part. The $\Delta I = 1/2$ rule is only approximate, an obvious violation being in the $K \rightarrow 2\pi$ decays where

$$\frac{I = 3/2 \text{ amplitude}}{I = 1/2 \text{ amplitude}} \sim 5\% .$$

Two approaches have been used to "explain" the $\Delta I = 1/2$ rule:

- (1) Arguments are advanced to suggest that the $\Delta I = 3/2$ part of \mathcal{L}_{eff} is dynamically suppressed (e.g., current algebra and PCAC lead to the $\Delta I = 1/2$ rule in several cases--see, e.g., A8 and M4).

(2) Pieces are added to \mathcal{L}_{eff} which cancel the $I = 3/2$ part (the deviations are then due to electromagnetic breaking of isospin symmetry. While $5\% > \alpha$, $5\% \sim (m_{\pi^+} - m_{\pi^0})/m_{\pi}$, which is presumably electromagnetic in origin.) These schemes always involve the introduction of neutral currents (whose couplings to leptons must be forbidden or suppressed--see, e.g., L10 and M4).

(Another, rather radical, explanation is to suppose that quarks exist but satisfy Bose statistics. In the absence of electromagnetic effects and in the approximation that the mass of the intermediate vector Boson is infinite, this gives an exact $\Delta I = 1/2$ rule.)^(L17)

1.2. CP Violation

The observation of the decay $K_L^0 \rightarrow 2\pi$ and that

$$\frac{\Gamma(K_L^0 \rightarrow \pi^+ e^- \bar{\nu})}{\Gamma(K_L^0 \rightarrow \pi^- e^+ \bar{\nu})} \neq 1$$

$$\frac{\Gamma(K_L^0 \rightarrow \pi^+ \mu^- \bar{\nu})}{\Gamma(K_L^0 \rightarrow \pi^- \mu^+ \bar{\nu})} \neq 1$$

indicates that CP symmetry is violated. The CPT theorem then implies T violation.

At present there is no definite agreement about the parameters which characterize these effects or the theory behind them (for a review of the experimental situation, containing references to the pertinent literature, see G1). Some of the theories proposed predict substantial T violating effects in neutrino reactions. Tests for T violation will be discussed in Chapters 2 and 3.

1.3. The Intermediate Vector Boson (IVB)

The hypothesis that the weak interactions are mediated by an IVB is very old. The simplest possibility is to introduce two charged vector bosons (W^+ and W^-), which interact only weakly and electromagnetically, and write:

$$\mathcal{L}_{\text{weak}} = g_W J_\lambda W^\lambda + \text{hermitian conjugate} \quad (1.11)$$

To lowest order in q^2/M_W^2 , this generates \mathcal{L}_{eff} above to order g_W^2 , with

$$g_W^2/M_W^2 = G/\sqrt{2}$$

Experimentally, $M_W > 1.8 \text{ GeV}$, independent of the branching ratio. (P15)

In decay processes, the IVB produces very small deviations ($\sim q^2/M_W^2$) from the predictions of \mathcal{L}_{eff} , which are almost impossible to observe if M_W is several GeV.

$\mathcal{L}_{\text{weak}}$ (1.11) suffers from exactly the same difficulties as \mathcal{L}_{eff} . It is not renormalizable. It does not yield the $\Delta I = 1/2$ rule unless neutral W 's are introduced (whose coupling to leptons must be suppressed). In attempts to impose the $\Delta I = 1/2$ rule, various conjectures have been made about the SU(2) and SU(3) properties of W 's, (L13, L10, M4) but they are not of great importance for neutrino reactions.

More complicated schemes involving intermediate bosons will be discussed in Section 1.5.

1.4. Limitations of the Phenomenological Theory

We have already mentioned the fact that if \mathcal{L}_{eff} (Eq. 1.1 and 1.9) or $\mathcal{L}_{\text{weak}}$ (Eq. 1.11) is used in perturbation theory, infinite results are obtained which cannot be removed by renormalization. Attempts to sum up the singular terms (F4) indicate that an increasing number of counter terms must be introduced in each order to render all matrix elements finite. (L3, L4) If this is so, such an approach could only give a phenomenological theory.

On the other hand, the effective Lagrangian philosophy, according to which higher-order terms are simply discarded, must fail at sufficiently high energies. ^(L2)

For example, \mathcal{L}_{eff} predicts that the process $\nu_{\mu} e^{-} \rightarrow \nu_e \mu^{-}$ is purely s-wave and that when the electron is left-handed in the center-of-mass system the cross section is

$$\sigma = 8 G^2 E_{\nu}^2 / \pi$$

where E_{ν} is the center-of-mass neutrino energy. The s-wave cross section, however, is limited by unitarity to be $< \pi \lambda^2$, which is only satisfied for $E_{\nu} < 320$ GeV in this case (corresponding to $E_{\nu}^{\text{lab}} < 10^5$ GeV). * (Violation of exact unitarity occurs, of course, in any theory in a finite order of perturbation theory.) The introduction of an IVB postpones the unitarity crisis to higher energies but does not remove it.

Attempts to calculate higher-order weak processes indicate that the energy/momentum λ at which the conventional theory fails may be quite small. For example, the Bjorken limiting technique ^(B21) can be used to calculate the most divergent part of the second-order weak matrix element for $K_L^0 \rightarrow \mu^+ \mu^-$, using naive canonical commutators ^(I2); the new experimental limit ^(C21) gives $\lambda \gtrsim 14$ GeV in the IVB theory, and $\lambda \lesssim 5$ GeV in the current-current theory. **

*A better limit is obtained for $\nu_{\mu} e^{-} \rightarrow \nu_e \mu^{-}$ than for $\nu_e e \rightarrow \nu_e e$, because the partial wave T matrix for inelastic reactions satisfies $|T| = |e^{2i\delta}| < 1$, while for elastic reactions, $|T| = |i - i e^{2i\delta}| < 2$. ^(I1)

**The most divergent contributions to other processes, such as $K^+ \rightarrow \pi^+ \nu \bar{\nu}$ and $\nu p \rightarrow \nu p$ can be calculated in the same way. ^(I2) In the IVB theory, present experimental limits give $\lambda < 250$ GeV and $\lambda < 1000$ GeV, respectively, in these examples.

Attempts to calculate the $K^0 - \bar{K}^0$ mass difference, ^(M9) which, unfortunately, involve many assumptions, give $\lambda \approx 4$ GeV with an IVB and $\lambda \approx 3$ GeV in the current-current theory. These estimates of λ would imply that the conventional theory will fail at momentum transfers available at NAL.

1.5. Some Alternative Theories of Weak Interactions

Any theory of weak interactions must obviously reproduce the successful applications of \mathcal{L}_{eff} at low energies. In view of the elegant structure of \mathcal{L}_{eff} , and associated hypotheses, such as current algebra, we would like the current-current interaction to emerge from alternative theories in a natural way. With the exception of the very radical theory of Lee and Wick, either the reduction to \mathcal{L}_{eff} in alternative theories appears artificial/accidental (this is dubbed "conspiracy" by Gell-Mann et al.) ^(G8) or the theories have not been shown to be finite ("evasion"). Nevertheless, it may be useful to review briefly the essential ideas of some of these theories, since they suggest specific forms for the deviations from the predictions of \mathcal{L}_{eff} which should be sought in neutrino reactions. (Reviews of unconventional theories of weak interactions by Shabalin ^(S8) and Segrè ^(S4) have been very useful in preparing this section.)

A. Models with Strongly Interacting IVB's

Several models have been proposed in which W's exist which interact strongly with each other and/or with hadrons. It is conjectured (but not proved) that the strong interactions might somehow provide an effective cut-off (λ) and render the weak interactions finite. Further motivation is provided by the speculation that in such theories $\lambda \sim M_W$, which could explain the value $\lambda \sim 5$ GeV indicated by some calculations of second-order weak effects, and by the feeling that heavy particles should enjoy strong interactions. (An argument sometimes advanced in support

of these theories is that, unless W's have strong interactions, the Born terms in electromagnetic processes such as $e^+ e^- \rightarrow W^+ W^-$ will violate unitarity at center-of-mass energy $\sim M_W/\sqrt{\alpha}$. * This difficulty, like the violations of unitarity by \mathcal{L}_{eff} , may only be apparent, however; the Lagrangian is hermitian so that if the field theory were soluble, the solution would be unitarity.)

Ingenious arguments have been advanced to reconcile the models with existing experimental data. We will not enter into details but simply list the main qualitative implications of the two classes of models:

- (a) Models in which W's interact strongly with each other but not with hadrons ^(F2, M5, O1) typically imply:

$\nu N \rightarrow \mu W + \dots$ in order g_W^2 competing with the lowest order process ($\sim g_W \alpha$) allowed by all models. (There is an extra suppression in one model. ^(M5, O1))

$\nu N \rightarrow \nu N$ in order g_W^3 .

$K_S^0 \rightarrow \mu^+ \mu^-$ in order g_W^3 .

Form factors in $e^+ e^- \rightarrow W^+ W^-$

(CP noninvariance can be neatly incorporated in these models. ^(O1))

For recent speculations based on these models, we refer to an interesting paper by Bjorken and Appelquist. ^(B27)

*In the special case that the anomalous magnetic moment of the W is zero, the energy is M_W/α . ^(T4)

(b) Models in which the W's interact strongly with hadrons. (C5, E5, M5, P13)

It is necessary to require that the strong interactions conserve the number of W's modulo 2 in order to prevent too large a rate for $\nu N \rightarrow \mu + \dots$

These models typically imply:

$$\nu N \rightarrow \mu W + \dots$$

in order g_W . This is probably only compatible with the muon fluxes observed deep underground if $M_W > 10 \text{ GeV}$ (K1, B27).

$$\nu N \rightarrow \nu N$$

in order g_W^2 . In most models the cross section vanishes at zero momentum transfer (C5) so there is no contradiction with experiment.

$$pp \rightarrow WW + \dots$$

strongly. If $M_W \sim 10 \text{ GeV}$, experiments at CERN ISR will certainly confirm or disprove this prediction.

$$\text{Form factors in } e^+e^- \rightarrow W^+W^-.$$

(Some difficulties with these theories are discussed in B27.)

B. The model of Gell-Mann, Goldberger, Kroll and Low (G8)

These authors observe that the propagator $\Delta_{\mu\nu}^{ij}$, which couples the currents J_μ^i and J_ν^j , can be made to behave as $1/k^2$ as $k^2 \rightarrow \infty$, provided $i \neq j$. If, for example, in addition to the usual IVB (mass m_W) a scalar boson (mass m_S) is introduced, which has a derivative coupling with J_μ , then to lowest order:

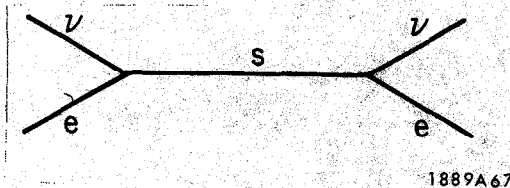
$$\Delta_{\mu\nu}^{ij} = g_W^2 \frac{-g_{\mu\nu} + \frac{k_\mu k_\nu}{M_W^2}}{k^2 - M_W^2} + \frac{g_i^* g_j k_\mu k_\nu}{k^2 - M_S^2} \quad (1.12)$$

The g_i can clearly be chosen so as to eliminate the leading $k_\mu k_\nu$ term as $k^2 \rightarrow \infty$,

provided $i \neq j$. In this theory, the leading divergences occur only in the diagonal interactions ($i = j$), which may be quite unconnected with the off-diagonal ($i \neq j$) interactions, which include all those so far observed (a cure for the diagonal divergences is not given). This reminds us of the great importance of testing the predictions of the V-A theory for processes such as $\nu e \rightarrow \nu e$; in all other cases the predictions for neutrino reactions are the same as in the conventional theory.

C. The Model of Lee and Wick^(L9)

The divergences of the weak interactions could all be removed if the second term in the expression (1.12) for $\Delta_{\mu\nu}^{ij}$ entered with a minus sign. Formally this requires the introduction of negative metric states and at first sight it leads to violations of unitarity, e. g., the amplitude corresponding to the diagram



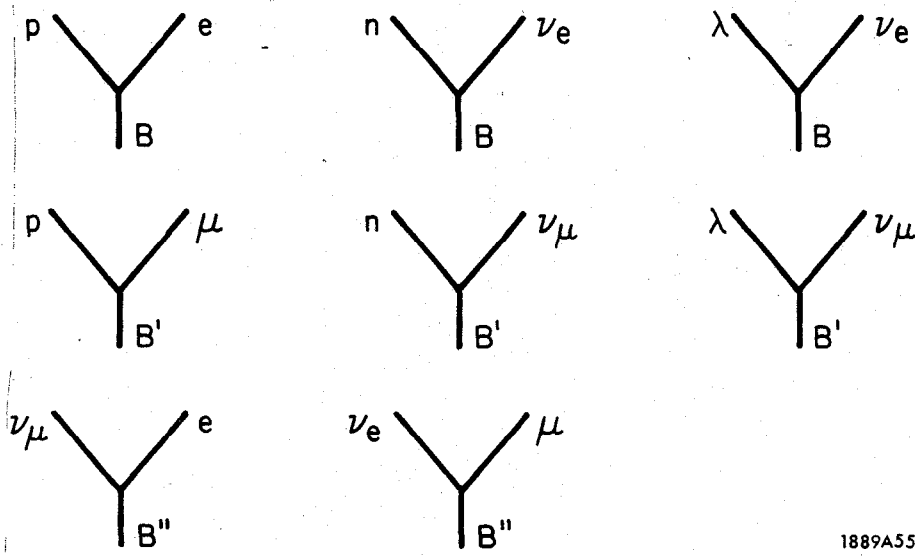
has the opposite sign than in the usual theory--the imaginary part of this amplitude gives the probability of producing s , which is therefore negative. Lee and Wick observed that this does not matter if s is unstable (i. e., has a complex mass), since it cannot be produced in this case. More formally, the S matrix connects stable asymptotic states--provided these have positive metric the S matrix can be unitary, although unstable states have negative metric. The negative metric states cause violations of causality but the times involved are very small in the laboratory and there is no conflict with experience.

The more conservative version of the Lee-Wick theory for weak interactions introduces a negative metric spin zero boson for each positive metric IVB. This theory is renormalizable but it still suffers from the same difficulty as electrodynamics--namely, that it may imply infinite mass differences between hadrons in the same isomultiplet. A completely finite theory can be constructed if two vector bosons of opposite metric and also two scalar bosons of opposite metric are introduced in place of each IVB in the conventional theory. ^(L5)

An interesting feature of this, and other theories involving scalar bosons, is that the heavier boson generally decays electromagnetically to the lighter. ^(L5) If $M_{J=1} > M_{J=0}$, the theory is harder to test, since $W_{J=1} \rightarrow W_{J=0} + \gamma$ and $W_{J=0} \rightarrow$ hadrons, since it does not couple to the lepton current in the approximation that the lepton mass is zero (we will discuss the detection of W's by observing their hadronic decays in Section 3.9B).

D. The Model of Tanikawa and Watanabe ^(T1)

This model describes leptonic and semileptonic interactions in terms of the exchange of scalar/pseudoscalar bosons B and is, therefore, renormalizable. The fundamental vertices are



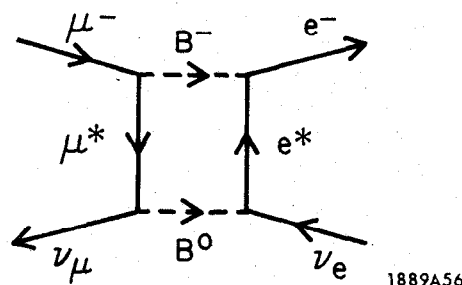
1889A55

where p , n , and λ could be the known particles thus denoted, or a triplet of quarks. At momentum transfers and energies $\ll M_B$, the lowest order diagrams reduce to point-like couplings of scalar and pseudoscalar currents whose relative weight is chosen so that the matrix element can be rewritten in the usual (V-A) current-current form by making a Fierz transformation. With a suitable choice of coupling constants, the model correctly reproduces the observed leptonic and semileptonic decays and does not contradict any experimental results.^(S6) Many observable effects are obviously predicted: a resonance in νp and $\bar{e}p$ scattering,^(K9) parity violation of order G in ep scattering, etc.^(L21) This is a "conspiracy" theory--the way \mathcal{L}_{eff} emerges at low energies is inelegant, CVC is only a low-energy approximation, universality is somewhat accidental, current algebra is irrelevant, etc.

E. The Models of Kummer, Segrè, Shabalin, and Christ

This theory, originally introduced by Kummer and Segrè,^(K13) and later elaborated in different ways by Shabalin^(S7,S9) and Christ,^(C19) (see also G20 and P12), treats the observed weak interactions as fourth-order effects. The theory is renormalizable and can be shown to simulate the conventional theory at low energies by using the Fierz transformation.

μ decay is described in lowest order by the diagram



where μ^* and e^* are postulated heavy leptons and $B^{\pm,0}$ postulated heavy bosons. To describe weak processes involving hadrons, heavy fermions must be introduced.^(S7,C19) The various versions of the theory do not manifestly contradict

experiment, although rather speculative arguments are needed to show this in some cases (P violating effects in nuclear physics tend to come out rather large-- see, however, S9). The most striking feature of these models is the large number of peculiar particles introduced. These models, like that of Tanikawa and Watanabe, remind us once again of the importance of looking for new phenomena in neutrino reactions.

CHAPTER 2

GENERAL PROPERTIES OF NEUTRINO REACTIONS

In this chapter we shall discuss tests of some of the hypotheses about the weak interactions reviewed in Chapter 1. Details will be postponed to Chapter 3 if they require elaborate phenomenological descriptions of particular processes. Some of these tests are summarized in Table 1 (including obvious tests not discussed in the text).

2.1. Tests of the current-current interaction and properties of the lepton current

Consider the process:

$$\nu(k)/\bar{\nu}(k) + A(p) \longrightarrow \ell(k')/\bar{\ell}(k') + B(p') \quad (2.1)$$

where the four momenta are indicated in brackets and B need not be a single-particle state. Assuming $\mathcal{L}_{\text{eff}}(1.1)$, the cross section is proportional to

$$m_{\mu\nu} W^{\mu\nu} \quad (2.2)$$

where*

$$m_{\mu\nu}^{\nu, \bar{\nu}} = \langle k | j_{\mu}^{\pm}(0) | k' \rangle \langle k' | j_{\nu}^{\mp}(0) | k \rangle \quad (2.3)$$

$$W_{\mu\nu}^{\nu, \bar{\nu}} = \frac{1}{2} \langle A | J_{\mu}^{\mp}(0) | B \rangle \langle B | J_{\nu}^{\pm}(0) | A \rangle (2\pi)^3 \delta^4(k+p-k'-p') \quad (2.4)$$

All the results in this section will follow simply from the tensor structure of $W_{\mu\nu}$ and $m_{\mu\nu}$; they are unchanged if an IVB exists, since its propagator may be

*Recall that with our normalization $\langle \ell(k') | j_{\mu}^{-}(0) | \nu(k) \rangle = \bar{u}(k') \gamma_{\mu} (1 - \gamma_5) u(k)$ and $\langle \bar{\ell}(k') | j_{\mu}^{+}(0) | \bar{\nu}(k) \rangle = \bar{v}(k) \gamma_{\mu} (1 - \gamma_5) v(k')$ in the conventional theory. We have introduced the notation J_{μ}^{+}, j_{μ}^{+} for currents which increase the charge of the states on which they act, and $J_{\mu}^{-} = (J_{\mu}^{+})^{\dagger}, j_{\mu}^{-} = (j_{\mu}^{+})^{\dagger}$ for currents which decrease it.

absorbed into the definition of J_μ ($J_\mu \rightarrow \Delta_{\mu\alpha} J_\alpha$). If the dynamical variables which characterize the states B(A) are summed over (averaged), except the momenta p and p' , then quite generally we may write:

$$\begin{aligned} \bar{\sum} \sum W_{\mu\nu} = & -g_{\mu\nu} W_1 + \frac{p_\mu p_\nu}{M^2} W_2 - i \frac{\epsilon_{\mu\nu\alpha\beta} p^\alpha q^\beta}{2M^2} W_3 + \frac{q_\mu q_\nu}{M^2} W_4 \\ & + \frac{(p_\mu q_\nu + p_\nu q_\mu)}{2M^2} W_5 + i \frac{(p_\mu q_\nu - p_\nu q_\mu)}{2M^2} W_6 \end{aligned} \quad (2.5)$$

$$(q = k - k' = p' - p)$$

where M is the mass of the target A and the W_i are real functions of $\nu = q \cdot p$ and q^2 , which depend on the reaction in question.* It follows from the positive

*The W_i are sometimes defined by putting $g_{\mu\nu} \rightarrow g_{\mu\nu} - \frac{q_\mu q_\nu}{q^2}$,

$$p_\mu p_\nu \rightarrow \left(p_\mu - \frac{q_\mu q \cdot p}{q^2} \right) \left(p_\nu - \frac{q_\nu q \cdot p}{q^2} \right), \quad W_i \rightarrow W'_i \text{ in Eq. (2.5).}$$

This has the disadvantage that the W'_i are constrained to satisfy the condition

$$\text{that } \left(W'_i + \frac{\nu^2 W'_2}{q^4} + W'_4 \right) \text{ and } \left(\frac{-\nu W'_2}{q^2} + \frac{W'_5}{2} \right) \text{ be finite as } q^2 \rightarrow 0.$$

semidefinite form of $W_{\mu\nu}$ that* (L14, D7):

$$0 \leq \frac{1}{2M^2} \sqrt{\nu^2 - M^2 q^2} |W_3| \leq W_1 \leq \left(1 - \frac{\nu^2}{M^2 q^2}\right) W_2$$

$$q^2 W_4 + \nu W_5 \leq M^2 W_1 - \frac{\nu^2 W^2}{q^2} \quad (2.6)$$

$$\frac{1}{4} (W_5^2 + W_6^2) \leq \left(q^2 W_4 + \nu W_5 - M^2 W_1 + M^2 W_2 \right) \frac{M^2 W_1}{\nu^2 - M^2 q^2} + W_2 W_4$$

An expansion similar to Eq. (2.5) holds for $\bar{\Sigma} \Sigma m_{\mu\nu}$ in terms of k and q . Hence, whatever the explicit form of the lepton and hadron currents:

$$\bar{\Sigma} \Sigma m_{\mu\nu} \bar{\Sigma} \Sigma W^{\mu\nu} = A + B k \cdot P + C (k \cdot P)^2, \quad (2.7)$$

a quadratic polynomial in the laboratory energy $E_\nu = \frac{k \cdot P}{M}$ whose coefficients A , B and C depend on ν , q^2 , and the reaction in question. (L14, P2) It follows that if the interaction is of the current-current form then $E_\nu^2 \frac{d^2 \sigma}{dq^2 d\nu}$ is a quadratic polynomial in E_ν (cf Eq. 2.10 and 2.11) and therefore only three combinations of structure functions are obtained if the final lepton polarization is not observed. An alternative way to obtain the same result is to note that the current-current form implies that only spin 0 and 1 are exchanged in the t channel. (G14, G15) Hence,

$\bar{\Sigma} \Sigma m_{\mu\nu} \bar{\Sigma} \Sigma W^{\mu\nu}$ is a quadratic polynomial in $\cos \theta t$. Since

$$\cos \theta t \sim (s - u) - \frac{m^2 (M^2 - M_B^2)}{q^2} \quad (2.8)$$

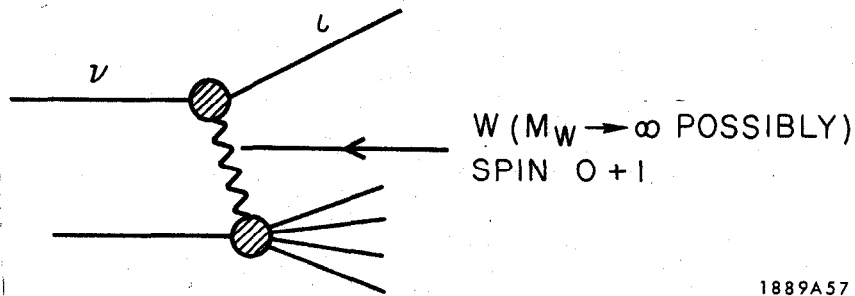
$$s = (k + P)^2 = M^2 + 2 M E_\nu$$

$$u = (k' - P)^2 = M^2 + m^2 + 2 \nu - 2 M E_\nu$$

*To derive this result, note that from its definition the diagonal elements of the matrix $W_{\mu\nu}$ must be positive semidefinite in any frame. A necessary and sufficient condition is that all the subdeterminants of $W_{\mu\nu}$ are positive semidefinite.

this result is equivalent to that already given.

Equation (2.7) and other such theorems discussed below are frequently referred to as consequences of locality. In fact, they depend only on the assumption that the only coupling between the hadrons and the leptons is due to a single (four) vector exchange, viz:



1889A57

The coupling of the currents may be mediated by an IVB and both the lepton and hadron vertices may have a completely non-local structure, but the theorems are still true. Exchange of spins > 1 violates the theorems even if the coupling is local. However, such couplings necessarily involve derivatives and might, therefore, be defined as non-local; with this definition, the theorems are consequences of locality and the assumption that the interaction is due to a single exchange between the leptons and hadrons.

If polarizations are not measured, there is one other relation which follows from the current-current form alone. ^(P6) The orientation of the hadronic system relative to the leptons is described by an azimuthal angle ϕ defined by $\cos \phi = \frac{\vec{n} \cdot \vec{q} \times \vec{K}}{|\vec{q} \times \vec{K}|}$, where \vec{n} is a unit vector parallel to $\vec{k} \times \vec{k}'$ and \vec{K} is some vector constructed from the hadronic variables. Apart from ϕ , the hadronic system can be described entirely in terms of variables which make no reference to the leptons (polarizations being described with respect to hadronic momenta). Under a rigid rotation of the entire hadron system through ϕ' around \vec{q} (taken here to be the z-axis), the leptons

being held fixed:

$$(J_x + iJ_y, J_x - iJ_y, J_z) \rightarrow (e^{i\phi'} [J_x + iJ_y], e^{-i\phi'} [J_x - iJ_y], J_z).$$

The amplitude, therefore, has the ϕ dependence $\alpha + \beta e^{i\phi} + \gamma e^{-i\phi}$ and the differential cross section with the other variables held fixed is given by:

$$\frac{d\sigma}{d\phi} = a + b \cos \phi + c \sin \phi + d \cos 2\phi + e \sin 2\phi \quad (2.9)$$

Summing over all the other variables except for ν and q^2 , the laboratory cross section has the general form^(P7):

$$\begin{aligned} \frac{d^3\sigma}{d|q^2|d\nu d\phi} &= \frac{1}{E_\nu^2} \left(f_1 + f_2 E_\nu + f_3 E_\nu^2 + (f_4 + f_5 E_\nu) \sigma \cos \phi \right. \\ &\quad \left. + (f_6 + f_7 E_\nu) \sin \phi + f_8 \sigma^2 \cos 2\phi + f_9 \sigma^2 \sin 2\phi \right) \\ \sigma^2 &= |\vec{q} \times (\vec{k} + \vec{k}')|^2 \end{aligned} \quad (2.10)$$

$$= -q^2 \left(4E_\nu \left(E_\nu - \frac{\nu}{M} \right) + q^2 \right) + 2m^2 \left(q^2 - \frac{\nu}{M} \right) + m^4$$

$$f_i = f_i(\nu, q^2)$$

At this point it is convenient to introduce the explicit form of the lepton current (1.2). The double differential cross section is then given by:

$$\begin{aligned} \frac{d^2\sigma^{\nu, \bar{\nu}}}{d|q^2|d\nu} &= \frac{G^2}{32\pi M E^2} \bar{\sum} \sum m_{\mu\nu} \bar{\sum} \sum W^{\mu\nu} \\ &= \frac{G^2}{8M^2\pi E^2} \left[2(m^2 - q^2)W_1^{\nu, \bar{\nu}} + (4EE' + q^2 - m^2)W_2^{\nu, \bar{\nu}} - \frac{m^2(q^2 - m^2)}{M^2} W_4^{\nu, \bar{\nu}} \right. \\ &\quad \left. - \frac{2Em^2}{M^2} W_5^{\nu, \bar{\nu}} \pm \frac{W_3^{\nu, \bar{\nu}}}{M^2} (E(q^2 + m^2) + E'(q^2 - m^2)) \right] \end{aligned}$$

$$= \frac{G^2}{2\pi M^2} \frac{E'}{E} \left(\cos^2 \theta/2 W_2^{\nu, \bar{\nu}} + 2 \sin^2 \theta/2 W_1^{\nu, \bar{\nu}} \mp \frac{E+E'}{M} \sin^2 \theta/2 W_3^{\nu, \bar{\nu}} \right) + 0(m^2) \quad (2.11)$$

where θ is the angle between the directions of the initial and final leptons in the laboratory. The final lepton's polarization is given by:

$$P_{\nu, \bar{\nu}}^L = \mp \pm \frac{m^2 \left(2W_1 \cos^2 \frac{\theta}{2} + W_2 \sin^2 \frac{\theta}{2} \mp W_3 \frac{(E-E')}{M} \cos^2 \frac{\theta}{2} + \frac{4E'^2}{M^2} \sin^2 \frac{\theta}{2} W_4 - \frac{2E'}{M} \sin^2 \frac{\theta}{2} W_5 \right)}{2E'^2 \left(2W_1 \sin^2 \frac{\theta}{2} + W_2 \cos^2 \frac{\theta}{2} \mp \frac{(E+E')}{M} \sin^2 \frac{\theta}{2} W_3 \right)} + 0(m^2)$$

$$P_{\nu, \bar{\nu}}^P = \pm \frac{m \sin \theta \left(2W_1 - W_2 + \frac{W_5 E'}{M} \pm \frac{W_3 E}{M} \right)}{2E' \left(\cos^2 \frac{\theta}{2} W_2 + 2 \sin^2 \frac{\theta}{2} W_1 \mp \frac{E+E'}{M} \sin^2 \frac{\theta}{2} W_3 \right)} + 0(m^2) \quad (2.12)$$

$$P_{\nu, \bar{\nu}}^T = - \frac{m}{M} \sin \theta \frac{2W_6}{2W_1 \sin^2 \frac{\theta}{2} + W_2 \cos^2 \frac{\theta}{2} \mp \frac{E+E'}{M} \sin^2 \frac{\theta}{2} W_3} + 0(m^2)$$

where the longitudinal (L), perpendicular (P), and transverse (T) polarization vectors have been chosen so that their space components are orthogonal in the laboratory frame and satisfy

$$\begin{aligned} \vec{S}^L &\propto \vec{k}' \\ \vec{S}^T &\propto \vec{k} \times \vec{k}' \\ \vec{S}^P &\propto \vec{S}^L \times \vec{S}^T \end{aligned} \quad (2.13)$$

It may be that at high energies the factorization of \mathcal{L}_{eff} into leptonic and hadronic parts still obtains but the exchange of other spins plays a role. Generally, if spin J is exchanged the invariant matrix element squared, summed over spins, etc., will be a $2J^{\text{th}}$ order polynomial in $\cos \theta_t$ (2.8). A direct test for scalar and tensor currents is that they cause the helicity of the final lepton

to be opposite to that of the initial neutrino in the approximation $m = 0$; with only vector and/or axial vector currents, the helicity is unchanged if $m = 0$. Cheng and Tung have discussed other tests for the presence of scalar and tensor currents. (C16)

The general theorems discussed here are all violated by electromagnetic effects. It might be feared that with a nuclear target of charge Z , corrections of order $Z\alpha$ could occur. Nachtmann has studied this problem^(N1), and has shown that the corrections to Eq. (2.7) are characterized by $Z\alpha/E'R$, where E' is the energy of the outgoing lepton and R is the nuclear radius. Nachtmann finds corrections $\approx 5\%$ in uranium.

2.2. Tests of properties of the hadron current

A. Selection Rules

$$\Delta Y \leq 1 \text{ and } \Delta Y = \Delta Q$$

The simplest reactions forbidden by these selection rules are listed in Table 2. The branching ratios for the "forbidden" processes depend on the square of the violation parameter (y). Roe has pointed out^(R8) that K^0 production provides a test which is linear in y , since

$$\begin{aligned} \bar{\nu} p \rightarrow \mu^+ \Lambda^0 (K^0 + y \bar{K}^0) & \quad (y = 0 \text{ if } \Delta Y \leq 1 \text{ only}) \\ \nu n \rightarrow \mu^- p (K^0 + y' \bar{K}^0) & \quad (y' = 0 \text{ if } \Delta Y = \Delta Q \text{ only}) \end{aligned}$$

If $y/y' \neq 0$, the observed states K_S and K_L occur in unequal numbers and this can be detected in a suitable apparatus.

$$\Delta I = 1/2 \text{ in } \Delta Y = 1 \text{ transitions}$$

For the reactions involving a single baryon or baryon resonance with $I = 1$ in the final state, this rule gives^(L13):

$$\frac{\sigma(\bar{\nu} n \rightarrow \Sigma^-)}{\sigma(\bar{\nu} p \rightarrow \Sigma^0)} = \frac{\sigma(\bar{\nu} n \rightarrow Y^{*-})}{\sigma(\bar{\nu} p \rightarrow Y^{*0})} = 2. \quad (2.14)$$

In Eq. (2.14) and below, the presence of the appropriate lepton in the final state is understood. In reactions with two stable hadrons in the final state we find:

$$\frac{\sigma(\bar{\nu}n \rightarrow \Sigma^0 \pi^-)}{\sigma(\bar{\nu}n \rightarrow \Sigma^- \pi^0)} = 1$$

$$\frac{\sigma(\bar{\nu}n \rightarrow \Lambda^0 \pi^-)}{\sigma(\bar{\nu}p \rightarrow \Lambda^0 \pi^0)} = \frac{\sigma(\bar{\nu}n \rightarrow \Sigma^- \eta^0)}{\sigma(\bar{\nu}p \rightarrow \Sigma^0 \eta^0)} = 2 \quad (2.15)$$

The $\Delta I = 1/2$ rule also gives a number of "triangular inequalities" for this class of reactions. (L13) The "triangular inequalities" between quantities σ_1 , σ_2 , and σ_3 are defined to be:

$$\sqrt{\sigma_1} + \sqrt{\sigma_2} \geq \sqrt{\sigma_3}$$

$$\sqrt{\sigma_1} + \sqrt{\sigma_3} \geq \sqrt{\sigma_2}$$

$$\sqrt{\sigma_2} + \sqrt{\sigma_3} \geq \sqrt{\sigma_1} \quad (2.16)$$

The triplets $\sigma_{1,2,3}$ for which these inequalities hold are:

σ_1	σ_2	σ_3	
$\sigma(\nu p \rightarrow pK^+)$	$\sigma(\nu n \rightarrow pK^0)$	$\sigma(\nu n \rightarrow nK^+)$	
$\sigma(\bar{\nu}n \rightarrow \Xi^- K^0)$	$\sigma(\bar{\nu}p \rightarrow \Xi^0 K^0)$	$\sigma(\bar{\nu}p \rightarrow \Xi^- K^+)$	
$\sigma(\bar{\nu}n \rightarrow nK^-)$	$\sigma(\bar{\nu}p \rightarrow n\bar{K}^0)$	$\sigma(\bar{\nu}p \rightarrow pK^-)$	(2.17)
$2\sigma(\bar{\nu}n \rightarrow \Sigma^0 \pi^0)$	$\sigma(\bar{\nu}p \rightarrow \Sigma^+ \pi^-)$	$\sigma(\bar{\nu}p \rightarrow \Sigma^- \pi^+)$	
$2\sigma(\bar{\nu}p \rightarrow \Sigma^0 \pi^0)$	$\sigma(\bar{\nu}p \rightarrow \Sigma^+ \pi^-)$	$\sigma(\bar{\nu}p \rightarrow \Sigma^- \pi^+)$	

|\Delta I = 1| for \Delta Y = 0 Transitions

This rule gives

$$\frac{\sigma(\nu p \rightarrow N^{*++})}{\sigma(\nu n \rightarrow N^{*+})} = \frac{\sigma(\bar{\nu} n \rightarrow N^{*-})}{\sigma(\bar{\nu} p \rightarrow N^{*0})} = 3 \quad (2.18)$$

and triangular inequalities (cf. Eq. 2.16) for:

$$\begin{array}{ccc} \frac{\sigma_1}{2\sigma(\nu n \rightarrow p\pi^0)} & \frac{\sigma_2}{\sigma(\nu p \rightarrow p\pi^+)} & \frac{\sigma_3}{\sigma(\nu n \rightarrow n\pi^+)} \\ 2\sigma(\nu n \rightarrow \Sigma^0 K^+) & \sigma(\nu p \rightarrow \Sigma^+ K^+) & \sigma(\nu n \rightarrow \Sigma^+ K^0) \\ 2\sigma(\bar{\nu} p \rightarrow n\pi^0) & \sigma(\bar{\nu} n \rightarrow n\pi^-) & \sigma(\bar{\nu} p \rightarrow p\pi^-) \\ 2\sigma(\bar{\nu} p \rightarrow \Sigma^0 K^0) & \sigma(\bar{\nu} n \rightarrow \Sigma^- K^0) & \sigma(\bar{\nu} p \rightarrow \Sigma^- K^+) \end{array} \quad (2.19)$$

Charge symmetry of the \Delta Y = 0 current

The charge symmetry condition (1.3) relates the form factors in pairs of processes such as $\nu_\mu p \rightarrow \mu^- p \pi^+$ and $\bar{\nu}_\mu n \rightarrow \mu^+ n \pi^-$, for example.

Note that it does not give equal cross sections since the ν and $\bar{\nu}$ currents are different. If the lepton spins are summed over, however, the lepton tensor is unchanged when $\nu \leftrightarrow \bar{\nu}$ except that the V-A interference term changes sign. Therefore, for $\Delta Y = 0$ reactions

$$\sum_{\text{lepton spins}} \left[d\sigma \left(\begin{array}{l} \nu p \rightarrow \mu^- a (I_3 = 3/2) \\ \nu n \rightarrow \mu^+ b (I_3 = 1/2) \end{array} \right) - d\sigma \left(\begin{array}{l} \bar{\nu} n \rightarrow \mu^+ a (I_3 = -3/2) \\ \bar{\nu} p \rightarrow \mu^- b (I_3 = -1/2) \end{array} \right) \right]$$

is proportional to the V-A interference term.

If all final states are summed over, the charge symmetry condition gives:

$$\begin{aligned} W_i^{\nu p} &= W_i^{\bar{\nu} n} \\ W_i^{\bar{\nu} p} &= W_i^{\nu n} \end{aligned} \quad (\Delta Y = 0) \quad (2.20)$$

for the W_i (Eq. 2.5). This gives obvious relations between (e. g.) the cross sections for ν and $\bar{\nu}$ on deuterium. For the quasi-elastic process the charge symmetry condition is:

$$\langle p | J_\lambda^{0+} | n \rangle = - \langle n | J_\lambda^{0-} | p \rangle \quad (2.21)$$

which, combined with the identity $\langle p | J_\lambda^{0+} | n \rangle^* = \langle n | J_\lambda^{0-} | p \rangle$, gives strong restrictions (see Section 3.3).

Absence of second-class currents

This hypothesis is the same as the charge symmetry condition if the $\Delta Y = 0$ semileptonic part of \mathcal{L}_{eff} conserves T, as we saw in Section 1.1D. If T is not conserved, this hypothesis implies phase conditions for form factors--see Section 3.3.

B. CVC and PCAC (Adler's theorem^{A3})

An obvious consequence of CVC is that it reduces the number of independent vector form factors, which are then related to form factors measured in electro-production by the isotriplet current hypothesis. These relations will be extensively exploited in Chapter 3. Here we shall discuss a theorem due to Adler which leads to direct tests of CVC and PCAC.

Consider the case when the lepton continues forward in the direction of the incident neutrino ($\theta = 0$). We shall neglect the lepton's mass so that the lepton and neutrino helicities are the same because of the factor $\gamma_\lambda (1 - \gamma_5)$ in the coupling. The spin is therefore conserved when $\theta = 0$ and j_λ can be written as some linear combination of k_λ and k'_λ . With $\theta = 0$, however, $\vec{k} \propto \vec{k}'$ and k_λ and k'_λ are also proportional in the approximation $k'^2 = k^2 = 0$. We can therefore write

$$j_\lambda \propto q_\lambda = k_\lambda - k'_\lambda \quad (\theta = 0, m = 0), \quad (2.22)$$

unless $q_\lambda = 0$, as it is for elastic scattering in these conditions. Equation (2.22) implies that:

(a) If CVC is correct, then only the axial current contributes when $\theta = 0$.

Parity violating effects should therefore vanish in this configuration.

(b) Assuming CVC, the matrix element is proportional to $q_\lambda A_\lambda$. This then implies $\sigma^\nu(\theta=0) \propto \sigma_\pi$, assuming PCAC. Putting in the correct factors we find (in the notation of Eq. 2.1):

$$\begin{aligned} \frac{M^4 d^2 \sigma_{\bar{\nu}, \nu \rightarrow F}}{d|q^2| dW^2} \Big|_{\theta=0} &= \frac{M^2 G^2 \cos^2 \theta f_\pi^2}{4 \pi^2} \frac{E'}{E} \frac{M^2}{p_\pi W} \sigma_{\pi^\pm \rightarrow F}^{(W)} \left(1 + \frac{q_0 m^2}{2k'_0 (q^2 - M_\pi^2)} \right)^2 \\ &= 4.0 \times 10^{-14} \frac{E'}{E} \frac{M^2}{p_\pi W} \sigma_{\pi^\pm \rightarrow F}^{(W)} \left(1 + \frac{q_0 m^2}{2k'_0 (q^2 - M_\pi^2)} \right)^2 \quad (2.23) \end{aligned}$$

where

$$W^2 = M^2 + q^2 + 2\nu$$

$$q^2 \Big|_{\theta=0} = m^2 - 2EE' + 2E \sqrt{E'^2 - m^2}$$

$\sigma_{\pi^\pm \rightarrow F}^{(W)}$ = pion cross section for the same target and final state F at center-of-mass energy W.

p_π = pion center-of-mass momentum at center-of-mass energy W.

Following Adler, we have assumed that pion scattering is dominated by p waves in extrapolating to zero mass in Eq. (2.23) (the choice of extrapolation procedure is clearly irrelevant at large energies) and we have retained the lepton mass in the pion pole term which might be important. The numerical constant was obtained using the Goldberger-Treiman value of $f_\pi (= \sqrt{2} M g_A / g_{NN\pi} \simeq 0.86 M_\pi)$.

The main problem in comparing Eq. (2.23) with experiment is that there are no events with $\theta \equiv 0$ and rapid variations may occur in this neighborhood due to terms which vanish at $q^2 = 0$. One inelastic reaction for which detailed phenomenological descriptions are available which could be fitted to the data at small q^2 and used to extract $\left. \frac{d\sigma}{dq^2} \right|_{\theta=0}$ is N^* production. However, the success of Eq. (2.23) for N^* production (or single π production) would not necessarily constitute a new test of PCAC. This is because the success of the Goldberger-Treiman relation ensures that Adler's theorem is satisfied for the Born term for single pion production. Therefore in most dynamical models of this process, in which both $\sigma(\nu N)$ and $\sigma(\pi N)$ are proportional to the Born terms enhanced in the same way, Adler's theorem is automatically satisfied.

An important point about the comparison of Eq. (2.23) with experiment is that $q^2 \simeq -4EE' \sin^2 \frac{\theta}{2}$ is generally a more appropriate variable in which to expand than θ (as has been emphasized by Piketty and Stodolsky^(P16)). Therefore, the range of θ for which Eq. (2.23) is a good approximation decreases with increasing EE' . If EE' (and hence q^2) is not known so that Eq. (2.23) can only be compared to experiment for small θ , then the relevant range of θ may be very small since $\left. \frac{d\sigma}{d \cos \theta} \right|_{\theta=0} \sim EE'$. (The actual range of q^2 or θ for which Eq. (2.23) is a good approximation depends on the reaction in question, of course.)

A subtle consequence of Eq. (2.23) is that the forward neutrino cross section should vary with different nuclear targets like the pion cross section^(B7, B8) (this is often called the "A^{2/3}" law--actually $\sigma_\pi \sim A^{0.75}$ at high energies). Such a phenomenon is by now well known in the electromagnetic case.

Experiments have been done to test these predictions. We shall discuss them and give more details of the theory in Section 3.8 after more phenomenological machinery has been assembled. Here we only remark that the Adler-Weisberger relation can be considered a successful test of Adler's relation for an integral over $\sigma^{\bar{\nu}} - \sigma^{\nu}$ if we accept the current algebra hypothesis.

Current Algebra

The only direct tests of the commutators (1.6 - 1.8) are Adler's sum rules^(A5):

$$\int_0^{\infty} W_2^{\bar{\nu}}(\nu, q^2=0) - W_2^{\nu}(\nu, q^2=0) d\nu = 4 M^2 \cos^2 \theta_c \langle I_3 \rangle \quad (\Delta Y=0) \quad (2.24)$$

$$\int_0^{\infty} (W_2^{\bar{\nu}}(\nu, q^2=0) - W_2^{\nu}(\nu, q^2=0)) d\nu = M^2 \sin^2 \theta_c \langle 3Y + 2I_3 \rangle \quad (\Delta Y=1) \quad (2.25)$$

Separating the quasi-elastic contribution and using Adler's PCAC theorem (2.23), Eq. (2.24) immediately reduces to the celebrated Adler-Weisberger relation. This has been frequently discussed and we will not dwell on the derivation.

Adler has derived sum rules which depend on the commutators (1.3 - 1.5) in unintegrated form, e. g:

$$[F_0^k(\vec{x}, 0), F_0^l(0)] = \delta(\vec{x}) i f^{klm} F_0^m(0), \text{ etc.} \quad (2.26)$$

For two reasons we shall only discuss Adler's so-called β sum rule:

- (1) The " α " and " γ " sum rules involve suspect assumptions about high energy behavior which are untrue in free field theories and also in Regge models.
- (2) They rely on commutators involving space components of currents which are model dependent. Some such sum rules will be discussed in Section 3.6.

If $W_{\mu\nu}$ (Eq. 2.4) is averaged over initial spins and summed over final states, it may be written in the form:

$$W_{\mu\nu}^{\bar{\nu}} = \bar{\sum} \int \frac{d^4x}{4\pi} e^{iq \cdot x} \langle p | [J_{\mu}^+(x), J_{\nu}^-(0)] | p \rangle \quad (2.27)$$

(The introduction of a commutator in place of $J_\mu^+(\mathbf{x})J_\nu(0)$ is allowed since the extra term only contributes in the unphysical region where $\mathbf{q} \cdot \mathbf{P} < 0$.) The simplest derivation of the sum rule starts from:

$$\begin{aligned} \int d\mathbf{q}_0 W_{00}^{\bar{\nu}} &= \sum \int \frac{d^3\mathbf{x}}{2} e^{-i\bar{\mathbf{q}} \cdot \bar{\mathbf{x}}} \langle p \left| \left[J_0^+(\bar{\mathbf{x}}, 0), J_0^-(0) \right] \right| p \rangle \\ &= \langle 4I_3 \cos^2 \theta_c + (3Y + 2I_3) \sin^2 \theta_c \rangle P_0 M^2. \end{aligned} \quad (2.28)$$

We then write $d\mathbf{q}_0 = d\nu / \sqrt{\vec{\mathbf{P}}^2 + M^2}$, where $\nu = \mathbf{q} \cdot \mathbf{P}$ and choose a frame where $\vec{\mathbf{q}} \cdot \vec{\mathbf{P}} = 0$; note that the integration is at varying $q^2 = \nu^2 / (\vec{\mathbf{P}}^2 + M^2) - \vec{\mathbf{q}}^2$. Finally Eq. (2.28) is divided by P_0 and the limit $|\vec{\mathbf{P}}| \rightarrow \infty$ is taken. Assuming that the limiting process and the integration can be interchanged and using Eq. (2.5) we get the fixed q^2 sum rule

$$\int_{-\infty}^{+\infty} d\nu W_2^{\bar{\nu}}(\nu, q^2) = \langle 4I_3 \cos^2 \theta_c + (3Y + 2I_3) \sin^2 \theta_c \rangle M^2 \quad (2.29)$$

Using the crossing property:

$$W_i^\nu(\nu, q^2) = -W_i^{\bar{\nu}}(-\nu, q^2) \quad (i \neq 5), \quad (2.30)$$

$$(W_5^\nu(\nu, q^2) = W_5^{\bar{\nu}}(-\nu, q^2)) ,$$

which follows directly from (2.27), Eq. (2.29) may be written in the final form:

$$\int_0^\infty (W_2^{\bar{\nu}}(\nu, q^2) - W_2^\nu(\nu, q^2)) d\nu = \langle 4 \cos^2 \theta_c I_3 + (3Y + 2I_3) \sin^2 \theta_c \rangle M^2 \quad (2.31)$$

This equation reduces to (2.24) and (2.25) at $q^2 = 0$. Using Eq. (2.11), (2.31) may be written in the form:

$$E \lim_{\nu \rightarrow \infty} \left(\frac{d\sigma^{\bar{\nu}P}}{d|q^2|} - \frac{d\sigma^{\nu P}}{d|q^2|} \right) = \frac{G^2}{\pi} \left(\cos^2 \theta_c + 2 \sin^2 \theta_c \right) \quad (2.32)$$

(m = 0)

which suggest a simple interpretation in terms of "point-like" constituents in the nucleon which we shall discuss in Section 3.6.

2.3. T Violation

If time reversal invariance symmetry held then (given the properties of the lepton current under T) it is easy to see that W_6 (Eq. 2.5) would be zero for the quasi-elastic process and for the case when all final states are summed. In the approximation that (2.12) applies (lowest order in G and $\alpha = \frac{e^2}{4\pi} = 0$) $W_6 = 0$ implies that in the laboratory the final lepton has no polarization transverse to the plane in which \vec{k} and \vec{k}' lie. (L11, B15, A2, C2) We shall now derive this result directly. (L25, B5)

If time reversal invariance holds:

$$\begin{aligned} |M(\alpha \rightarrow \beta)|^2 &= \langle \alpha | T^+ | \beta \rangle \langle \beta | T | \alpha \rangle \\ &= |M(\beta' \rightarrow \alpha')|^2 = \langle \beta' | T^+ | \alpha' \rangle \langle \alpha' | T | \beta' \rangle \end{aligned} \quad (2.33)$$

where α' and β' are the time reversal states corresponding to α and β (spins and momenta reversed). If in addition the T matrix satisfies $T_{\alpha\beta} = T_{\alpha\beta}^+ e^{i\delta\alpha\beta}$ (δ real) then:

$$|M(\alpha \rightarrow \beta)|^2 = |M(\alpha' \rightarrow \beta')|^2 \quad (\text{if } T = T^+ e^{i\delta}) \quad (2.34)$$

This forbids transverse lepton or baryon polarization which could only occur because of a term $\sim \vec{s} \cdot (\vec{k} \times \vec{k}')$ which is odd under $\alpha, \beta \rightarrow \alpha', \beta'$.

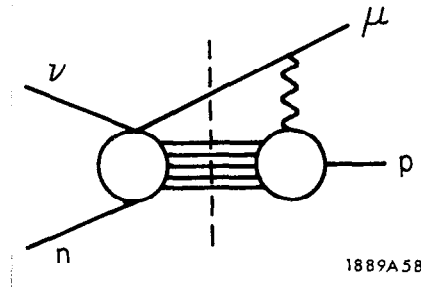
We shall now show that $T = T^+$ in the approximation $\alpha = 0$ both for the quasi-elastic process and for the case when all final states are summed over by using the unitarity relation to order G:

$$T_{\text{weak}} - T_{\text{weak}}^+ = i T_{\text{weak}}^+ (T_{\text{strong}} + \alpha T_{\text{e.m.}}) + i (T_{\text{strong}}^+ + \alpha T_{\text{e.m.}}^+) T_{\text{weak}} \quad (2.35)$$

$$T = T_{\text{strong}} + \alpha T_{\text{e.m.}} + G T_{\text{weak}}$$

For the quasi-elastic process $|\alpha\rangle = |\nu, \text{nucleon}\rangle$ and $|\beta\rangle = |\text{lepton}, \text{nucleon}\rangle$. T_{strong} gives zero acting on these states which are stable under strong interactions. Therefore $T_{\text{weak}}^+ = T_{\text{weak}} + 0(\alpha)$ in this case and the theorem is proved.

Electromagnetic corrections will occur due to the diagram:



The leading correction ($\sim G^2 \alpha$) is due to the interference of this diagram and the usual first-order weak process. This involves the imaginary part of the amplitude in which the intermediate particles are on mass shell (indicated by the dashed line.) These corrections have been bounded in an interesting paper by DeRafael and de Rujula^(D4) which we shall discuss in Section 3.3d.

When a complete set of final states $|\beta\rangle$ is summed over, the states may be taken to be eigenstates of the S matrix for strong interactions. The complete set of intermediate states inserted between T^+ and T in Eq. (2.35) may also be taken to consist of eigenstates of S_{strong} . It follows from Eq. (2.35) that $T_{\text{weak}} = T_{\text{weak}}^+ e^{i\delta} + 0(\alpha)$ in this case and the theorem is proved.

Note that the T violating structure function W_6 is bounded in terms of the others (Eq. 2.6 and 3.77). The inequalities require that $W_6 = 0$ in the deep inelastic region ($\nu \rightarrow \infty$, ν/q^2 fixed) if either $\sigma_s = 0$ (Eq. 3.68) or the weak current is conserved.^(D7) Both these conditions are expected to hold in the deep inelastic region according to currently fashionable theories (See section 3.6).

In other processes, transverse polarizations will only be forbidden by T invariance in the approximation that final state interactions are negligible (for a discussion see C9 and references therein). T invariance gives further restrictions for scattering from polarized targets but these do not seem worth discussing at present.

CHAPTER 3
PHENOMENOLOGICAL DESCRIPTIONS OF NEUTRINO REACTIONS

3.1. Neutrino Beams

We begin this chapter with a brief discussion of some experimental aspects of neutrino physics.* First we shall discuss neutrino beams of the type used at CERN and elsewhere, and then the monoenergetic neutrino beam which will be built at NAL.

At proton accelerators neutrino beams have usually been produced in the way which is schematically illustrated in Fig. 2. Important points to notice are:

1. Incident proton beams produce far more forward-going positive particles than negative particles (typically $\pi^+/\pi^- \sim 5-10/1$). Therefore ν beams (from π^+ and K^+ decay) will be much more intense than $\bar{\nu}$ beams (from π^- and K^- decay)--see, e. g., Fig. 5. Furthermore the contamination of $\bar{\nu}$ beams by ν 's (due to imperfect defocusing) will be much worse than the contamination of ν beams by $\bar{\nu}$'s. (The contamination must be accurately estimated in order to make tests of lepton conservation.)
2. The principal decay modes of π 's and K 's are $\pi \rightarrow \mu + \nu_\mu$ and $K \rightarrow \mu + \nu_\mu$. The beam therefore mainly consists of muon neutrinos. There are some ν_e 's ($\bar{\nu}_e$'s) which come chiefly from the decays $K^\pm \rightarrow \pi^0 e^\pm \nu_e$ ($\bar{\nu}_e$) and $\mu^\pm \rightarrow e^\pm \nu_e$ (ν_e) $\bar{\nu}_\mu$ (ν_μ)--see, e. g., Fig. 6. (It is important to estimate the ν_e ($\bar{\nu}_e$) background in order to test lepton conservation and measure or put limits on $\nu_e - e$ elastic scattering.)

*References to discussions of experimental techniques and developments at various laboratories may be traced from C7, C11, H3, and B36.

3. The energy of neutrinos from $\pi_{\mu 2}$ and $K_{\mu 2}$ decay is given by

$$E_{\nu} = \frac{M_{\pi}^2 - M_{\mu}^2}{2(E_{\pi} - p_{\pi} \cos \theta)} \approx \frac{E_{\pi}}{2} \quad \text{if } \theta = 0, \quad E_{\pi} \gg M_{\pi} \quad (\pi \rightarrow \mu \nu) \quad (3.1)$$

$$E_{\nu} = \frac{M_K^2 - M_{\mu}^2}{2(E_K - p_K \cos \theta)} \approx E_K \quad \text{if } \theta = 0, \quad E_K \gg M_K \quad (K \rightarrow \mu \nu)$$

where E_{ν} is the laboratory energy and θ the angle the neutrino makes with the parent meson's direction. It is therefore clear that the high energy part of the neutrino spectrum comes from K decay.

It may be possible in the future to "tag" the neutrinos in the broad spectrum neutrino beam described above. ^(H2) Otherwise the neutrino energy must be deduced by adding up the energy in the final state and a precise knowledge of the neutrino spectrum is necessary to interpret the results. Measurement of the spectrum usually proceeds in two ways:

1. The primary proton flux is continuously monitored. The flux of secondary pions and kaons is measured in a preliminary experiment (precise knowledge of the K/π ratio is essential since, as we shall see, there is a better way to measure the flux of ν 's from π decay; alternative measurements of the ν flux from K decay are hard to perform). Using the known properties of the focusing system, the hadron flux in the decay tunnel, and hence the neutrino flux, can be calculated.
2. The muon flux from the decays $\pi/K \rightarrow \mu \nu$ is measured thus providing a rather direct measurement of the ν flux. To this end detectors are placed in the shielding, the depth the muon penetrates giving its energy. There are two difficulties:

- (a) Low energy μ 's cannot be detected in this way since they only penetrate to small depths where the hadron flux is still appreciable.
- (b) Only the $\pi \rightarrow \mu\nu$ flux is well determined by this method. This is because the spectra of forward going μ 's from π and K decay are similar (the maximum energy being approximately the energy of the parent in both cases) and the π/K ratio is so large. Because of the larger K mass, the angular distribution of μ 's from K decay is broader than that of μ 's from π decay. It may be possible to exploit this fact to monitor the $K \rightarrow \mu\nu$ spectrum.

As a consequence of these facts the spectrum in the last CERN experiment was only well determined from about 1 - 4 GeV. Outside this range the first method was used ("renormalized" by the second) but it could not be considered very reliable since the K/π ratio was not well known.

It is obviously desirable to devise alternative methods of measuring the K flux. Other possibilities such as detecting γ 's from the decays $K^\pm \rightarrow \pi^\pm \pi^0 \rightarrow \pi^\pm \gamma\gamma$ perpendicular to the beam might be entertained but problems of neutron background probably make this impossible.

In Fig. 3 - 6 we show the broad band neutrino spectra anticipated in various beams of the type described above. A "monoenergetic" neutrino beam will be built at NAL,^(C7) using an idea proposed some years ago^(T3) (related designs were proposed earlier^{P14}). A collimated π/K beam of well defined momentum is introduced into the decay tunnel. The target is designed and positioned to subtend a very small angle θ at the possible decay points. The spectrum is easily calculated using Eq. (3.1) and has the shape illustrated in Fig. 7.

Only a very rough measurement of the final state energy is necessary to distinguish neutrinos from the two energy bands. The flux can be measured by the

method already described. In the proposed beam, which is described in C7 (where details of the design, backgrounds from K_{l3} decays, etc., may be found), the two bands have energy spreads of $\pm 6\%$, and it is calculated that the NAL machine running at 500 GeV can give $\sim 10^7$ ν 's with energy 250 ($\pm 6\%$) GeV/pulse in this apparatus. Even if the gap between the bands turns out to be largely filled in, the results will still be much easier to interpret than those obtained with a conventional beam (however, the number of events will be much less). With the usual broad-band spectrum the flux falls roughly exponentially as a function of energy so that a small error in deducing the neutrino energy from the energy of the final state can lead to a large error in the cross section.

There is one other method of measuring the neutrino flux if we believe the conventional theory of weak interactions. In this case, neglecting the muon mass:

$$\left. \frac{d\sigma}{d|q^2|} \right|_{q^2=0}^{\nu n \rightarrow \mu^- p} = \left. \frac{d\sigma}{d|q^2|} \right|_{q^2=0}^{\bar{\nu} p \rightarrow \mu^+ n} = \frac{G^2 \cos^2 \theta_c}{2\pi} \left(1 + \left| \frac{g_A}{g_V} \right|^2 \right), \quad (3.2)$$

which can be used to deduce the incident flux with hydrogen and, perhaps, deuterium targets. This method is not very reliable with nuclear targets since the cross section is strongly suppressed at small q^2 because of the Pauli principle (see Section 3.3) and this effect turns out to be very model-dependent. At large energies the quasi-elastic cross section is expected to be energy-independent (see Section 3.3) so that it can be used to determine the shape of the spectrum without knowledge of the form factors or the influence of the Pauli principle and the Fermi motion. However, this depends on being able to identify quasi-elastic events which is not easy with nuclear targets (due to reabsorption of produced π 's, etc.)

Despite this, such a method was used in the early spark chamber experiments at CERN, following a suggestion by M. M. Block, and revealed that the flux was

about twice as large as originally thought. Block pointed out that there is a region ($0.1 \text{ GeV}^2 \lesssim Q^2 \lesssim 0.2 \text{ GeV}^2$) where Q^2 is large enough to escape the main effects of the exclusion principle yet small enough so that the result is insensitive to the axial form factor. Quasi-elastic events in this region, therefore, give the absolute flux if they can be identified with a nuclear target.

While on the subject of targets, we might remark that while counter experiments can use enormous targets and may be preferable for examining particular reactions, bubble chambers can more easily reveal possible surprises in high-energy neutrino reactions, such as violations of selection rules (but it may be necessary to employ them in conjunction with other devices to determine all the energy in the final state if a broad spectrum is used). In either case the advantages of using targets containing complex nuclei (better stopping power in bubble chambers as well as higher target mass) must be weighed against the difficulties of interpretation due to nuclear reabsorption and other effects at small q^2 . It would be rash to dwell further on this subject in view of the many studies of experimental techniques now in progress.

3.2. Neutrino Lepton Interactions

The neutrino lepton interactions which are allowed in the usual theory and might be observed directly are

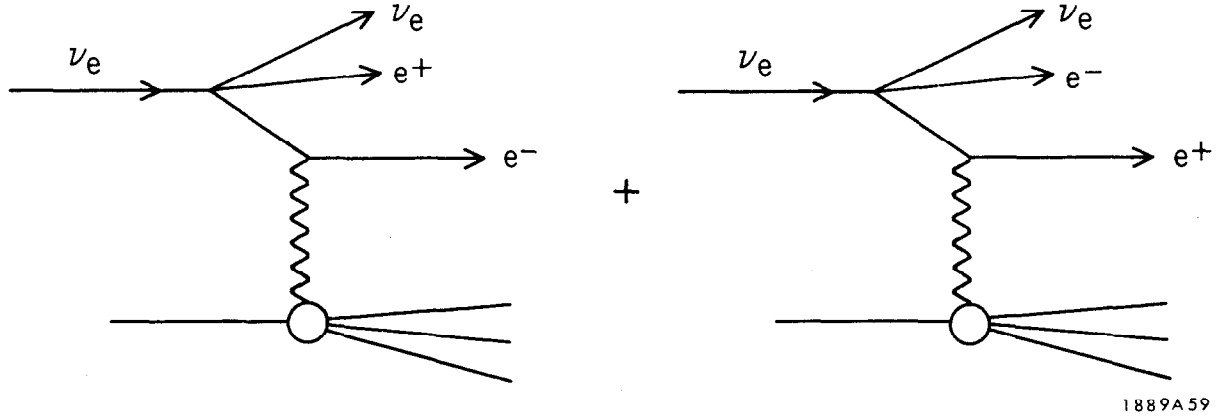
$$\nu_{\mu} + e^{-} \rightarrow \mu^{-} + \nu_e \quad (3.3)$$

$$\nu_e + e^{-} \rightarrow \nu_e + e^{-} \quad (3.4)$$

$$\bar{\nu}_e + e^{-} \rightarrow \bar{\nu}_e + e^{-} \quad (3.5)$$

$$\bar{\nu}_e + e^{-} \rightarrow \bar{\nu}_{\mu} + \mu^{-} \quad (3.6)$$

In addition, leptonic interactions can take place in the electromagnetic field of a target nucleus, e. g.:



A. Interactions with electron targets

The existence of μ decay implies the existence of the processes (3.3) and (3.6). The limits for (3.4) and (3.5) were given on page 19 ; on the basis of the conventional theory, we shall conclude that there is little chance of measuring the cross sections for these processes directly in the near future. However, the conventional theory may be totally misleading at high energies.

An essential point is that even at NAL energies the center-of-mass energy is very low: $s = 2m_e E_\nu < 0.5 \text{ GeV}^2$, $S_{av.} \sim 0.01 \text{ GeV}^2$. Therefore, the cross sections are very small since dimensionally $\sigma \sim G^2 s$ and $G^2 S_{av.} \sim 10^{-39} \text{ cm}^2$. In fact, assuming a 200-GeV proton beam, a target of 70 m^3 of liquid hydrogen (the hypothetical 25' chamber) and a "typical experiment" Nezrick calculated^(N6):

$\nu_\mu e^- \rightarrow \mu^- \nu_e$	215 events
$\nu_e e^- \rightarrow \nu_e e^-$	2.5 events
$\bar{\nu}_e e^- \rightarrow \bar{\nu}_e e^-$	0.8 events
$\bar{\nu}_e e^- \rightarrow \bar{\nu}_\mu \mu^-$	0.02 events

The low rates for $\nu_e / \bar{\nu}_e$ processes are due to the relatively feeble $\nu_e / \bar{\nu}_e$ flux. The reactions (3.4) and (3.5) will be hard to detect positively because of

background problems. For these reasons, we shall only discuss reaction (3.3) in detail here. Cross sections for the other processes are related as $s \rightarrow \infty$ by:

$$\begin{aligned} \lim_{s \rightarrow \infty} \sigma(\nu_{\mu} e^{-} \rightarrow \nu_e \mu^{-}) &= \lim_{s \rightarrow \infty} \sigma(\nu_e e^{-} \rightarrow \nu_e e^{-}) \\ &= 3 \times \lim_{s \rightarrow \infty} \sigma(\bar{\nu}_e e^{-} \rightarrow \bar{\nu}_{\mu} \mu^{-}) = 3 \times \lim_{s \rightarrow \infty} \sigma(\bar{\nu}_e e^{-} \rightarrow \bar{\nu}_{\mu} \mu^{-}) \end{aligned} \quad (3.7)$$

in the usual theory.

Let us examine the extra information which can be obtained by observing the reaction (3.3) which cannot be obtained from μ decay.^(J4) Assuming a point interaction without derivative couplings we may write quite generally:

$$\mathcal{H} = \frac{1}{\sqrt{2}} \bar{\mu} \gamma_{\lambda} (1 - \gamma_5) e \bar{\nu}_{\mu} \gamma_{\lambda} (g_V - g_A \gamma_5) \nu_e + h \cdot c + \mathcal{H}' \quad (3.8)$$

μ decay can be used to eliminate \mathcal{H}' , which contains e and μ in different combinations, but it obviously cannot determine g_A/g_V as long as the neutrinos are not observed.^(J3) (The usual theory has $g_A/g_V = 1$, in which case (3.8) reduces immediately to the usual \mathcal{H}_{eff} by a Fierz transformation provided $\mathcal{H}' = 0$.) Although the limits on \mathcal{H}' are not very good, we shall assume $\mathcal{H}' = 0$. In this case^(J4):

$$\begin{aligned} \frac{d\sigma(\nu_{\mu} e^{-} \rightarrow \nu_e \mu^{-})}{d\cos\theta} &= \frac{(s - m_{\mu}^2)^2}{32\pi s} (|g_V|^2 + |g_A|^2) (A + B - \lambda(A - B)) \\ A &= \left[(s + m_e^2) - (s - m_e^2) \cos\theta \right] \left[(s + m_{\mu}^2) - (s - m_{\mu}^2) \cos\theta \right] \\ B &= 4s^2 \\ \lambda &= + \frac{2 \operatorname{Re}(g_V^* g_A)}{|g_V|^2 + |g_A|^2} \quad (= 1 \text{ in the conventional theory}) \end{aligned} \quad (3.9)$$

where θ is the angle between the incident ν_{μ} and the μ^{-} in the center of mass. The θ distribution clearly determines λ , the most striking λ dependence being

$$\frac{d\sigma(\theta = 0)}{d\sigma(\theta = \pi)} \xrightarrow{s \gg m_e^2} \frac{1}{2} (1 + \lambda) \quad (3.10)$$

a result which can be derived directly from the fact that the μe vertex conserves helicity as $s \rightarrow \infty$. If a few hundred events are obtained at NAL, it will be possible to determine λ approximately.

B. Interactions in the electromagnetic field of a nucleus

The cross sections for these processes can be calculated exactly to order $G^2 \alpha^2$ in terms of known quantities if \mathcal{L}_{eff} is assumed for leptonic interactions (the existence of an IVB would only alter the results by adding terms of order M_μ^2/M_W^2). The dominant process is that in which the nucleus (of charge Ze) recoils coherently. The first detailed calculations were done by Czyz, Sheppey and Walecka^(C28) (approximate results having been obtained previously^(B14,K2,K12,S5)) who found:

$$\sigma(\nu_\mu Z \rightarrow \mu^- e^+ \nu_e Z) \xrightarrow{E \rightarrow \infty} \frac{5Z^2 \alpha^2 G^2}{72 \pi^2} E_\nu \beta \left\{ \ln\left(\frac{2E_\nu}{\beta}\right) + \frac{1}{3} \ln\left(\frac{2E_\nu \beta}{m_\mu^2}\right) - \frac{193}{90} - \frac{\beta^2}{150 m_\mu^2} \right\} \quad (3.11)$$

$$\sigma(\nu_\mu Z \rightarrow \mu^- \mu^+ \nu_\mu Z) \xrightarrow{E \rightarrow \infty} \frac{5Z^2 \alpha^2 G^2}{72 \pi^2} E_\nu \beta \left\{ \frac{4}{3} \ln\left(\frac{2E_\nu \beta}{m_\mu^2}\right) - \frac{332}{45} - \frac{2\beta^2}{75 m_\mu^2} \right\} \quad (3.12)$$

using a nuclear form factor

$$F(q^2) = \frac{1}{(1 - q^2/\beta^2)^2} \quad \beta = \frac{\sqrt{20}}{R_0} = 1.2 A^{1/3} \text{ fm} .$$

Results obtained with an exponential form factor are also given in C28 as are the cross sections for processes with incident ν_e 's (neither choice of form factor gives a good fit to the observed charge distribution--see, e. g., Fig. 3 of L24--the two forms were supposed to bracket the actual behavior as $Q^2 \rightarrow \infty$). The asymptotic formulae (3.11) and (3.12) are compared with the exact cross section in Fig. 8. Cross sections for various nuclei are given in Fig. 9.

In order to distinguish these four fermion events from other processes which yield a muon pair ($\nu_\mu \text{Pb} \rightarrow \mu^- \pi^+ (\rightarrow \mu^+ \nu) + \dots$, $\nu_\mu \text{Pb} \rightarrow \mu^- W^+ (\rightarrow \mu^+ \nu) + \dots$) the distributions in the muon variables must be calculated. This has been done by Fujikawa^(F13) (whose results are quoted in H3) and by Løvseth and Radomski.^(L24) These calculations are of interest in their own right since the results can eventually be confronted with experiment. At present the most important results concern the experimental signature of the four fermion processes.

Unfortunately it is the author's impression that Fujikawa's results disagree with those of Løvseth and Radomski (compare, e. g., Fig. 6 of L24 with Fig. 16 of F13) but it is hard to pin this down since, except in a few cases, they plot different distributions. There is agreement that the μ^- tends to continue in the direction of the ν and take most of its energy. However, in Ref. H3 it is claimed, on the basis of Fujikawa's calculations, that the muons have transverse momentum 0 - 50 MeV (see Table 3). In contrast Løvseth and Radomski find (e. g.) for $\nu_\mu \text{Pb} \rightarrow \nu_\mu \mu^+ \mu^- \text{Pb}$ that $\langle P_{\mu^+}^{t3} \rangle \simeq \langle P_{\mu^-}^{t3} \rangle \simeq 70$ MeV at $E_\nu = 1.5$ GeV increasing to $\langle P_{\mu^+}^{t3} \rangle \simeq 200$ MeV and $\langle P_{\mu^-}^{t3} \rangle \simeq 290$ MeV at $E_\nu = 40$ GeV (their quantity P^{t3} is almost the transverse momentum at small angles). This apparent discrepancy is very serious since the ability to distinguish the four fermion processes from other reactions in the experiment to be performed at NAL^(H3) hinges on the characteristics of the transverse momentum distributions. The authors of this NAL proposal give the estimates in Table 3, on the basis of which they conclude that the four fermion cross sections can be measured to $\pm 10\%$ in 30 - 60 days running time. Løvseth and Radomski using their larger value of the transverse momentum are less optimistic. In view of this apparent disagreement, we do not quote detailed results here. It is comforting that a third independent calculation is under way.^(S11)

3.3. Quasi-elastic Neutrino Scattering ($\Delta Y = 0$)

A. General Remarks

The hadronic current describing the process

$$\nu(k_1) + n(p_1) \longrightarrow \ell^-(k_2) + p(p_2)$$

may be written

$$\begin{aligned} \langle p(p_2) | J_\lambda^+ | n(p_1) \rangle &= \cos \theta_c \bar{u}(p_2) \Gamma_\lambda u(p_1) \\ \Gamma_\lambda &= \gamma_\lambda F_V^1(q^2) + \frac{i \sigma_{\lambda\nu} q^\nu \xi F_V^2(q^2)}{2M} + \frac{q_\lambda F_V^3(q^2)}{M} \\ &\quad + \gamma_\lambda \gamma_5 F_A(q^2) + \frac{q_\lambda \gamma_5 F_p(q^2)}{M} + \frac{\gamma_5 (p_1 + p_2)_\lambda F_A^3(q^2)}{M} \\ &= \gamma_\lambda \left(F_V^1 + \frac{(M_1 + M_2) \xi F_V^2}{2M} \right) + \frac{q_\lambda F_V^3}{M} - \frac{(p_1 + p_2)_\lambda \xi F_V^2}{2M} \\ &\quad + \gamma_\lambda \gamma_5 \left(F_A + \frac{(M_2 - M_1) F_A^3}{M} \right) + i \gamma_5 \frac{\sigma_{\lambda\nu} q^\nu F_A^3}{M} + \frac{q_\lambda \gamma_5 F_p}{M} \\ &\quad \cdot \left(q = k_1 - k_2 = p_1 - p_2, \quad M = \frac{M_1 + M_2}{2} \right) \end{aligned} \tag{3.13}$$

The relation to the form factors used by some other authors is given in the appendix (we keep $M_1 \neq M_2$ for convenience in going to the $\Delta Y \neq 0$ case and introduce $\xi = \mu_p - \mu_n$ so that $F_V^2(0) = 1$ if the isotriplet current hypothesis is correct). Experimental results for β decay at $q^2 \simeq 0$ agree with Eq. (3.15) below within the errors and give $F_A(0) = -1.23 \pm 0.01$.

For the process:

$$\bar{\nu}(k_1) + p(p_1) \longrightarrow \ell^+(k_2) + n(p_2)$$

the current is

$$\langle n(p_2) | J_\lambda^- | p(p_1) \rangle = \cos \theta_c \bar{u}(p_2) \tilde{\Gamma}_\lambda u(p_1) = \langle p(p_1) | J_\lambda^+ | n(p_2) \rangle^* \quad (3.14)$$

$$\tilde{\Gamma}_\lambda(p_1, p_2) = \gamma_0 \Gamma_\lambda^+(p_2, p_1) \gamma_0$$

The various hypotheses about J_λ discussed in Chapter 1 restrict the form factors as follows:

- (1) T invariance \rightarrow All form factors real (apart from an arbitrary overall phase factor which we take to be real henceforth).
- (2) Charge symmetry $\rightarrow F_V^{1,2}$, F_A and F_P real. $F_{V,A}^3$ imaginary.
- (3) No second-class currents $\rightarrow F_{V,A}^3 = 0$ (\equiv T invariance + charge symmetry).
- (4) CVC $\rightarrow F_V^3 = 0$.
- (5) Isotriplet current

$$F_V^1(q^2) = [F_1^p(q^2) - F_1^n(q^2)] = \text{Dirac electromagnetic isovector form factor.} \quad (3.15)$$

$$\xi = \mu_p - \mu_n = 3.71 \quad (\mu = \text{anomalous magnetic moment})$$

$$F_V^2(q^2) = \frac{\mu_p F_2^p(q^2) - \mu_n F_2^n(q^2)}{\mu_p - \mu_n} = \text{Pauli electromagnetic isovector form factor.}$$

In terms of the Sachs form factors

$$F_V^1(q^2) = \left(1 - \frac{q^2}{4M^2}\right)^{-1} \left[G_E^V(q^2) - \frac{q^2}{4M^2} G_M^V(q^2) \right] \quad (3.16)$$

$$\xi F_V^2(q^2) = \left(1 - \frac{q^2}{4M^2}\right)^{-1} \left[G_M^V(q^2) - G_E^V(q^2) \right]$$

Experimentally, the G's are described to within $\pm 10\%$ by:

$$G_E^V(q^2) = \frac{1}{\left(1 - \frac{q^2}{0.71 \text{ GeV}^2}\right)^2} \quad (3.17)$$

$$G_M^V(q^2) = \frac{1 + \mu_p - \mu_n}{\left(1 - \frac{q^2}{0.71 \text{ GeV}^2}\right)^2}$$

Important points to notice about the quasi-elastic process are:

- (1) If polarizations are not measured, only 3 combinations of the 6 complex form factors can be determined according to the general theorems in Section 2.1. We have

$$\frac{d\sigma}{d|q^2|} \left(\begin{array}{c} \nu \text{ n} \rightarrow \ell^- \text{ p} \\ \bar{\nu} \text{ p} \rightarrow \ell^+ \text{ n} \end{array} \right) = \frac{M^2 G^2 \cos^2 \theta_c}{8\pi E_\nu^2} \left[A(q^2) \mp B(q^2) \frac{(s-u)}{M^2} + \frac{C(q^2)(s-u)^2}{M^4} \right] \quad (3.18)$$

$$(s-u = 4ME_\nu - q^2 - m^2)$$

The relation between ν and $\bar{\nu}$ experiments follows from Eq. (2.8) and (2.11). To derive this relation directly^(B6), note that if electromagnetic corrections are neglected $T = T^+$ for these processes (see Chapter 2.3) so that

$$\sum_{\text{spins}} \left| M_{\nu \text{ n} \rightarrow \ell^- \text{ p}} \right|^2 = \sum_{\text{spins}} \left| M_{\ell^- \text{ p} \rightarrow \nu \text{ n}} \right|^2 \quad (3.19)$$

Because of CPT invariance, the spin averaged lepton tensors (2.3) satisfy:

$$m_{\mu\nu}(\ell^-(k_2) \rightarrow \nu(k_1)) = m_{\mu\nu}(\bar{\nu}(k_1) \rightarrow \ell^+(k_2)) \left[= m_{\mu\nu}(\bar{\nu}(-k_1) \rightarrow \ell^+(-k_2)) \right]. \quad (3.20)$$

Hence

$$\begin{array}{c} d\sigma(s, t, u) = d\sigma(u, t, s) \\ \nu \text{ n} \rightarrow \ell^- \text{ p} \quad \bar{\nu} \text{ p} \rightarrow \ell^+ \text{ n} \end{array} \quad (3.21)$$

In terms of the form factors in (3.13) (putting $M_1 = M_2$ now) the functions A, B and C (3.18) are given explicitly by (see, e. g., M4, P4 or A2):

$$\begin{aligned}
A = & \frac{(m^2 - q^2)}{4M^2} \left[\left(4 - \frac{q^2}{M^2}\right) |F_A|^2 - \left(4 + \frac{q^2}{M^2}\right) |F_V^2|^2 - \frac{q^2}{M^2} |\xi F_V^2|^2 \left(1 + \frac{q^2}{4M^2}\right) \right. \\
& - \frac{4q^2 \operatorname{Re} F_V^{1*} \xi F_V^2}{M^2} + \frac{q^2}{M^2} \left(4 - \frac{q^2}{M^2}\right) |F_A^3|^2 \\
& \left. - \frac{m^2}{M^2} \left(|F_V^1|^2 + |F_A + 2F_P|^2 + \left(\frac{q^2}{M^2} - 4\right) \left(|F_V^3|^2 + |F_P|^2 \right) \right) \right] \quad (3.22) \\
B = & + \frac{q^2}{M^2} \operatorname{Re} F_A^* \left(F_V^1 + \xi F_V^2 \right) + \frac{m^2}{M^2} \operatorname{Re} \left[\left(F_V^1 + \frac{q^2}{4M^2} \xi F_V^2 \right)^* F_V^3 - \left(F_A + \frac{q^2 F_P}{2M^2} \right)^* F_A^3 \right] \\
C = & \frac{1}{4} \left(|F_A|^2 + |F_V^1|^2 - \frac{q^2}{M^2} \left| \frac{\xi F_V^2}{2} \right|^2 - \frac{q^2}{M^2} |F_A^3|^2 \right)
\end{aligned}$$

(2) Unless some of the form factors behave very differently from the others, A, B and C (3.18) will be of the same order of magnitude. Since A, B and C presumably fall off rapidly with Q^2 , only C is measured as $s \rightarrow \infty$. To obtain the maximum information neutrinos of ~ 1 GeV are required.

(3) The contributions of the form factors F_P and $F_V^3 \sim m^2 \left(J_\lambda \sim q_\lambda F_P / F_V^3; q_\lambda j^\lambda \sim m \right)$ and are therefore hard to detect unless these form factors are unexpectedly large.

(4) In the approximation $m = 0$ the only contribution of second-class currents $\sim |F_A^3|^2$. The absence of interference terms between the two classes of currents means that it would be hard to detect second-class currents with small form factors.

B. Cross Sections in the Conventional Theory and Theoretical Ideas about the Axial Form Factors

In the conventional theory, in which the hypotheses listed on page 58 are satisfied, there are two unknown form factors in elastic neutrino scattering: F_A and F_P . F_A can be determined rather directly by measuring $d\sigma^\nu - d\sigma^{\bar{\nu}}$ which, because of the assumption of charge symmetry (page 39), depends only on the V-A interference term:

$$\frac{d\sigma^{\nu n \rightarrow \ell^- p}}{d|q^2|} - \frac{d\sigma^{\bar{\nu} p \rightarrow \ell^+ n}}{d|q^2|} = \frac{G^2 \cos^2 \theta_c}{4\pi M^2 E_\nu^2} (s-u) q^2 F_A^* G_M^V \quad (3.23)$$

Up to now extensive $\bar{\nu}$ experiments have not been performed, nor are the ν experiments nearly accurate enough to allow $F_A(q^2)$ and $F_P(q^2)$ to be determined. The usual procedure is to assume the functional form

$$F_A(q^2) = -1.23 / \left(1 - \frac{q^2}{M_A^2}\right)^n \quad (3.24)$$

and to use a model for F_P or neglect its contribution ($\sim m^2$). The results of model calculations with $n = 2$ are shown in Fig. 10 - 13 (cross sections are given in M4 for a wide range of form factors).

Experiments have not even been able to determine the best value of n up to now but $n = 2$ is usually assumed by analogy to the electromagnetic case. This is very unsatisfactory. The remarkable scaling law $G_E(q^2)/G_M(q^2) \simeq \text{const.}$ suggests that G_E and G_M describe the same distribution of "stuff" inside the nucleon and we might therefore be tempted to assume that the axial form factor is similar. In the absence of a dynamical understanding of the scaling law, however, we have no criterion to decide which combination (if any) of the axial form factors should

behave like G_E and G_M (an unusual choice of form factors which has some advantages has been discussed by Ketley).^(K7) On the other hand, the experimental discovery of such a combination might shed light on the scaling law.

There is one piece of evidence in favor of taking $n = 2$ in Eq. (3.24). $F_A(q^2)$ can be calculated in terms of single pion electroproduction data near threshold using PCAC and current algebra. The results of one calculation rule out $n = 1$ and give $M_A = 1.34 \pm 0.05$ GeV with $n = 2$.^(N5) However, other authors (e.g. F15) find different results. The data is probably not good enough to make a reliable determination of F_A by this method at present. (When the processes $ep \rightarrow ep \pi^0$ and $ep \rightarrow en \pi^+$ have been separated it will be possible to check the reliability of the method by using it to calculate a combination of the known form factors G_M and G_E .)

Near $q^2 = 0$ we expect F_P to be dominated by the pion pole:

$$\frac{F_P(q^2)}{M} \simeq \frac{\sqrt{2} g_{NN\pi} f_\pi}{q^2 - M_\pi^2}, \quad (q^2 \simeq 0). \quad (3.25)$$

PCAC gives

$$F_P(q^2) \simeq \frac{2M^2 F_A(0)}{q^2} \left[\frac{1}{1 - q^2/M_\pi^2} - \frac{F_A(q^2)}{F_A(0)} \right], (q^2 \simeq 0) \quad (3.26)$$

which agrees with Eq. (3.25) provided

$$\left| \frac{1}{F_A(0)} \frac{\partial F_A}{\partial q^2} \right|_{q^2=0} \ll \frac{1}{M_\pi^2},$$

which is presumably the case. According to these formulae $F_P(q^2)$ is much larger than $F_A(q^2)$ near $q^2 = 0$ and this is borne out by experiments on μ capture. There is no reason to believe Eq. (3.25) or (3.26) away from $q^2 \simeq 0$. However, if we believed that the axial current would be conserved if M_π were zero, then $F_P(q^2) = (2M^2 F_A(q^2))/(M_\pi^2 - q^2)$ might be a reasonable approximation for all q^2 .

Some authors have normalized $F_p(q^2)$ to $-\sqrt{2} g_{NN\pi} f_\pi/M_\pi^2$ at $q^2 = 0$ and given it the same q^2 dependence as F_V^1 or G_E^V for $q^2 < 0$. This implies an abrupt change of behavior at $q^2 = 0$. With $F_p \propto F_V^1$ (e. g.) it gives

$$\left. \frac{\partial F_p}{\partial Q^2} \right|_{q^2 = -\epsilon} = - \frac{F_p(0)}{0.71 \text{ GeV}^2}$$

while the assumption that the pion pole dominates in $0 < q^2 < M_\pi^2$, which is implicit in this choice of normalization, yields

$$\left. \frac{\partial F_p}{\partial Q^2} \right|_{q^2 = +\epsilon} = - \frac{F_p(0)}{M_\pi^2} .$$

This procedure of normalizing near the pole certainly overestimates F_p for small Q^2 (the contribution of F_p to the cross section from large Q^2 is negligible if F_p falls off like $1/Q^2$ or faster as $Q^2 \rightarrow \infty$).

With this dubious choice of q^2 dependence F_p can make a substantial contribution to the cross section, although it enters multiplied by $\frac{m}{M}$, because $F_p(0) \simeq -90F_A(0)$. Thus with $F_p(q^2) = F_p(0) F_V^1(q^2)$ Yamaguchi found^(Y2) that it contributed $\sim 20\%$ to the cross section for $E_\nu \sim M$, although its contribution was negligible for $E_\nu \gg M$ and $E_\nu \ll M$. We believe that this is like to be a gross exaggeration of the effect of F_p .

We conclude that the contribution of F_p is probably not more than a few percent. In the absence of more compelling theoretical arguments it is probably best to ignore F_p until the experiments are accurate enough to check any model or parameterization adopted for it.

The results expected from a ν or $\bar{\nu}$ experiment at Argonne are shown in Table 4 where the errors expected in the determination of various parameters

are shown. The ν experiment can measure M_A (Eq. 3.24) but it is very insensitive if other parameters are allowed to vary. The $\bar{\nu}$ experiment is able to determine M_A and any large derivations from CVC, although there are many fewer events. However, if a good fit cannot be achieved with CVC, it would perhaps be more natural to keep CVC but abandon the assumption $F_A^3 = 0$.

C. Polarization Measurements

The quasi-elastic cross section when both the final lepton and baryon polarizations are measured has been given by Adler^(A2) for $\Delta Y = 0$ and $\Delta Y = \pm 1$ reactions (see also E2, K7 and P4--the relation between our form factors and those used by these authors is given in the appendix). Here we will make some simplifying assumption and try to pick out the leading terms.

In the approximation $m = 0$ the lepton vertex conserves helicity. Interesting lepton polarization effects are therefore proportional to m and hard to measure. The polarizations may be obtained directly from Eq. (2.12) using

$$\begin{aligned}
W_i &= 2 \delta(2\nu + q^2) \omega_i \\
\omega'_1 = \omega_1 &= |F_A|^2 - \frac{q^2}{4M^2} \left(|F_A|^2 + |F'_v + \xi F_v^2|^2 \right) \\
\omega'_2 = \omega_2 &= |F_A|^2 + |F'_v|^2 - \frac{q^2}{M^2} \left(\left| \frac{\xi F_v^2}{2} \right|^2 + |F_A^3|^2 \right) \\
\omega'_3 = \omega_3 &= 2 \operatorname{Re} F_A^* F'_v \\
\omega'_4 = 4\omega_4 + \omega_2 - 2\omega_5 &= -|F'_v|^2 - |F_A + 2F_P|^2 + \left(4 - \frac{q^2}{M^2} \right) \left(|F_v^3|^2 + |F_P|^2 \right) \\
\omega'_5 = \omega_5 - \omega_2 = \operatorname{Re} & \left\{ 2 \left[\left(F'_v + \frac{q^2 \xi F_v^2}{2M^2} \right)^* F_v^3 - \left(F_A + \frac{q^2 F_P}{2M^2} \right)^* F_A^3 \right] \right. \\
\omega'_6 = \omega_6 = \operatorname{Im} & \left. \right\}
\end{aligned} \tag{3.27}$$

The ω'_i occur naturally if the hadron tensor $W_{\mu\nu}$ is expanded in terms of $p + p'$ and q rather than p and q . They are much more convenient than the ω_i for many purposes in the quasi-elastic case.*

The unpolarized cross section essentially determines $\omega_{1,2,3}$ (dropping terms of order m^2). Polarization effects are, therefore, only of interest insofar as they contain information about $\omega_{4,5,6}$. Note that the contributions of $\omega_{4,5,6}$ vanish as $q^2 \rightarrow 0$ ($\theta \rightarrow 0$). Since most of the events presumably occur at small q^2 , it will therefore be hard to obtain useful information from lepton polarization measurements. The deviation of the longitudinal lepton (antilepton) polarization from -1 (+1) is hardly amenable to measurement being of order m^2 (unless the V-A lepton current gives an incorrect description at high energies). The perpendicular polarization is proportional to $m \sin \theta$ but we note that the extra structure function which it determines (ω_5) enters multiplied by E' and, unfortunately, as θ and Q^2 increase,

* E.g., in terms of the ω'_i the coefficients A, B and C (Eq. 3.18 and 3.22) have the simple form^(P4):

$$4M^2 A = (m^2 - q^2) \left(8M^2 \omega'_1 - (4M^2 - q^2) \omega'_2 + m^2 \omega'_4 \right)$$

$$2M^2 B = -q^2 \omega'_3 \pm m^2 \omega'_5$$

$$4C = \omega'_2$$

Note that $\omega'_i \nu n \rightarrow \mu^- p = \omega'_i \bar{\nu} p \rightarrow \mu^+ n$

$$\omega'_5 \nu n \rightarrow \mu^- p = -\omega'_5 \bar{\nu} p \rightarrow \mu^+ n \quad (i \neq 5)$$

ω'_5 vanishes if there are no second-class currents.

E' decreases. We conclude that longitudinal and perpendicular lepton polarizations are not very useful tools in practice. We will discuss the transverse polarization in the next section.

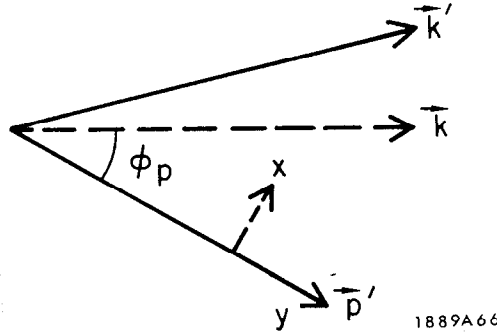
It is hard to measure the baryon polarization unless the apparatus is designed with that purpose in mind. Jovanic and Block^(J6) have considered surrounding a deuterium target with Al spark chambers; the transverse and perpendicular polarizations are measured when the nucleon rescatters from the Al plates. Alternatively this could be achieved by inserting Al plates in a bubble chamber. This might be worth while at NAL energies at which the unpolarized quasi-elastic cross section depends only on $C(q^2)$ in Eq. (3.22) which contains little information on its own. We shall see below that the polarizations depend on quite different combinations of form factors than $C(q^2)$.

Before giving detailed formulae we consider some general properties. When $\theta_{\mu\nu} = \pi \left(Q^2 = Q_{\max}^2 = 4ME^2/(M+2E) + 0(m^2) \right)$ it follows from angular momentum conservation that in the approximation $m = 0$ the final baryon is 100% longitudinally polarized (with negative helicity in the center of mass and laboratory) because the conventional lepton vertex conserves helicity. As $\theta_{\mu\nu} \rightarrow 0 \left(Q^2 \rightarrow 0(m^2) \right)$ angular momentum conservation requires that in the center of mass the transverse and perpendicular polarizations vanish; the longitudinal polarization is, of course, known and is almost 100% (with negative helicity) because $g_A/g_V \approx -1$ (this polarization is completely perpendicular in the laboratory because $\vec{q} = \vec{p}'$ is essentially perpendicular to \vec{k} for infinitesimal Q^2). Interesting polarization effects, therefore, occur at intermediate Q^2 .

In the conventional theory the cross section when the final baryon is perpendicularly polarized may be written^(B32):

$$\begin{aligned}
\frac{d\sigma^{\uparrow x}}{d|q^2|} - \frac{d\sigma^{\downarrow x}}{d|q^2|} &= \frac{G^2 \cos^2 \theta_c \sin \phi_p}{2\pi} \left\{ -2 F_A F'_V - \frac{-q^2}{2M^2} \left[F_A \xi F_V^2 \right. \right. \\
&\quad \left. \left. + \frac{M}{E} F'_V (F'_V + \xi F_V^2 + F_A) \right] + \frac{q^4}{16M^2} \frac{M}{E} \left(\left| \xi F_V^2 \right|^2 + \xi F_V^2 (F'_V + F_A) \right) \right\} \\
\left(\sin \phi_p = \sqrt{\frac{4M^2 E^2 + q^2 (M^2 + 2ME)}{(4M^2 - q^2) E^2}} + 0 \left(\frac{m^2}{E^2} \right) \right)
\end{aligned} \tag{3.28}$$

where \uparrow_x (\downarrow_x) indicates laboratory polarization \parallel (anti \parallel) to x defined by:



Equation (3.28) provides another way to determine F_A . If this were inconsistent with the result obtained from the differential cross section, we would have to turn to the general case with all form factors retained which is given, e. g., in A2 and P4. Here we give only the limit of the polarization as $E \rightarrow \infty$ with Q^2 fixed, which is the interesting part for experiments at NAL:

$$P^X(\text{perp}) = - \sqrt{\frac{4M^2}{4M^2 - q^2}} \frac{\left[2 \operatorname{Re} \left(F_V^1 + \frac{q^2}{4M^2} \xi F_V^2 \right)^* F_A - \frac{q^2}{M^2} \operatorname{Re} \left(F_V^1 + \xi F_V^2 \right)^* F_A^3 \right]}{\left| F_A \right|^2 + \left| F'_V \right|^2 - \frac{q^2}{4M^2} \left| \xi F_V^2 \right|^2 - \frac{q^2}{M^2} \left| F_A^3 \right|^2} + 0 \left(\frac{1}{E} \right). \tag{3.29}$$

Longitudinal polarization cannot be measured by rescattering the baryon. It is therefore inaccessible unless the apparatus is in a magnetic field so that the

direction of the polarization is different at the production point and the point of rescattering. Here we give the leading terms in the general case as $E \rightarrow \infty$, with Q^2 fixed:

$$P^Y(\text{long}) = 2 \sqrt{\frac{-q^2}{4M^2 - q^2}} \frac{\text{Re} \left(2 F'_V + \frac{q^2 \xi F_V^2}{2M^2} \right)^* F_A^3 - \text{Re} \left(F'_V + \xi F_V^2 \right)^* F_A}{|F_A|^2 + |F'_V|^2 - \frac{q^2}{4M^2} |\xi F_V^2|^2 - \frac{q^2}{M^2} |F_A^3|^2} + O\left(\frac{1}{E}\right) \quad (3.30)$$

The polarizations with incident autineutrinos are given, e.g., in (A2) and (P4) (they can be deduced from Eq. (3.42) and (3.43) below in the conventional theory). The general arguments above still apply except that the helicity is now positive when $\theta_{\mu\nu} = \pi$, in the approximation $m = 0$. The results of a model calculation with incident autineutrinos are shown in Fig. 25 and 26.

D. T Violating Effects

In Section 2.3 we discussed the fact that, in the absence of electromagnetic corrections, transverse polarizations (out of the reaction plane) would indicate T violation. The transverse lepton polarization is given by Eq. (3.27) and (2.12). The cross section when the final baryon is polarized along $\vec{S}_{\text{trans}} \sim \vec{k} \times \vec{k}'$ is given by^(A2,P4):

$$\left(\frac{d\sigma(+S_{\text{trans}})}{d|q^2|} - \frac{d\sigma(-S_{\text{trans}})}{d|q^2|} \right)_{\substack{\text{final} \\ \text{baryon} \\ \text{polarized}}} = \frac{G^2 \sqrt{-q^2(4M^2 E^2 + q^2) + q^2(2ME + M^2)}}{8\pi M^3 E^2} \\ \times \text{Im} \left[(4ME + q^2) \left(\left[F'_V + \xi F_V^2 \right]^* \frac{\xi F_V^2}{2} - F_A^* F_A^3 \right) + 2M^2 F_A^* \left(F'_V + \frac{q^2 \xi F_V^2}{4M^2} \right) \right. \\ \left. + q^2 F_A^{3*} \left(F'_V + \xi F_V^2 \right) \right] \quad (3.31)$$

These effects can be estimated^(B15, F12) in the theory of T violation due to Cabibbo^(C2) who introduced second-class currents with form factors comparable to the first-class form factors but 90° out of phase (second-class currents must be introduced if we wish to have T violation without abandoning the charge symmetry condition). Using the limit on F_V^3 from μ capture it turns out that it gives a very small contribution^(B15) and we shall ignore it (unless we abandon CVC, $F_V^3 = 0$ in any case). Results obtained with $F_A^3 = i(\xi F_V^2/2)$ and the conventional dipole fit for the other form factors are shown in Fig. 14c. The baryon polarization is insensitive to F_p . However, the muon polarization is proportional to the divergence of the axial current (W_6 vanishes if $\partial_\mu A_\mu = 0$) and this is sensitive to the choice of F_p . The results in Fig. 14 were obtained using Eq. (3.26). Berman

and Veltman^(B15) obtained much larger results following essentially the same prescription as Yamaguchi which probably greatly exaggerates F_p , as we argued in Section 3.3B.

If substantial transverse polarization is found, sceptics might attribute it to electromagnetic corrections (although we would expect them to be of order α). This loophole has been closed for baryon polarizations of the magnitude given by taking $F_A^3 = i(\xi F_V^2/2)$, however, by De Rafael and de Rujula^(D4) who have bounded the electromagnetic effects which simulate T violation by using the Schwartz inequality to bound the contribution of each half of the diagram on page 46 in terms of known data. The bound is shown in Fig. 14; it is presumably comfortably satisfied since much information is lost in the use of the Schwartz inequality.

E. Nuclear Effects

Up to now all neutrino experiments have used complex nuclei as targets. This complicates the analysis since the nuclear effects turn out to be quite model dependent. Eventually the quasi-elastic form factors will be accurately measured by experiments on hydrogen and deuterium (we return to the nuclear effects in the latter case at the end of this section) and the experiments on nuclei will give interesting information about nuclear structure.

Even to speak of quasi-elastic neutrino scattering on nucleons bound in nuclei is to picture the nucleus as a collection of almost free nucleons and we shall neglect many body terms, off-mass shell effects, etc. The most important nuclear effects are due to

1. The Fermi motion
2. The Pauli principle
3. Rescattering and absorption of recoiling hadrons

The last effect obscures the interpretation because it allows processes such as $\nu N \rightarrow \mu N \pi$ to be mistaken for the quasi-elastic process when the pion is re-absorbed. This effect is discussed in (L23) and (B45). The Fermi motion spreads out the quasi-elastic peak in $q^2 - \nu$ space. We neglect it here referring to (L23, L22, Y5) for discussion and references.

The most important nuclear effect is due to the Pauli principle. In a simple Fermi gas model the quasi-elastic process is only allowed if the momentum of the recoiling proton (neutron) lies outside the Fermi sphere of protons (neutrons) present initially. A simple calculation gives the result that in this model the cross section per neutron is equal to the cross section on a free neutron multiplied by^(G2, B14)

$$1 - N^{-1} D \quad (3.32)$$

where

$$\begin{aligned} D &= Z && \text{for } 2x < u - v \\ &= \frac{1}{2} A \left\{ 1 - \frac{3x}{4} (u^2 + v^2) + \frac{x^3}{3} - \frac{3}{32x} (u^2 - v^2)^2 \right\} && \text{for } u - v < x < u + v \\ &= 0 && \text{for } x > u + v \end{aligned} \quad (3.33)$$

$$x = \frac{|\vec{q}|}{2k_f}, \quad u = \left(\frac{2N}{A}\right)^{1/3}, \quad v = \left(\frac{2Z}{A}\right)^{1/3}$$

(N, Z, A) = (neutron, proton, nucleon) number

k_F is the Fermi momentum and $|\vec{q}| = \sqrt{(q^2 + m^2)/4M^2 - q^2}$ is the three-momentum transfer to a stationary target neutron (the same formula holds for the process $\bar{\nu}p \rightarrow \mu^+n$ with $N \leftrightarrow Z$). The function $1 - N^{-1}D$ is plotted in Fig. 15 and 16 for two cases.

We have recently carried out extensive calculations using shell model wave functions and the kinematics which would obtain if the target were a single stationary

nucleon^(B11) (this paper contains many references to previous work on this subject and on the related problem of μ capture). In this approach spin is important and it is necessary to distinguish three exclusion factors:

$$D_{S,T,L} = - \left(\psi \left| \sum_{n \neq m} e^{i\vec{q} \cdot (\vec{x}_n - \vec{x}_m)} \tau_n^- \tau_m^+ (1, \sigma_{xn} \sigma_{xm}, \sigma_{zn} \sigma_{zm}) \right| \psi \right) \quad (3.34)$$

where \vec{x}_n are the coordinates of the nucleons, σ_{xn} the x component of the spin operator for the nth nucleon, τ_n^\pm the isospin raising (lowering) operators, ψ the ground state wave function and \vec{q} is taken to be along the z axis. The cross section per neutron in the conventional theory in the approximation $m = 0$ is given by

$$\frac{d\sigma}{d\Omega} = \frac{1}{64\pi^2 M^2} \left(\frac{E'}{E} \right)^2 \left(|\alpha|^2 (1 - N^{-1} D_S) + (|\beta_x|^2 + |\beta_y|^2) (1 - N^{-1} D_T) \right) \quad (3.35)$$

$$|\alpha|^2 = 8 G^2 \cos^2 \theta_c \left(\frac{(E + E')^2}{1 - q^2/4} + q^2 \right) \left| F_V' + q \frac{F_V^2}{4 M^2} \right|^2$$

$$|\beta_x|^2 + |\beta_y|^2 = 8 G^2 \cos^2 \theta_c \left(\left[\frac{(E + E')^2}{1 - q^2/4} - q^2 \right] \left[\frac{-q^2}{4} |F_V' + \xi F_V^2|^2 + |F_A|^2 (1 - q^2/4) \right] + 2 \left(F_V' + \xi F_V^2 \right) F_A q^2 (E + E') \right)$$

The exclusion factors $D_{S,T,L}$ obtained using harmonic oscillator wave functions are plotted in Fig. 15 and 16 for two cases.

The main differences between the shell model and the Fermi gas model are:

1. Spin effects are important in the shell model near $q^2 = 0$, as evidenced by the fact that $D_S \neq D_T \neq D_L$ and $d\sigma/dq^2 \Big|_{q^2=0} \neq 0$ for symmetric ($N=Z$) nuclei except in the case of closed shells. These effects are

very sensitive to configuration-mixing and are probably greatly exaggerated in Fig. 15 and 16 where only the simplest configurations were used. However, for $Q^2 \gtrsim 0.02 \text{ GeV}^2$ the three shell model exclusion factors are approximately equal and the choice of wave function is presumably not very important.

2. The shell model is much more dilute than the Fermi gas model (which is based on central, and not average, nuclear densities) and the exclusion effect is therefore less.

In the absence of detailed electromagnetic experiments on the quasi-elastic peak in nuclei we have no real reason to prefer one particular model and it is distressing that the models discussed here differ by $\sim 20\%$ for $Q^2 \sim 0.05 - .1 \text{ GeV}^2$. We recommend trying both models and assigning errors to cover the difference.

Equations (3.34) and (3.35) can be applied to a deuterium target. A simple calculation gives

$$\left. \frac{\left(\frac{d\sigma}{dq^2}\right)_{\nu d}}{\left(\frac{d\sigma}{dq^2}\right)_{\nu n}} \right|_{q^2=0} = \frac{\frac{2}{3} \left(\frac{g_A}{g_V}\right)^2}{1 + \left(\frac{g_A}{g_V}\right)^2} = 0.39 \quad (3.36)$$

independent of the choice of space wave function (at $\vec{q}=0$ the vector current does not contribute since it does nothing but turn a neutron \longleftrightarrow proton leading to a state which is forbidden by the Pauli principle; the axial current flips the spin in addition but its contribution is reduced since some states are forbidden). Block^(B33) has calculated the exclusion factors in the closure approximation using a Hulthen wave function; he found that to $\sim \pm 1\%$ the deuterium/neutron cross section ratio is not sensitive to E_ν or to the choice of form factors. The ratio is shown in Fig. 17. Corrections to the closure approximation have not been studied.

The problem of neutrino scattering on deuterium (and nuclei) has recently been studied by Belavin and Gurvits^(B4) who suggest that in certain configurations $(\sigma(\nu d)/\sigma(\nu n))$ should be equal to $(\sigma(\pi^+ d \rightarrow p p \pi^0)/\sigma(\pi^+ n \rightarrow p \pi^0))$ to a good approximation. However, they do not take account of the vital spin effects which are different in the ν and π cases.

F. Experimental Results

Information about the quasi-elastic process has been obtained in both the bubble chamber^(B45) and the spark chamber experiments^(H5) at CERN and in a spark chamber experiment at ANL.^(K15)

In the latter experiment obvious multiparticle events were eliminated but otherwise inelastic events could not be distinguished. After imposing various cuts to reduce the remaining inelastic background, it was allowed for by making a 10% overall subtraction (estimated assuming N^* dominance and using the model of Berman and Veltman).^{*}(B16) The results are shown in Fig. 18 and 19; the theoretical curve for free neutrons was obtained using CVC, $F_{V,A}^3 = F_p = 0$ and a dipole fit for F_A with $M_A^2 = 0.71 \text{ GeV}^2$. The experiment is notable for the conspicuous absence of the exclusion effect which is especially surprising in view of its established effect in μ capture; this might be attributed to an incorrect allowance for inelastic events.

*The Berman-Veltman cross section agrees approximately with the available data but this may be fortuitous since they overestimated the vector couplings by a factor $\sqrt{3/2}$ due to a misinterpretation of a previous paper. With the correct vector couplings, their cross section is unchanged at $Q^2 = 0$ but reduced at large Q^2 .

The CERN spark chamber group analyzed the events initiated in the Al plates in essentially the same way. A dipole form was used for F_A and $M_A = 0.65^{+0.45}_{-0.40}$ GeV was obtained from fitting the q^2 distribution of events with $E_\nu > 1.4$ GeV which is shown in Fig. 20 (this method is insensitive to the spectrum since $\sigma(E_\nu)$ --Fig. 10--is approximately constant at this energy) and the angular distribution of all events.

In the CERN bubble chamber experiment it was easier to isolate the quasi-elastic process, background being estimated using Monte Carlo programs. Again CVC was used with $F_p = F_{V,A}^3 = 0$ and a dipole form adopted for F_A . $M_A = 0.7 \pm 0.2$ GeV was obtained by fitting both $\sigma_\nu(E_\nu)$ --Fig. 21--and the differential cross section (using a Fermi gas model)--Fig. 22. Exactly the same result was also obtained by taking the cross section for events with $Q^2 > 0.3 \text{ GeV}^2$ where nuclear effects should be unimportant; in this case $E_\nu \gtrsim 1$ GeV and the shape of the spectrum is not important.

3.4. Quasi-elastic Neutrino Scattering ($\Delta Y = \pm 1$)

The most general forms of the currents in the processes $\nu(\bar{\nu}) N \rightarrow \ell^-(\ell^+) Y$ are the same as in the $\Delta Y = 0$ reactions [Eqs. (3.13) and (3.14)] except that $\cos \theta_c \rightarrow \sin \theta_c$. T invariance again implies that all the form factors are relatively real. Unless the conventional theory fails badly at high energies it will be a long time before accurate measurements of $\Delta Y = 1$ cross sections are available and we shall therefore work in the approximation $m = 0$ in this section (the general case is given, e. g., in A2, P4). In this approximation the differential cross section

is given by:

$$\frac{d\sigma^{\nu, \bar{\nu}}}{d|q|^2} = \frac{G^2 \sin^2 \theta}{32 M^2 \pi E^2} \left(-8 M^2 q^2 \omega_1'' - 4(M^2 \nu^2 - q^2) \omega_2'' \pm 2(s-u) q^2 \omega_3'' + (s-u)^2 \omega_2'' \right) \quad (3.37)$$

where

$$\begin{aligned} \nu &= q \cdot P = M_1 (E - E'), \quad M_2^2 = M_1^2 + 2\nu + q^2 \\ \omega_1'' &= \frac{(M_-^2 - q^2)}{4M^2} \left| F'_V + \xi F_V^2 \right|^2 + \frac{(M_+^2 - q^2)}{4M^2} \left| F_A \right|^2 \\ \omega_2'' &= \left| F_A + \frac{M_-}{M} F_A^3 \right|^2 + \left| F'_V + \xi F_V^2 - \frac{M_+ \xi F_V^2}{2M} \right|^2 - \frac{q^2}{M^2} \left| \frac{\xi F_V^2}{2} \right|^2 - \frac{q^2}{M^2} \left| F_A^3 \right|^2 \\ \omega_3'' &= 2 \operatorname{Re} F_A^* (F'_V + \xi F_V^2) \\ M_{\pm} &= \sqrt{M_1^2 + 2\nu + q^2} \pm M_1 = M_2 \pm M_1 \end{aligned} \quad (3.38)$$

According to the $\Delta Y = \Delta Q = \pm 1$ selection rule, the only reactions of this type on neutron or proton targets are:



The $\Delta I = 1/2$ rule gives:

$$d\sigma(\Sigma^0) = 1/2 d\sigma(\Sigma^-) \quad (3.40)$$

In the Cabibbo scheme in the limit of exact SU(3) symmetry^(C4, B31, S10):

$$\begin{aligned}
\langle p | J_\lambda^+ | n \rangle &= \cos \theta \bar{u} \left(\gamma_\mu (F_p^1 - F_n^1) + \frac{i \sigma_{\lambda\nu} q^\nu}{2 M_p} (\mu_p F_p^2 - \mu_n F_n^2) \right. \\
&\quad \left. + \gamma_\lambda \gamma_5 F_A + q_\lambda \gamma_5 \frac{F_p^2}{M_p} \right) u \\
\langle p | J_\lambda^+ | \lambda \rangle &= -\sqrt{\frac{3}{2}} \sin \theta \bar{u} \left(\gamma_\lambda F_p^1 + \frac{i \sigma_{\lambda\nu} q^\nu}{M_p + M_\lambda} \mu_p F_p^2 \right. \\
&\quad \left. + \frac{(1 + 2x(q^2))}{3} \left[\gamma_\lambda \gamma_5 F_A + \frac{2 q_\lambda \gamma_5 F_p^2}{M_p + M_\lambda} \right] \right) u \\
\langle n | J_\lambda^+ | \Sigma^- \rangle &= \frac{\sin \theta}{\sqrt{2}} \bar{u} \left(\gamma_\lambda (F_p^1 + 2 F_n^1) + \frac{i \sigma_{\lambda\nu} q^\nu}{M_n + M_\Sigma} (\mu_p F_p^2 + \mu_n F_n^2) \right. \\
&\quad \left. - (1 - 2x(q^2)) \left[\gamma_\lambda \gamma_5 F_A + \frac{2 q_\lambda \gamma_5 F_p^2}{M_n + M_\Sigma} \right] \right) u \tag{3.41}
\end{aligned}$$

where F_p and F_n are the corresponding electromagnetic proton and neutron form factors and x measures the ratio of f/d couplings for the axial current. In principle x need not be the same for F_A and F_p but since we are working in the approximation $m = 0$ here F_p does not contribute anyway.

Of course, we do not know how to take account of SU(3) breaking. Perhaps the simplest assumption, which seems as reasonable as any, is to keep $F_{V,A}^3 = 0$ and use Eq. (3.41) with the physical masses and the constant value of x given by decay processes (a prescription anticipated in labelling the masses in (3.41), although they are of course equal in the limit in which (3.41) applies). The total

cross section obtained with a prescription which is approximately the same in the case $M = 0.89$ GeV is shown in Fig. 23 and 24. Marshak et al.^(M4) used dispersion relations to make monopole models of the form factors; they give curves for $\sigma(E_\nu)$ and $d\sigma/dq^2$ obtained in this and several other ways.

Although high statistics experiments for the processes under discussion are remote, the prospects for measuring the final hyperon polarization are good since it is analyzed by the decay $\rightarrow N\pi$ (of course Σ^0 decays to $\Lambda\gamma$ very rapidly which will make it hard to observe the Σ^0 production process at all; with nuclear targets it is also hard to observe Σ^- production since $\Sigma^- \xrightarrow{\text{charge exchange}} \Sigma^0 \rightarrow \Lambda\gamma$, which will obscure observation of Λ production). The general arguments in Section 3.2C still apply: in the approximation $m = 0$, the hyperon is 100% longitudinally polarized with positive helicity when $\theta_{\mu\nu} = \pi$ and longitudinally (perpendicularly) polarized in the center of mass (laboratory) with a value depending essentially on g_A/g_V when $\theta_{\mu\nu} = 0$. The final hyperon polarization in the approximation adopted above ($F_{V,A}^3 = 0$, all other form factors relatively real, $m = 0$) can be obtained from^(P4)

$$\frac{d\sigma^{\bar{\nu}}(s')}{d|q^2|} = \frac{1}{2} \frac{d\sigma}{d|q^2|} \Big|_{\text{av}} - \frac{G^2}{32\pi M_1^2 E^2} \left[b_1 (s' \cdot P) + b_2 (s' \cdot n) - i b_3 \epsilon_{\mu\nu\alpha\beta} s'^{\mu} P^{\nu} q^{\alpha} n^{\beta} \right] \quad (3.42)$$

where s'_{μ} is the hyperon polarization, which satisfies $s'^2 = -1$, $s' \cdot p' = 0$, and

$$P = p + p'$$

$$n = k + k'$$

$$\begin{aligned}
b_1 = \text{Re} & \left[(s-u)^2 \frac{\xi_{F_V}^2 F_A}{M_1+M_2} + (s-u) \left\{ (M_1+M_2) |F_A|^2 \right. \right. \\
& + (M_1-M_2) |F_V^1|^2 + (M_1^2+q^2-M_2^2) \frac{\xi_{F_V}^2 F_V^1}{M_1+M_2} \left. \left. \right\} \right. \\
& \left. + 2M_1 (M_2^2-q^2-M_1^2) F_A^* F_V^1 + (M_1-M_2) \left((M_1+M_2)^2 - q^2 \right) \frac{F_A^* \xi_{F_V}^2}{M+M'} \right] \\
b_2 = \text{Re} & \left[(s-u) F_A^* \left(2M_1 F_V^1 - \left((M_1+M_2)^2 - q^2 \right) \frac{\xi_{F_V}^2}{M_1+M_2} \right) \right. \\
& + (M_1+M_2) \left[(M_2-M_1)^2 - q^2 \right] |F_V^1|^2 + (M_2-M_1) \left[(M_2+M_1)^2 - q^2 \right] |F_A|^2 \\
& \left. + \left[(M_2^2-M_1^2)^2 - q^2 (2M_2^2+2M_1^2-q^2) \right] \frac{F_V^1 \xi_{F_V}^2}{M_1+M_2} \right] \tag{3.43}
\end{aligned}$$

$$b_3 = 0$$

The general form of the b_i is given, for example, by Pais^(P4) who also gives a convenient set of polarization vectors s'_μ whose space components are orthogonal in the laboratory. Using these (with the directions defined by the figure on Page 67 and $\vec{s}'_{\text{trans}} \propto \vec{k} \times \vec{k}'$) we obtain the high-energy limit of the polarized cross sections in the general case in the approximation $m^2 = 0$:

$$\begin{aligned}
\frac{d\sigma^{\uparrow y}}{d|q^2|} - \frac{d\sigma^{\downarrow y}}{d|q^2|} &\xrightarrow{E \rightarrow \infty} \frac{G^2 \sin^2 \theta_c}{\pi \sqrt{q^4 - 2q^2(M_1^2 + M_2^2) + (M_1^2 - M_2^2)^2}} \\
&\times \operatorname{Re} \left\{ 2(-q^2 + (M_1 - M_2)^2) \left[F_v^1 + \frac{q^2 \xi F_v^2}{(M_1 + M_2)^2} \right]^* F_A^3 \right. \\
&\left. - \left[(-q^2 + M_1^2 - M_2^2) F_v^1 - \frac{2q^2 M_2 \xi F_v^2}{M_1 + M_2} \right]^* F_A \right\} \quad (3.44)
\end{aligned}$$

$$\begin{aligned}
\frac{d\sigma^{\uparrow x}}{d|q^2|} - \frac{d\sigma^{\downarrow x}}{d|q^2|} &\xrightarrow{E \rightarrow \infty} -\frac{G^2 \sin^2 \theta_c}{\pi} \sqrt{\frac{-q^2}{q^4 - 2q^2(M_1^2 + M_2^2) + (M_1^2 - M_2^2)^2}} \\
&\times \operatorname{Re} \left\{ \left[2M_2 F_v^1 + (M_2^2 - M_1^2 + q^2) \frac{\xi F_v^2}{M_1 + M_2} \right]^* F_A \right. \\
&\left. + \frac{2((M_1 - M_2)^2 - q^2)}{M_1 + M_2} (F_v^1 + \xi F_v^2)^* F_A^3 \right\} \quad (3.45)
\end{aligned}$$

$$\begin{aligned}
\frac{d\sigma(+s'_{\text{trans}})}{d|q^2|} - \frac{d\sigma(-s'_{\text{trans}})}{d|q^2|} &\xrightarrow{E \rightarrow \infty} \frac{G^2 \sin^2 \theta_c \sqrt{-q^2}}{\pi(M_1 + M_2)} \\
&\times \operatorname{Im} \left\{ (F_v^1 + \xi F_v^2)^* \xi F_v^2 - 2F_A^* F_A^3 \right\} \quad (3.46)
\end{aligned}$$

This high-energy limit is the most amenable part experimentally. With F_A , F_v^1 and F_v^2 approximately determined from the unpolarized cross section, the longitudinal and perpendicular polarizations provide a sensitive test for the

"second class" form factor F_A^3 . Transverse polarization is again indicative of T violation in the approximation $\alpha = 0$.

Marshak et al., ^(M4) have computed the total polarization using various models; some of their results are shown in Fig. 25 and 26.

3.5. N*(1238) Production

A. General Remarks

The literature on N*(1238) production may be divided into three classes of papers based on:

1. Dynamical calculations using dispersion relations
2. Isobar models
3. Higher symmetries and quark models

In the subsequent sections we shall outline the main features of these models and compare them with each other and with the data. Here we discuss a few general properties. We cannot even hope to discuss the kinematics fully (a detailed discussion takes 26 pages of Adler's monumental 122-page paper, ^(A6) to which we refer), let alone do justice to all the published papers.

The assumed isovector property of J_λ gives

$$\frac{\sigma(\nu p \rightarrow \mu^- N^{*++})}{\sigma(\nu n \rightarrow \mu^- N^{*+})} = \frac{\sigma(\bar{\nu} n \rightarrow \mu^+ N^{*-})}{\sigma(\bar{\nu} p \rightarrow \mu^+ N^{*0})} = 3 \quad (3.47)$$

For the experimentally observed process of $N\pi$ production the $\Delta I = 1$ rule gives the triangular inequalities (Eq. 2.19) which imply:

$$\frac{\sigma(\nu p \rightarrow \mu^- p \pi^+)}{\sigma(\nu n \rightarrow \mu^- p \pi^0) + \sigma(\nu n \rightarrow \mu^- n \pi^+)} \leq 3$$

$$\frac{\sigma(\bar{\nu} n \rightarrow \mu^+ n \pi^-)}{\sigma(\bar{\nu} p \rightarrow \mu^+ n \pi^0) + \sigma(\bar{\nu} p \rightarrow \mu^+ p \pi^-)} \leq 3 \quad (3.48)$$

the upper limits being reached when the ratio of the $I=1/2$ to $I=3/2$ amplitudes is zero.

Another subject which can be discussed in a model-independent way is the density matrix of the N^* ; Berman and Veltman^(B16) have given its general form. (For a rather general discussion of the density matrix in this and other processes, see F8.) They have also given the general form of the angular distribution of the produced pion assuming that the resonant ($J=3/2$) partial wave dominates (see Adler for the complete case). In this approximation the T matrix satisfies $T = T^\dagger e^{i\delta}$ (δ real) and time reversal invariance therefore implies (see Section 2.3) that the parity violating triple product $\left[\vec{q}_\pi \cdot (\vec{k} \times \vec{k}') \right]_{N^* \text{ c. of m.}}$ is absent in the decay angular distribution which is, therefore, symmetric in Adler's angle δ (his Fig. 2) or equivalently in the angle ϕ defined in Fig. 27. This symmetry is violated by interference with other (nonresonant) partial waves which are out of phase; near resonance, the phase difference is $\sim 90^\circ$ and Adler finds^(A6) that an appreciable asymmetry may occur in his model (for a more general discussion of such apparent T-violating effects, see C9).

Using the angles defined in Fig. 31, Berman and Veltman found that the angular distribution of the final pion in the N^* rest frame when $\alpha \rightarrow 0$ is given by

$$D(\theta, \phi) = 1 + 3 \cos^2 \theta + 0 \left(\frac{E - E'}{M} \sin \alpha/2 \right) + 0 \left(\frac{M' - M}{M} \sin \alpha/2 \right) \quad (3.49)$$

This result follows immediately from CVC and Adler's theorem (Eq. 2.21):

$j_\lambda(\alpha=0) \propto q_\lambda$ in the approximation $m = 0$. Kinematically, therefore, when $\alpha = 0$ the process is equivalent to pseudoscalar + nucleon $\rightarrow N^* \rightarrow N + \pi$ which is a p wave process with the form (3.49) (note that this is independent of PCAC). The range of α for which (3.49) is a good approximation and the range of validity of Adler's theorem are, therefore, related questions. As discussed on page 42,

q^2 ($\approx -4 E^2 \sin^2 \alpha/2$ in this case) is probably a better variable than α in which to expand and Eq. (3.49) may only apply for very small values of α at large energies. We return to this question in the case of one particular model at the end of Section 3.5C.

B. Dynamical Calculations

The first calculations of N^* production by neutrinos were made by Bell and Berman using the static model.^(B9) Subsequent authors have used the static model as a starting point in finding solutions to the dispersion relations or to determine coupling constants in the isobar model. It seems worthwhile, therefore, to outline a static isobar model calculation^(B10) since it can be treated briefly yet explicitly.

Consider the process

$$\nu(k) + P(p) \rightarrow \mu^-(k') + P(p') + \pi^+(q') \quad (3.50)$$

in the center-of-mass of the final hadrons

$$\vec{p}' + \vec{q}' = \vec{p} + \vec{q} = 0 \quad (3.51)$$

We assume that the $J = 3/2$ state dominates so that the dependence of the amplitude on the final hadron states is only through a quantity with the appropriate transformation properties which can be taken to be a two-spinor three vector \vec{R} satisfying

$$\vec{\sigma} \cdot \vec{R} = 0 \quad (3.52)$$

The invariant amplitude generally involves eight terms (Eq. 3.58) (sixteen if $J = 3/2$ dominance is not assumed); we shall work to lowest order in \vec{q} here so that:

$$\begin{aligned} M &= \vec{C} \cdot (\vec{R}^* p) \\ \vec{C} &= C_A \vec{j} + C_V \vec{j} \times i\vec{q} \end{aligned} \quad (3.53)$$

where \vec{j} is the space component of the lepton current j_λ in the chosen reference system (Eq. 3.51) and j_0 has been eliminated using $q \cdot j = 0$ (m^2) ≈ 0 .

We shall also consider the amplitude for the process

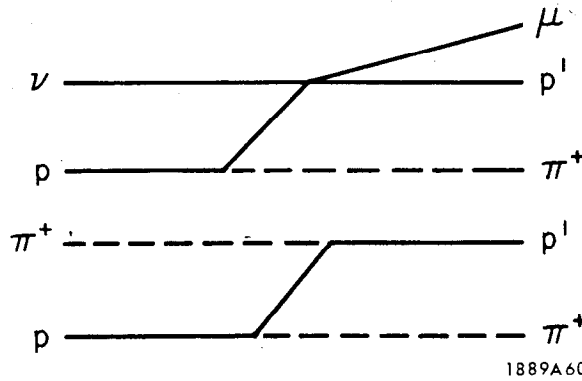
$$\pi^+(q) + P(p) \rightarrow \pi^+(q') + P(p') \quad (3.54)$$

in the resonant region, which we write

$$i\vec{q} \cdot (\vec{R}^* p) \quad (3.55)$$

absorbing a multiplicative constant in \vec{R} .

The conventional dispersion relation for these processes, like the static model, amounts largely to a resonant final state enhancement of the one-nucleon exchange diagrams:



These differ only at the upper vertex. Writing the usual covariant vertices, making a small \vec{q} approximation, extracting the part which can excite the Δ resonance and comparing Eq. (3.53) with Eq. (3.55), we get:

$$C_A = \left| \frac{g_A}{g_V} \right| \frac{GM}{g}, \quad C_V = \frac{-\xi G}{2g} \begin{pmatrix} \xi = \mu_p - \mu_n \\ = 4.7 \end{pmatrix} \quad (3.56)$$

where $g = 13.5$ is the pion nucleon coupling constant. The value of C_A agrees with that predicted by PCAC (which is automatically satisfied for the Born term by virtue of the success of the Goldberger-Treiman relation). Using the isotriplet current hypothesis, the vector coupling gives the Chew-Low relation^(C17)

for $\sigma(\gamma p \rightarrow \pi^0 p) / \sigma(\pi^0 p \rightarrow \pi^0 p)$ which works surprisingly well in the resonant region--see, e. g., Fig. 3 of B10. (The corresponding relation for charged pion photoproduction does not work so well because of substantial S-wave and $I=1/2$ contributions omitted here.) From Eq. (3.53) we obtain, in terms of laboratory variables:

$$\begin{aligned} \frac{d^2 \sigma}{d|q^2| dW^2} = \frac{W^2 P(W)}{2\pi^2 M^2 E^2} & \left\{ |C_A|^2 \left(\frac{Mq_0 + q^2}{Wq_3} \right)^2 \left[(E+E')^2 - q_3^2 \right] \right. \\ & - |C_A|^2 \frac{q^2}{q_3^2} \left[(E+E')^2 + q_3^2 \right] - \operatorname{Re} C_A^* C_V \frac{4q^2 M(E+E')}{W} \\ & \left. - |C_V|^2 q^2 \frac{M^2}{W^2} \left[(E+E')^2 + q_3^2 \right] \right\} \quad (3.57) \end{aligned}$$

$$W^2 = (p+q)^2 = M^2 + q^2 + 2Mq_0$$

$$q_3^2 = q_0^2 - q^2 \quad ,$$

$$P(W) = \frac{\sigma_\pi(W)}{4P_\pi W}$$

$$4P_\pi^2 W^2 = W^2 - M^2 - m_\pi^2 - 4M^2 m_\pi^2$$

which is the same as the original result of Bell and Berman apart from factors arising from a Lorentz transformation (which $\rightarrow 1$ as $M \rightarrow \infty$), the static approximation having been made by them in the laboratory. The cross section for antineutrinos incident on neutrons is the same except that the V-A interference term changes sign.

Turning now to more sophisticated calculations we cannot do better than to quote Adler's description of his work^(A6):

"The general method is to write fixed momentum transfer dispersion relations for the invariant amplitudes. Under the dispersion integrals we approximate the imaginary parts of the amplitudes by keeping only multipoles which excite the (3,3) resonance and which are dominant in Born approximation. We then project out integral equations for these multipoles; an examination of the nearest left-hand singularity structure of the multipoles shows enough of a resemblance to the familiar case of pion-nucleon scattering to allow a simple approximate solution to the integral equations. We guess this approximate solution by the heuristic procedure of first studying the static-nucleon limit of the integral equations. We then check numerically that the guess is a reasonably self-consistent solution to the integral equations when no static approximation is made, so that our final answer is not a static limit result."

As well as nucleon exchange, pion exchange was included in the Born approximation (it contributes only to the vector part). The results were compared with a large number of PCAC-current algebra predictions, one bad discrepancy being interpreted as being due to the neglect of vector meson exchange. Adler found that his model agreed well with electroproduction data for $Q^2 < 0.6 \text{ GeV}^2$ but gave too small a cross section for larger Q^2 . He therefore multiplied the whole neutrino cross section by a correction factor, which ensured that the vector part agreed with the electroproduction data after the appropriate isospin rotation. Other authors have employed similar methods. We refer to Adler for a comparison with earlier work and references.

In these models, the q^2 dependence is determined by the form factors in the Born terms; a dipole is usually adopted for the nucleon's axial form factor. Although the static model is only plausible for small $|\vec{q}|$, it can be extended to all q^2 in the same way. Assuming $M_A^2 = 0.71 \text{ GeV}^2$, Eq. (3.56) and (3.57) give

$$\lim_{E \rightarrow \infty} \int_0^{1.39 \text{ GeV}} \frac{dW}{2} \left(\frac{d\sigma^{\nu p \rightarrow N^*}}{dW} + \frac{d\sigma^{\nu n \rightarrow N^*}}{dW} \right) = 3.7 \times 10^{-39} \text{ cm}^2$$

while Adler (Fig. 28) found $3.5 \times 10^{-39} \text{ cm}^2$ for this quantity. This supports the belief that the static model contains the most important terms in Adler's dispersion treatment. For $\sigma^{\nu n \rightarrow N^*}$ alone, however, the models do not agree so well since Adler has a substantial nonresonant $I = 1/2$ contribution.

Some of Adler's results are shown in Fig. 28 - 30.

Another dispersion calculation has recently been done by Zucker^(Z1) who obtained a much larger cross section which approaches:

$$\lim_{E \rightarrow \infty} \sigma^{\nu p \rightarrow N^{*++}} \simeq 1.2 \times 10^{-38} \text{ cm}^2$$

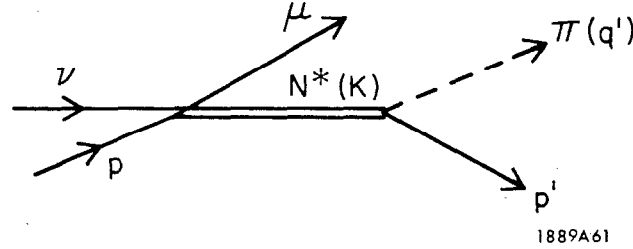
(which, to anticipate, agrees much better with the data, Fig. 35, than Adler's result). As usual, the amplitude had the form $A^{\ell h c} D^{-1}$ where $A^{\ell h c}$ is the left-hand cut given by the Born terms and D^{-1} is a final state enhancement factor determined entirely by strong interactions. The Born terms differed from Adler's mainly in the vector part which was essentially the same as in Walecka and Zucker's model of electroproduction^(W1) and contained an important contribution from ω exchange. In electroproduction, the normalization of the D^{-1} function was treated as a parameter and an excellent fit was obtained for the $N^*(1238)$ (better than Adler's at large Q^2) and for higher resonances. The same D^{-1} was then used to make an absolute calculation of ν production.

In this model the ω exchange contribution to the photoproduction amplitude is about half the size of the other contributions with which it interferes destructively. If the ω exchange is omitted, $A^{\ell h c}$ is much the same as Adler's. (The inclusion of ω exchange does not change the q^2 behavior very much for the $N^*(1238)$ but Walecka and Zucker find that it is essential to get a good fit to higher resonances.) Since Adler's results also fit photoproduction, we infer that D^{-1} (Zucker) $\simeq 2 D^{-1}$ (Adler). The axial part of $A^{\ell h c}$ is approximately the same in both calculations so that Zucker's axial amplitude ($\sim A^{\ell h c} D^{-1}$) must be about twice Adler's. This accounts for his larger cross section.

The $N^*(1238)$ makes the dominant contribution to the Adler-Weisberger calculation of g_A/g_V (see, e.g., W4) which relies on Adler's theorem (2.23). Unless the success of this calculation is fortuitous, Zucker's model for ν production must, therefore, be wrong at $q^2 \simeq 0$ since it violates Adler's theorem by a large amount. (Adler, not unnaturally, approximately satisfies his own theorem.) However, it could be argued that this only shows that the model is wrong for one amplitude in one region and such models are not expected to work well for individual amplitudes at all q^2 . (Z2) Another point is that if ω exchange is so important, the success of the absolute prediction of (e.g.) the Chew-Low (static) model for photoproduction must, in our opinion, be regarded as accidental since it includes no ω contribution. (Such absolute calculations should be regarded with some suspicion, since the solution of the Omnes equation for D^{-1} is sensitive to assumptions about high-energy behavior, but one is reluctant to deny significance to the success of the very straightforward static model calculations.) However, it is true that Walecka and Zucker find that ω exchange is essential to fit higher resonances.

C. Isobar Models

In the isobar model the N^* is treated as an elementary particle in the Feynman diagram



If the N^* is described by a Rarita-Schwinger spinor U_α (the relativistic generalization of the quantity \vec{R} in the previous section; see Veltman^(V1) for a convenient review of the properties of U_α) then, quite generally, the matrix element for N^* production may be written:

$$\begin{aligned} \frac{G}{\sqrt{2}} \bar{U}_\alpha(K) & \left(\left[\frac{C_3^V}{M} \gamma_\lambda + \frac{C_4^V}{M^2} K_\lambda + \frac{C_5^V}{M^2} P_\lambda \right] \gamma_5 F^{\lambda\alpha} + C_6^V j^\alpha \gamma_5 \right. \\ & \left. + \left[\frac{C_3^A}{M} \gamma_\lambda + \frac{C_4^A}{M^2} K_\lambda \right] F^{\lambda\alpha} + C_5^A j^\alpha + \frac{C_6^A p^\alpha q \cdot j}{M^2} \right) U(p) \end{aligned} \quad (3.58)$$

($F_{\lambda\alpha} = q_\lambda j_\alpha - q_\alpha j_\lambda$)

The differential cross section has been given explicitly by Albright and Liu^(A11,A12) with all terms retained and by Kim^(K8) with $C_6^V = 0$ (CVC) and $m = 0$ (in which case C_6^A does not contribute). The relation between our form factors and those used by these and other authors is given in the appendix.

The effectiveness of the various couplings may be judged from Fig. 31 and 32 which are taken from the paper of Albright and Liu.^(A12)

If T is conserved, the form factors are relatively real. The absence of second-class currents (or, equivalently, charge symmetry plus T conservation) implies that the hadronic currents in the processes $\nu p \rightarrow N^{*++}$ ($\nu n \rightarrow N^{*+}$) and $\bar{\nu} n \rightarrow N^{*-}$ ($\bar{\nu} p \rightarrow N^{*0}$) are the same. If J_λ^0 is an isovector, 3.47 holds. CVC implies $C_6^V = 0$ and the isotriplet current hypothesis gives:

$$\frac{C_i^V [\nu p \rightarrow \mu^- N^{*++}](q^2)}{\sqrt{3}} = C_i^V [\nu n \rightarrow \mu^- N^{*+}](q^2) = C_i^V [\gamma p \rightarrow N^{*+}](q^2) \quad (3.59)$$

All coupling constants quoted below are for N^{*+} production. The photo- and electroproduction data can be fitted with $C_4^V = C_5^V = 0$ which implies that the N^* is excited by an M1 transition in agreement with the quark model prediction. In their analysis of photoproduction data, Dalitz and Sutherland^(D1) found

$$C_3^V(0) = 2.05 \pm 0.04 \quad (3.60)$$

(in comparison with the Chew-Low (static model) value of 2.2 and the SU(6) prediction of 1.6). Gourdin and Salin^(G16) obtained essentially the same value but subsequent authors (e. g., Berman and Veltman,^(B16) Albright and Liu,^(A11,A12) Kim,^(K8) Dufner and Tsai^(D13)) failed to divine a hidden convention with respect to Clebsch-Gordan coefficients in their paper and deduced a value for C_3^V which was too big by a factor of $\sqrt{3/2}$.

Dufner and Tsai^(D13) extracted $C_3^V(q^2)$ from electroproduction data finding that it could be approximately fitted by:

$$\left[\frac{C_3^V(q^2)}{C_3^V(0)} \right]^2 = e^{-6.3 \sqrt{Q^2}} \left(1 + 9.0 \sqrt{Q^2} \right) \quad (Q^2 \text{ in } \text{GeV}^2) \quad (3.61)$$

i. e., the inelastic form factor C_3^V falls off faster than the elastic form factor (the ratio of (3.61) to the dipole fit to the elastic form factor (3.17) is ~ 0.7 at $Q^2 = 0.5 \text{ GeV}^2$ and 0.5 at $Q^2 = 1.6 \text{ GeV}^2$).

$C_5^A(0)$ can be obtained using PCAC which gives (again for $\nu n \rightarrow N^{*+}$)

$$C_5^A = \frac{-f_\pi g_{N^{*+}n\pi^+}}{M} = -1.2 \quad (3.62)$$

using $g_{N^{*+}n\pi^+} = 8.3$ (corresponding to $\Gamma(N^{*+} \rightarrow p\pi^+) = 120$ MeV) and $f_\pi = 0.97 m_{\pi^+}$. There is no general criterion which determines C_3^A or C_4^A ; comparison with the static theory gives the result that they are zero to lowest order in $|\vec{q}|/M$. Equations (3.60) and (3.62) give a value for C_A/C_V (3.53) in almost exact agreement with the static model result (3.56).

Salin^(S1) has developed a "hybrid" model in which the nucleon and pion exchange Born terms are added to the Feynman diagram for N^* production. He retained only the C_3^V and C_4^A couplings (so that, as observed by Adler, his model does not respect PCAC); C_3^V was determined using Eq. (3.59) and C_4^A by requiring self-consistency in the solution of dispersion relations.

We close this section by returning to the question of corrections to Eq. (3.49) in the Berman-Veltman model^(B16) in which $C_6^V = C_5^V = C_4^V = C_4^A = C_3^A = m = 0$ and $C_3^V(0)$ and $C_5^A(0)$ are given by (3.60) and (3.62) respectively. They give the complete expression for $D(\theta, \phi)$ in their model from which we can extract the leading terms at small α :

$$\begin{aligned} D(\theta, \phi) \sim & 1 + 3 \cos^2 \theta - \frac{6(M' - M)}{(M' + M)} \cos \phi \sin \theta \cos \theta \sin \alpha / 2 \\ & + \sin^2 \frac{\alpha}{2} \left[1 + \frac{4E}{\lambda M} + \frac{6E}{\lambda M} \cos^2 \theta + \frac{3(\lambda^2 M^2 + 2\lambda M E + E^2) \sin^2 \phi \sin^2 \theta}{\lambda^2 M^2} \right] \\ & + 0 \left(\frac{M' - M}{M} \sin^2 \frac{\alpha}{2} \right) + 0 \left(\sin^4 \frac{\alpha}{2} \right) \end{aligned} \quad (3.63)$$

$$\lambda = \frac{M C_A^5(0)}{(M + M') C_A^3(0)} \simeq -0.25$$

Note that with a pure vector coupling ($\lambda = 0$), Eq. (3.63) implies that the cross section vanishes at $\alpha = 0$ in agreement with Adler's theorem. Equation (3.63) shows that at large E the best expansion parameter is $q^2 \approx -4E^2 \sin^2 \alpha/2$ and not α . Using the fact that λ is small we find

$$\int D(\theta, \phi) d\phi \sim 1 + 3 \left(1 - \frac{2E^2}{\lambda^2 M^2} \sin^2 \alpha/2 \right) \cos^2 \theta \quad (3.64)$$

so that we can only expect the $1 + 3 \cos^2 \theta$ distribution to hold at very small values of α .

D. Higher Symmetries and Quark Models

SU(6) symmetry gives

$$C_A^5 (q^2=0)^{n \rightarrow N^{*+}} = \frac{2\sqrt{3}}{5} \left(\frac{g_A}{g_V} \right)^{n \rightarrow p} \quad (\text{A12, P10}) \quad (3.65)$$

$$C_V^3 (q^2=0)^{n \rightarrow N^*} = \frac{\sqrt{3}}{5} (1 + \xi) = 1.6 \quad (\text{G10, F14})$$

The calculation of C_V^3 is actually ambiguous since the contribution of the vector current (and of the remaining parts of the axial current) vanishes in the SU(6) limit $q_\mu \rightarrow 0$. Furthermore, it is not clear whether we should take $(g_A/g_V)^{n \rightarrow p} = -5/3$, which is the value given by SU(6), or the experimental value -1.23 ; the former gives a value for C_A^5 close to the PCAC result (Eq. 3.62) while the latter gives a value for $\Gamma(N^*)$ which is wrong by a factor of 2 if we accept PCAC.

Various prescriptions have been used to compare the SU(6) and quark model values for C_V^3 with photoproduction data; there seems to be general agreement that the prediction is too small (cf Eq. 3.65 and 3.60). In the quark model it is

clear that g_A/g_V for the quark should be adjusted to give the correct $(g_A/g_V)^{n \rightarrow p}$ and, consequently, a value for C_A^5 in disagreement with PCAC.

These models respect the isotriplet current hypothesis so that the vector current can be taken from electroproduction and the only new information is the value of $C_A^5(0)$ (the expected error can be judged from the failure of the prediction of $C_V^3(0)$). However, we can also calculate $C_A^5(0)$ using PCAC and this procedure is probably preferable. We conclude that, in general, models which apply at that zero momentum transfer (SU(6) and the non-relativistic quark model) give no information which is not otherwise available to the believer in PCAC, insofar as the isovector amplitude can be obtained from electroproduction data; tests of these models can be made by comparing them with electroproduction and (via PCAC) with pion cross sections.

Relativistic symmetries (U(6,6), etc.) give predictions for all q^2 , once a prescription for avoiding their inherent ambiguities has been adopted. (A13, A17, K5, K6) However, these models are--probably justly--no longer fashionable and it would not be appropriate to discuss them in detail here. We refer to Albright and Liu^(A13) for a comparison of various approaches involving these symmetries.

E. Comparison between Models

Calculations such as Adler's predict the nonresonant and the resonant pion production amplitudes. The isobar model gives a phenomenological description of the resonant part of the amplitude only; the nonresonant background can probably simply be subtracted by drawing a smooth background curve below the resonant peak without introducing intolerable errors.

Since the dispersion calculations must be done numerically, it is often hard to trace the origin of differences in the results obtained by different authors and it will be hard to assess disagreement with experiment. It would, therefore, be very useful if future authors would extract the effective values of the isobar couplings, as Bijtebier has done^(B20) in the case of Adler's model. His results are shown in Table 5. We refer to his paper for a careful comparison of the models of Adler, Salin, and Berman and Veltman.

The following seems a reasonable strategy for fitting the resonance production cross section in the isobar model:

1. Use the results of analysis of electroproduction data (e. g., that of Dufner and Tsai^(D13)) to fix the vector form factors.
2. Put $C_5^A(0) = -1.2$ (the PCAC value) and $C_3^A = C_4^A = 0$, as suggested by the static model. Try to fit the data, describing the q^2 dependence of C_5^A in terms of some parameters. The form of the quasi-elastic form factor F_A should be a starting point, in agreement with the predictions of the static model and dispersion calculations. Up to now this prescription is that of Berman and Veltman^(B16); it is, essentially, a sophisticated version of the static model (the reader may judge the reliability of this from the exposition above) and contains the main terms in Adler's model.
3. If the above method cannot fit the data (or only fit it at the price of giving C_5^A an "unreasonable" q^2 dependence), introduce C_4^A in addition, with a suitable parameterization. This is the prescription followed by Bijtebier.^(B20) Dispersion theorists seem to be agreed that C_3^A is very small so that it may be reasonable to keep it zero except as a last resort. The price of varying $C_4^A(0)$ in Adler's model has been discussed

in detail by Bijtebier; the variation is achieved by exploiting the arbitrary polynomial in the solution of the Omnès equation.

A final theoretical remark is that in most models $\bar{\sigma} \rightarrow \sigma^\nu$ as $E \rightarrow \infty$ (though this could be avoided by a suitable choice of form factors). In the static model and the models of Adler and of Berman and Veltman the sign of the V-A interference term is such that $\sigma^{\bar{\nu}n} < \sigma^{\nu p}$ at finite energies.

F. Experimental Results

We shall discuss the results of the 1967 CERN experiment for π production on the free protons in propane^(B46) (the results of the 1963-1964 experiment on Freon, which suggested a smaller cross section, may be found in Y4--see also Fig. 29 and 30). We refer to the experimental paper^(B46) for a discussion of background, cuts in the data, etc. The main results are shown in Fig. 33 - 35.

Important points to note are:

1. The data (Fig. 34) agrees with the $1+3 \cos^2 \theta$ distribution expected at small α (Eq. 3.49) if all events with $\sin^2 \alpha/2 < 0.1$ are taken.

This is very surprising, at least in the Berman-Veltman model (and therefore also in the static model and Adler's model which are closely related). Equation (3.64) indicates that if λ has the value $\approx -1/4$ predicted by these models, then the $1+3 \cos^2 \theta$ distribution should be a good approximation for events with $\sin^2 \alpha/2 \lesssim 10^{-3}$, ($E^2 \sim 4M^2$ being a reasonable value to take in Eq. (3.64) for the CERN experiment bearing in mind that $d\sigma/d \cos \alpha|_{\alpha=0} \sim E^2$). We conclude that either these models are incorrect or that the fit to $1+3 \cos^2 \theta$ is fortuitous (the approximate formulae (3.64) and (3.65) are quite irrelevant for $\sin^2 \alpha/2 < 0.1$ in the CERN experiment; the complete formula must be used and this requires a knowledge of the form factors).

2. The data (Fig. 34) shows a 2.9 standard deviation from symmetry in the angle ϕ for events with $\sin^2 \alpha/2 < 0.1$. Such an asymmetry can be caused either by interference with nonresonant background or by T violation (see page 82). This is true for all α , however, and the statistically more significant distribution of all the events is roughly symmetric in Adler's angle δ (and hence also in ϕ).
3. The total cross section is too large to be explained in Adler's model, the static model, or the (corrected) Berman-Veltman model except with a very large value of M_A (> 3 GeV). (The average cross section for $1 \text{ GeV} < E_\nu < 4 \text{ GeV}$ is $\sigma(\nu p \rightarrow \mu^- \pi^+ p) = (1.13 \pm 0.28) \times 10^{-38} \text{ cm}^2$ where the error is statistical and systematic.) It can be fitted with axial form factors equal to the vector form factor by introducing a coupling C_4^A while respecting the isotriplet current hypothesis and PCAC, as was done by Bijtebier^(B20) (see Table 5).
4. The data is not good enough to use $d\sigma/dq^2$ to test the models critically. In those models which agree with the static model for small Q^2 there must be more events at large Q^2 than previously expected, in order to double the predicted value of σ .

Bijtebier's model shows that the value of σ obtained in the CERN experiment can be fitted without abandoning the $q^2 = 0$ prediction of PCAC. However, all the other models which fit the data (Salin, Altarelli et al., Zucker) violate PCAC. This is distressing since, as we have repeatedly remarked, the PCAC prediction cannot be badly violated in the N^* region unless the success of the Adler-Weisberger relation is fortuitous.

3.6. Highly Inelastic Reactions

A. Kinematics

This section is devoted to the inclusive process in which only the final lepton is observed. It is useful to begin by introducing new dimensionless structure functions G_i :

$$W_1(\nu, q^2) = G_1(\omega, Q^2/M^2)$$

$$\frac{\nu W_i(\nu, q^2)}{M^2} = G_i(\omega, Q^2/M^2) \quad (i \neq 1) \quad (3.66)$$

$$\left(\nu = \mathbf{q} \cdot \mathbf{P} = M(E - E')_{\text{lab}}, \quad \omega = 2\nu/Q^2 \right)$$

In terms of the G_i the double differential cross section may be written:

$$\frac{d^2 \sigma^{\nu, \bar{\nu}}}{d\omega dy} = \frac{G^2 M E}{\pi \omega^2} \left[\left(1 - y - \frac{My}{2\omega E} \right) G_2^{\nu, \bar{\nu}} + \frac{y^2 G_1^{\nu, \bar{\nu}}}{\omega} \mp y \left(1 - \frac{y}{2} \right) \frac{G_3^{\nu, \bar{\nu}}}{\omega} \right] \quad (3.67)$$

$$(y = \nu/ME)$$

It is also useful to introduce hypothetical absorption cross sections for scalar, right-handed and left-handed currents:

$$\sigma_S = \frac{\pi}{\nu + q^2/2} \left[W_2 \left(\frac{\nu^2}{-q^2 M^2} + 1 \right) - W_1 \right]$$

$$\sigma_R = \frac{\pi}{\nu + q^2/2} \left[W_1 + \frac{1}{2} \sqrt{\frac{\nu^2}{M^4} - \frac{q^2}{M^2}} W_3 \right] \quad (3.68)$$

$$\sigma_L = \frac{\pi}{\nu + q^2/2} \left[W_1 - \frac{1}{2} \sqrt{\frac{\nu^2}{M^4} - \frac{q^2}{M^2}} W_3 \right]$$

These definitions are rather arbitrary; we have followed the convention of using the flux factor for a zero mass particle with the same $s = (q + P)^2$. Using Eq. (2.6), we see that the σ 's satisfy the simple positivity conditions:

$$\sigma_i \geq 0, \quad (3.69)$$

as expected since they are cross sections (albeit hypothetical ones).

On the basis of Regge theory, or the behavior of real cross sections, we might expect that

$$\sigma_i \xrightarrow[q^2 \text{ fixed}]{\nu \rightarrow \infty} \nu^{\alpha(0) - 1}$$

where $\alpha(t)$ is the trajectory function of the leading trajectory which can be exchanged in forward current scattering (recall that according to the optical theorem $\sigma \sim \text{Im} A(JN \rightarrow JN, \text{forward})$). This implies

$$\begin{aligned} W_1 &\xrightarrow{\nu \rightarrow \infty} \beta_1(q^2) \nu^{\alpha_1(0)} \\ W_2 &\xrightarrow{\nu \rightarrow \infty} \beta_2(q^2) \nu^{\alpha_2(0) - 2} \\ W_3 &\xrightarrow{\nu \rightarrow \infty} \beta_3(q^2) \nu^{\alpha_3(0) - 1} \end{aligned} \quad (3.70)$$

a result which can be derived more formally by making a t channel helicity analysis of elastic current-nucleon scattering and using the Regge model. The

Pomeron can contribute to W_1 and W_2 so that we expect $\alpha_{1,2}(0) = 1$.^{*} It cannot contribute to W_3 which is due to interference of the axial and vector currents ($\sim \text{Im}(J^V N \rightarrow J^A N, \text{forward})$), because these currents are supposed to have opposite G parity. A unit of G parity must, therefore, be exchanged and the leading trajectories have $\alpha_3(0) \sim 1/2$. The possible Regge trajectories for various combinations of structure functions are given in Table 6.

Although Regge behavior implies $\lim_{\nu \rightarrow \infty} (\sigma_R(\nu, q^2) - \sigma_L(\nu, q^2)) = 0$, it does not imply such a Pomeranchuk theorem for $\lim_{E \rightarrow \infty} (\sigma^\nu(E) - \sigma^{\bar{\nu}}(E))$; indeed this quantity is infinite in most of the models discussed below. Since we are only working to order G, unitarity reduces to a linear relation and we cannot begin to derive results such as the Froissart bound which depend essentially on the nonlinearity of the unitarity relation. Actually, no bounds can be rigorously derived even if we work to all orders in G because the exchange of neutrinos gives rise to infinite range forces (see, however, R9).

^{*}Actually the point $\alpha = 1$ is a nonsense point for W_2 , in the Regge jargon. The Pomeron, therefore, decouples unless either a fixed $J = 1$ pole is present which restores its contribution or the residue is singular as $t \rightarrow 0$.^(A1) Fixed poles may be present in weak and electromagnetic amplitudes and indeed they occur in models.^(A1) As $q^2 \rightarrow 0$ current conservation requires that the vector part of the structure functions satisfy

$$W_1 \sim -\nu^2 W_2 / M^2 q^2$$

so that if the Pomeron decouples from W_2 , it must also decouple from the photo-production amplitude W_1 ; experimentally this is not the case. The Adler relation (2.22) requires the Pomeron to couple to the axial part of W_2 for $q^2 \approx 0$.

The physical region for inelastic processes in the $\nu - Q^2$ plane is illustrated in Fig. 36. The only results which have been derived at all Q^2 for the inclusive process are the Adler sum rules (2.24 and 2.25). Most of the theoretical predictions pertain to the "deep inelastic" region where $S = M^2 + 2\nu - Q^2$ and Q^2 are large ($S > S_0$, $Q^2 > Q_0^2$); note that as $E_\nu \rightarrow \infty$ this tends to 100% of the physical region. These predictions assume scale invariance to which we now turn.

B. Scale Invariance

Bjorken^(B24) studied the structure functions G_i (Eq. 3.66) and argued that the limits

$$\lim_{\omega \text{ fixed}} Q^2 \rightarrow \infty (G_i(\omega, Q^2/M^2)) = F_i(\omega) \quad (3.71)$$

exist and are not zero. In discussing the consequences of this hypothesis it is useful to define structure functions which describe the production of non-strange (F_i) and strange (f_i) final states thus:

$$\tilde{F}_i(\omega) = \cos^2 \theta_c F_i(\omega) + \sin^2 \theta_c f_i(\omega) \quad (3.72)$$

We denote the structure functions which describe inelastic electron scattering off protons and neutrons by $G_{1,2}^{\gamma p, \gamma n}$ and their limits, as in (3.71), by $F_{1,2}^{\gamma p, \gamma n}$.

Bjorken's hypothesis is known as "scale invariance" because it is trivially satisfied if no scale is defined so that the dimensionless G_i can only depend on the one dimensionless variable available— ω . Scale invariance is suggested by the Adler sum rules (2.24 and 2.25) which may be written:

$$\int_1^\infty (G_2^{\bar{\nu}}(\omega, Q^2/M^2) - G_2^{\nu}(\omega, Q^2/M^2)) \frac{d\omega}{\omega} = \langle 4 \cos^2 \theta_c I_3 + \sin^2 \theta_c (3 Y + 2 I_3) \rangle \quad (3.73)$$

The simplest way to ensure the Q^2 independence of the left-hand side as $Q^2 \rightarrow \infty$ is to assume that the limit in Eq. (3.71) exists.

Experiments indicate that $G_{1,2}^{\gamma p, \gamma n}$ may satisfy Eq. (3.71)--or "scale."^(B25) They are approximately independent of Q^2 in the region $20 \text{ GeV}^2 > Q^2 > 1 \text{ GeV}^2$, $S = M^2 + 2\nu - Q^2 > 6.5 \text{ GeV}^2$ and $\nu < 12 \text{ GeV}^2$.* It seems that $F_2^{\gamma p} \neq F_2^{\gamma n}$.

Assuming scale invariance, Eq. (3.67) implies:

$$\frac{d^2 \sigma^{\nu, \bar{\nu}}}{d\omega dy} = \frac{G^2 M E}{\pi \omega^2} \left[(1-y) \tilde{F}_2^{\nu, \bar{\nu}}(\omega) + \frac{y^2 \tilde{F}_1^{\nu, \bar{\nu}}(\omega)}{\omega} \mp y \left(1 - \frac{y}{2}\right) \frac{\tilde{F}_3^{\nu, \bar{\nu}}(\omega)}{\omega} \right] \quad (3.74)$$

$$\left(E \gg M, \quad Q^2 > Q_0^2, \quad s > s_0 \right)$$

and, therefore,

$$\lim_{E \rightarrow \infty} \sigma^{\nu, \bar{\nu}}(E) = \frac{G^2 M E}{\pi} \int_0^\infty d\omega \left(\frac{\tilde{F}_2^{\nu, \bar{\nu}}(\omega)}{2\omega^2} + \frac{\tilde{F}_1^{\nu, \bar{\nu}}(\omega)}{3\omega^3} \mp \frac{\tilde{F}_3^{\nu, \bar{\nu}}(\omega)}{3\omega^3} \right) \quad (3.75)$$

The fact that $\sigma \sim E$ is a direct consequence of scale invariance since the only possibility is $\sigma \sim G^2 s = 2G^2 M E_\nu^{\text{lab}}$ in the absence of any scale.

Equation (2.12) for the perpendicular and longitudinal lepton polarizations may be written:

$$P_{\nu, \bar{\nu}}^P = \pm \frac{m}{2M} \sqrt{\frac{2My}{\omega E(1-y)}} \frac{2\tilde{F}_1 y + \tilde{F}_3(1-y) \pm \tilde{F}_3}{\left(\tilde{F}_2(1-y) + \frac{\tilde{F}_1 y^2}{\omega} \mp y \left(1 - \frac{y}{2}\right) \frac{\tilde{F}_3}{\omega} \right)} \quad (3.76)$$

$$P_{\nu, \nu}^L = \mp \pm \frac{m^2 y}{2ME} \frac{(2\tilde{F}_1 \mp \tilde{F}_3 + 2(1-y)\tilde{F}_4/\omega)}{\left(\tilde{F}_2(1-y) + \frac{\tilde{F}_1 y^2}{\omega} \mp y \left(1 - \frac{y}{2}\right) \frac{\tilde{F}_3}{\omega} \right)}$$

$$(E \gg M, Q^2 > Q_0^2, s > s_0, y \neq 1)$$

*The precise domain is drawn in B35. If the G_i are regarded as functions of $\omega' = (s + Q^2)/Q^2$ and Q^2/M^2 , the domain of Q^2 independence extends down to $s = 3.3 \text{ GeV}^2$ (ω' and ω are, of course, the same in Bjorken's limit).

In the scaling region the inequalities (2.6) become

$$\begin{aligned}
0 &\leq \left| \tilde{F}_3(\omega) \right| \leq 2 \tilde{F}_1(\omega) \leq \omega \tilde{F}_2(\omega) \\
-4 \tilde{F}_4 + 2 \omega \tilde{F}_5 &\leq 2 \omega \tilde{F}_1 + \omega^2 \tilde{F}_2 \\
\tilde{F}_5 \tilde{F}_1 - \tilde{F}_1^2 + \left(\tilde{F}_2 - \frac{2 \tilde{F}_1}{\omega} \right) \tilde{F}_4 &\geq \frac{1}{4} \left(\tilde{F}_5^2 + \tilde{F}_6^2 \right)
\end{aligned} \tag{3.77}$$

A useful form of the cross section in which the implications of these inequalities are transparent can be obtained using Eq. (3.68):

$$\frac{d^2 \sigma^{\nu, \bar{\nu}}}{d \omega d y} = \frac{G^2 M E}{\pi \omega^2} \frac{\nu W_2}{M^2} \left[(1-y) + \frac{y^2}{2} (R+L) \pm y \left(1 - \frac{y}{2} \right) (L-R) \right] \tag{3.78}$$

$$(E \gg M)$$

where

$$\begin{aligned}
0 \leq R &= \frac{\sigma_R}{\sigma_R + \sigma_L + 2 \sigma_S} \leq 1 \\
0 \leq L &= \frac{\sigma_L}{\sigma_R + \sigma_L + 2 \sigma_S} \leq 1
\end{aligned}$$

In going from a left-handed ν to a right-handed $\bar{\nu}$, $L \longleftrightarrow R$ so that the necessary sign change in Eq. (3.78) is obvious. The assumption that νW_2 scales implies that, however the other structure functions behave, $\sigma(E)$ rises at least linearly as $E \rightarrow \infty$ ^(B29) with:

$$\frac{1}{3} \int \frac{F_2^{\nu, \bar{\nu}}(\omega) d \omega}{\omega^2} \leq \lim_{E \rightarrow \infty} \frac{\pi}{G^2 M E} \sigma^{\nu, \bar{\nu}}(E) \leq \int \frac{F_2^{\nu, \bar{\nu}}(\omega) d \omega}{\omega^2} \tag{3.79}$$

Assuming that the other structure functions also scale, R and L are functions of ω only in the scaling region and

$$\lim_{E \rightarrow \infty} \sigma^{\nu(\bar{\nu})}(E) = \frac{G^2 M E}{\pi} \int \frac{d\omega}{\omega^2} X^{\nu(\bar{\nu})}(\omega) F_2^{\nu(\nu)}(\omega) \quad (3.80)$$

$$\frac{1}{3} \leq X^{\nu(\bar{\nu})} = \frac{1}{2} + \frac{1}{2} L(R) - \frac{1}{6} R(L) \leq 1 .$$

When we talk about the limit $E \rightarrow \infty$, we are indulging the hope that there is a region where E is large enough for our formulae to apply but still small enough for the conventional weak interaction theory to hold. The existence of an IVB would modify the results above and cause an apparent breakdown of scaling since it would require the substitution:

$$G^2 \rightarrow \frac{G^2}{\left(1 - \frac{q^2}{M_W^2}\right)^2} = \frac{G^2}{\left(1 - \frac{2y M E}{\omega M_W^2}\right)^2} . \quad (3.81)$$

C. Models and Sum Rules

We shall assume that inelastic lepton scattering exhibits scale invariance although scale invariance is broken by logarithmic terms in perturbation theory and such terms are not excluded by the SLAC data. We are, therefore, assuming that in the "deep inelastic region," or equivalently near the light cone in configuration space, the real world is smoother than perturbation theory suggests (see, e.g., A7 or J1). In fact, scale invariance requires that products of operators behave much as they do in free field theory in the appropriate limit. The simplest way to exploit this idea is to study models in which the nucleon is built from non-interacting particles in the most arbitrary way consistent with certain general

requirements (charge conservation, etc.). It turns out that there is some a posteriori justification for this "generalized parton model" since all the results can also be obtained in models with simple interaction Hamiltonians by either using the Bjorken-Johnson-Low^(BJL) expansion of time-ordered products^(B21, J5) or making formal expansions of operators on the light cone. These formal methods involve manipulations which fail in perturbation theory^(A9, J2) but we are already committed to the view that this may be irrelevant (for a recent lucid exposition of this view, see F11).

In all these approaches the structure functions are expressed in terms of quantities which cannot be calculated without making strong dynamical assumptions (these quantities are the distribution functions in the parton model and the values of matrix elements of certain operators in the formal approach). Since none of the models which attempt to give a detailed description of the structure functions has gained universal acceptance, we will not review them here.* However, it turns out that sum rules and relations between the structure functions can be obtained without further assumptions once we decide what the constituents of the nucleon are. These relations are very interesting because they depend directly on the spin and internal quantum numbers of the particles (or partons) in the underlying field theory which is chosen.

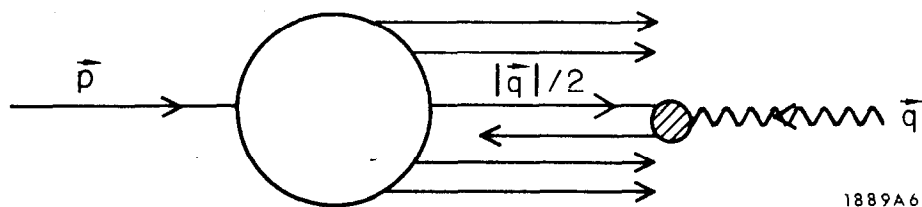
The SLAC data^(B35) require that the majority of the charged partons have spin 1/2 (see below). Since we wish to consider models in which Gell-Mann's current commutation relations obtain it is, therefore, rather natural to assume that

*However, we will give a very brief qualitative discussion at the end of this section of what might be expected on the basis of the free field or "parton" model.

For other approaches see, e. g., B25, B26, G11, L19, L1, D6.

the partons are quarks. We shall discuss such models below--first in parton language, in which the assumptions tested by each sum rule are transparent, and then from the more formal point-of-view of the BJL expansion. We shall only discuss the weak structure functions F_i which describe $\Delta Y=0$ reactions in the text. The results are summarized in Table 7; results for the $\Delta Y=1$ structure functions f_i are given in Table 8.

The parton model^(B28, D9, D12, F6) is supposed to apply in frames in which the proton has a large momentum \vec{P} , the i^{th} parton having momentum $x_i \vec{P}$. It is convenient to choose the Breit frame of the virtual photon (current) and the parton with which it interacts:*



In this frame

$$\begin{aligned} \nu &= |\vec{P}| |\vec{q}| \\ q^2 &= -\vec{q}^2 \end{aligned} \quad (3.82)$$

and the interacting parton has

$$x = \frac{|\vec{q}|}{2|\vec{P}|} = \frac{-q^2}{2\nu} = \frac{1}{\omega} \quad (3.83)$$

*The discussion here is very simplified. We do not wish to get embroiled in attempts to justify the model, transverse momentum cut-off, etc. Erudite readers will notice that the usual "justification" breaks down in the frame chosen because $q_0=0$. Nevertheless, the model works in that it gives the same results as in the conventional frames^(D8) and this frame has several heuristic advantages.

The Bjorken limit is therefore $|\vec{P}| \longrightarrow \infty$ with x fixed. The assumption that in this limit $0 \leq x_i \leq 1$ ensures that the scattering is incoherent, since the scattered parton travels in the opposite direction from the others, so that W_2 , for example, is given by

$$W_2 = \sum_i \int u_i(x) W_2^i(x, \nu, q^2) dx \quad (3.84)$$

where

$u_i(x)$ - probability of finding a constituent of the i^{th} type with a fraction x of the proton's longitudinal momentum.

The partons are supposed to have small momenta transverse to \vec{P} and to be on mass shell before and after the interaction so that $W^i \sim \delta(2\nu x + q^2)$ in the deep inelastic region; it is this δ function which gives scale invariance. The explicit forms of the W^i can be obtained from Eq. (3.27) (with $F_V^1 = Q_V^i$, $F_A = -Q_A^i$, where Q^i is the appropriate electromagnetic or weak charge of the i^{th} type of parton and the other form factors are zero), except that W_3 has the opposite sign for antiquarks.* Hence, for example**:

$$W_2^{i\gamma} = 2x_i Q_i^2 M^2 (2x_i \nu + q^2)$$

$$F_2^\gamma(x) = x \sum_{q=1}^6 u_q(x) Q_q^2 \quad (3.85)$$

where q labels the three sorts of quarks and their antiparticles.

*We assume a weak current $\bar{\psi} \gamma_\mu (1 - \gamma_5) \psi$ so that antiquark results can be obtained from quark results by replacing $\gamma_\mu (1 - \gamma_5)$ by $\gamma_\mu (1 + \gamma_5)$. The axial-vector interference term W_3 therefore changes sign.

**A factor x^2 occurs because W_2^i is the coefficient of $P_\mu^i P_\nu^i \simeq x_i^2 P_\mu P_\nu$ in the hadronic tensor. A factor x_i^{-1} occurs because Eq. (3.84) requires that the parton states are normalized to one parton per proton. With the covariant normalization used elsewhere the number of partons per proton = $2E^i/2E \simeq x^i$.

Two results can be obtained directly without looking at the explicit forms of the F_i . The first is the relation between $\sigma_S/\sigma_{R,L}$ and the spin of the parton. (C6, B28, G18) In the Breit frame a spin 0 parton carries no angular momentum in or out along \vec{q} ; hence it cannot absorb a transverse current and $\sigma_R = \sigma_L = 0$. If the parton has spin 1/2, its helicity is conserved by the electromagnetic and weak interaction when $|\vec{P}_i|/M_i \rightarrow \infty$ but since its direction is reversed it must absorb a unit of spin; in this case, therefore, $\sigma_S = 0$.* In terms of the structure functions, $\sigma_S = 0$ implies

$$2 F_1 = \omega F_2 . \quad (3.86)$$

Another immediate result is that the axial current is effectively conserved in the deep inelastic region^(L20) since we can neglect the parton's mass ($M_i/|\vec{P}_i| \rightarrow 0$). This gives

$$\begin{aligned} F_4 &= 0 \\ F_5 &= 2 F_1 \end{aligned} \quad (3.87)$$

Note that the second relation actually follows from (3.86) and the inequalities (3.77) (which also imply $F_6 = 0$ if (3.86) is assumed).

Since we assume the conventional isospin properties of the weak current, Eq. (2.20) is valid:

$$\begin{aligned} F_i^{\nu p} &= F_i^{\bar{\nu} n} \\ F_i^{\bar{\nu} p} &= F_i^{\nu n} \end{aligned} \quad (3.88)$$

* $\sigma_{S,R,L}$ are, in general, not invariant quantities. However, they are invariant under Lorentz transformations along \vec{q} , one of which connects the Breit frame with the laboratory. In the SLAC data $\sigma_S/\sigma_T = 0$ is "quite unlikely but not impossible." However, $\sigma_S/\sigma_T = -q^2/\nu^2$ fits the data and this is zero in the Bjorken limit.

and we are, therefore, left at this point with six independent structure functions which may be taken to be $F_1^{\gamma p}$, $F_1^{\gamma n}$, $F_1^{\nu p}$, $F_1^{\nu n}$, $F_3^{\nu p}$, and $F_3^{\nu n}$. Using an iso-spin reflection to equate the distributions $u_p(x)$, $u_{\bar{p}}(x)$, $u_n(x)$, etc., for a proton target with $u_n(x)$, $u_{\bar{n}}(x)$, $u_p(x)$, etc., for a neutron target (where p, n and λ denote the three types of quarks) and noting that in the processes of interest here $u_\lambda(x)$ and $u_{\bar{\lambda}}(x)$ occur only in the combination $u_\lambda(x) + u_{\bar{\lambda}}(x)$, we see that there are five independent distributions (which we take to be the distributions for a proton target). We can, therefore, derive one relation^(L18) which is:

$$12 \left(F_1^{\gamma p} - F_1^{\gamma n} \right) = \left(F_3^{\nu p} - F_3^{\nu n} \right) \quad (3.89)$$

This result depends directly on the nonintegral charges attributed to the quarks.

In the Sakata or Fermi-Yang model, for example, the factor 12 is replaced by 4.

The fact that all the contributions to the F_i are positive gives the useful inequality^(L18):

$$F_1^{\nu p} + F_1^{\nu n} \leq \frac{18}{5} \left(F_1^{\gamma p} + F_1^{\gamma n} \right) \quad (3.90)$$

The equality is reached when $u_\lambda(x) = u_{\bar{\lambda}}(x) = 0$ since the strange quarks contribute to electromagnetic processes but not to $\Delta Y = 0$ weak processes. This relation is also peculiar to the quark model; in the Sakata (or Fermi-Yang) model the λ is neutral (does not exist) and the corresponding relation is an equality (with 2 replacing 18/5).

Integrals over certain combinations of the $u_i(x)$ are determined by the proton's conserved quantum numbers:

$$\begin{aligned} \text{Strangeness} = 0 &= \int (u_\lambda(x) - u_{\bar{\lambda}}(x)) dx \\ \text{Charge} = 1 &= \int \frac{2}{3} (u_p(x) - u_{\bar{p}}(x)) - \frac{1}{3} (u_n(x) - u_{\bar{n}}(x)) dx \\ \text{Baryon number} = 1 &= \int \frac{1}{3} (u_p(x) + u_n(x) - u_{\bar{p}}(x) - u_{\bar{n}}(x)) dx \end{aligned} \quad (3.91)$$

Written in terms of ω these relations give the sum rules:

$$\int (F_1^{\nu n} - F_1^{\nu p}) \frac{d\omega}{\omega^2} = 1 \quad (3.92)$$

$$-\int (F_3^{\nu p} + F_3^{\nu n}) \frac{d\omega}{\omega^2} = 6 \quad (3.93)$$

Equation (3.92) is the Bjorken "backward" sum rule;^(B22) rewriting it in terms of F_2 using Eq. (3.88) we recognize it as the scaling limit of the Adler sum rule.^(A5) The latter depends only on the isospin properties of the current and is true in almost any reputable model which scales. The Bjorken sum rule depends on the spin of the constituents (the right-hand side is zero in spin 0 parton models or the algebra of fields). Equation (3.93)^(G18) depends on the baryon number attributed to the quarks (see footnote on page 106); the right-hand side is 2 in the Sakata and Fermi-Yang models. The verification of (3.89) and (3.93) would establish the "truth" of the quark model.

Some inequalities follow from the fact that $\int u_p(x) dx > 2$ and $\int u_n(x) dx > 1$ ^(L18) but they are almost certainly trivially satisfied by the data.* More interesting inequalities follow from energy momentum conservation^(L20) which reads

$$1 = \int dx x \sum_i u_i(x)$$

*The inequalities for integrals over the F_i which follow from this result are not all independent. The positivity domains for these integrals, and other quantities, have been discussed in a systematic way by Nachtman.^(N3) He also points out that

$$1/4 \leq \frac{F_2^{\gamma p}}{F_2^{\gamma n}} = \frac{4(u_p^+ + u_p^-) + u_n^+ + u_n^- + u_\lambda^+ + u_\lambda^-}{u_p^+ + u_p^- + 4(u_n^+ + u_n^-) + u_\lambda^+ + u_\lambda^-} \leq 4$$

which is well satisfied by the data.

or

$$1 - \epsilon = \int d\mathbf{x} \sum_{q=1}^6 u_q(\mathbf{x}) \quad (3.94)$$

$$(0 \leq \epsilon \leq 1)$$

where ϵ is the fraction of the momentum carried by neutral particles or gluons which have no weak or electromagnetic charge but can carry momentum; such gluons are necessarily present in renormalizable field theories of interacting quarks. This gives the inequality^(L20)

$$\int \left(F_2^{\gamma p} + F_2^{\gamma n} \right) \frac{d\omega}{\omega^2} \leq \frac{5}{9} \quad (3.95)$$

which is almost certainly satisfied experimentally unless surprises await us at high energies (the equality is reached when both $\epsilon = 0$ and $u_\lambda(x) = u_{\bar{\lambda}}(x) = 0$). We might hope to establish that $\epsilon \neq 0$ using electromagnetic data alone since^(L20)

$$\int F_2^{\gamma p, \gamma n} \frac{d\omega}{\omega^2} \geq \frac{1}{9} (1 - \epsilon) \geq \frac{1}{9} \quad (\text{if } \epsilon = 0), \quad (3.96)$$

but this inequality is satisfied by the proton data and probably by the neutron data--see Eq. (3.114) (the term thrown away in (3.96) to get an inequality in, e. g., the γp case is $\int d\mathbf{x} \frac{1}{3} (u_p(x) + u_{\bar{p}}(x))$; in simple models, this is $\geq \frac{1}{9}(1 - \epsilon)$). A measurement of ϵ is given by^(L20):

$$\epsilon = 1 + \int \left[\frac{3}{4} \left(F_2^{\nu p} + F_2^{\nu n} \right) - \frac{9}{2} \left(F_2^{\gamma p} + F_2^{\gamma n} \right) \right] \frac{d\omega}{\omega^2} \quad (3.97)$$

We shall see in the next section that the data give $\epsilon \neq 0$ (with large errors).

The formal derivation of sum rules for the inclusive process starts from the expression (2.27) for the hadronic tensor:

$$W_{\mu\nu} = \sum \int \frac{d^4x}{4\pi} e^{iq \cdot x} \langle P \left[\left[J_\mu^+(x), J_\nu(0) \right] \right] P \rangle = \frac{1}{2\pi} \text{Im} T_{\mu\nu}^{\nu, \bar{\nu}} \quad (3.98)$$

$$T_{\mu\nu} = i \int d^4x e^{iq \cdot x} \theta(x_0) \langle P \left[\left[J_\mu^+(x), J_\nu(0) \right] \right] P \rangle$$

If we consider $T_{\mu\nu}$ in the limit $q_0 \rightarrow i\infty$, we might expect an expansion of $J_\mu(x)$ in x_0 to converge. This gives the Bjorken-Johnson-Low theorem:

$$T_{\mu\nu} \xrightarrow{q_0 \rightarrow i\infty} i \sum_n \left(\frac{i}{q_0} \right)^{n+1} \int e^{-i\vec{q} \cdot \vec{x}} d^3x \langle P \left[\left[\frac{\partial^n J_\mu(\vec{x}, 0)}{\partial t^n}, J_\nu(0) \right] \right] P \rangle \quad (3.99)$$

Of course, the commutator may not be smooth enough to allow this expansion and, in fact, it turns out that the equal time commutators obtained by calculating $T_{\mu\nu}$ in perturbation theory and using Eq. (3.99) do not always exist. Even when they do exist, they do not always coincide with the values obtained by naive canonical manipulations. Equation (3.99) could actually be adopted as an operational definition of the equal time commutators. As discussed above, we shall assume that the real world is smoother than perturbation theory suggests and that this definition agrees with the naive canonical result (any other assumption would deprive the ensuing sum rules of their predictive power).

The next step is to expand $T_{\mu\nu}$ in terms of available tensors just as we expanded $W_{\mu\nu}$ (assuming T invariance now):

$$T_{\mu\nu} = -g_{\mu\nu} T_1 + \frac{P_\mu P_\nu T_2}{M^2} - \frac{i \epsilon_{\mu\nu\alpha\beta} P_\alpha q_\beta T_3}{2M^2} + \frac{q_\mu q_\nu T_4}{M^2} + \frac{(q_\mu P_\nu + q_\nu P_\mu) T_5}{2M^2} \quad (3.100)$$

The T_i are analytic functions in the complex ν plane. The discontinuities across the cuts from $-\infty$ to $-Q^2/2$ and $Q^2/2$ to ∞ are $4\pi W_i$. Using the asymptotic

behavior suggested by Regge theory, we can, therefore, write:

$$T_{2,3,5}^{\nu, q^2} = 2 \int_{-\infty}^{+\infty} \frac{W_{2,3,5}(\nu', q^2) d\nu'}{\nu' - \nu} \quad (3.101)$$

$$T_{1,4}(\nu, q^2) = T_{1,4}(0, q^2) + 2\nu \int_{-\infty}^{+\infty} \frac{W_{1,4}(\nu', q^2) d\nu'}{\nu'(\nu' - \nu)}$$

Substituting Eq. (3.101) into Eq. (3.100), taking the limit $q_0 \rightarrow i\infty$ in a frame in which $\bar{q} = 0$ with $\omega = 2P_0 / -q_0$ fixed ($|\omega| < 1$) and comparing the coefficients of ω with those given by Eq. (3.99) gives^(C25, B24):

$$\begin{aligned} L_{xx}^n &= 2 \int_0^\infty \frac{F_1^\mp}{\omega^{n+2}} d\omega & (n=0, 1, 2, 3, \dots) \\ L_{zz}^n &= \int_1^\infty (2F_1^\mp - \omega F_2^\mp) \frac{d\omega}{\omega^{n+2}} & (n=1, 2, 3, \dots) \\ L_{yx}^n &= i \int_1^\infty F_3^\pm \frac{d\omega}{\omega^{n+2}} & (n=0, 1, 2, \dots) \\ L_{oz}^n &= \int_1^\infty (F_5^\mp - \omega F_2^\mp) \frac{d\omega}{\omega^{n+2}} & (n=1, 2, 3, \dots) \\ L_{oz}^n - L_{oo}^n - L_{zz}^n &= 4 \int_1^\infty \frac{F_4^\mp}{\omega^{n+3}} d\omega & (n=1, 2, 3, \dots) \\ L_{\mu\nu}^n &= \lim_{P_0 \rightarrow \infty} i \left(\frac{i}{2P_0} \right)^{n+1} \int d^4x \delta(x_0) \left\langle P_z \left[\frac{\partial^n J_\mu^+(x)}{\partial t^n}, J_\nu^-(0) \right] \right\rangle_{P_z} \end{aligned} \quad (3.102)$$

where the upper (lower) sign holds for n even (odd) and we have used the crossing relation (2.30) to get:

$$F_i^\pm = F_i^\nu \pm F_i^{\bar{\nu}} \quad (3.103)$$

In the quark model the $n = 0$ sum rules give (3.92) and (3.93). The sum rules for $n > 1$ involve time derivatives of currents and we must, therefore, specify the interaction Hamiltonian which we take to consist of renormalizable interactions:

$$\mathcal{H}_I = g_S \xi \bar{\psi} \psi + i g_P \phi \bar{\psi} \gamma_5 \psi + g_V B_\mu \bar{\psi} \gamma^\mu \psi \quad (3.104)$$

In this case we can recover the parton results (3.86), (3.87), (3.89), and (3.90). Actually we obtain an infinite number of moments of (3.89) and (3.90), e. g.:

$$\int \phi(\omega) \frac{d\omega}{\omega^{2n+1}} = 0, \quad n = 1, 2, 3, \dots \quad (3.105)$$

$$\phi(\omega) = 12 \left(F_1^{\gamma P} - F_1^{\gamma n} \right) - \left(F_3^{\nu P} - F_3^{\nu n} \right)$$

However, if we assume that $\phi(\omega)$ does not change sign an infinite number of times, this implies $\phi(\omega) = 0$.^(L20)

To understand how we get these results, consider the case $g_V = 0$ (they are also true for $g_V \neq 0$ but the argument is more involved).^{*(L20)} The locality of

*After the completion of this paper and circulation of a preliminary draft, we received a paper from Gross and Treiman^(G19) in which, among other things, these results are derived in an elegant way in the case $g_V \neq 0$ using the light cone expansion. With our approach it is almost obvious that the results are true when $g_V \neq 0$; we can show that we can put $M_V = 0$ in calculating the infinite momentum commutators which are obtained from the free field ones by putting $i\partial_\mu \rightarrow i\partial_\mu + g_V B_\mu$. This does not change the sum rules, which only depend on the Lorentz and SU(3) properties of the commutators.

the commutators gives the general form:

$$\int d^4x \delta(x_0) \langle P_Z \left| \left[\frac{\partial^n J_\mu^+(x)}{\partial t^n}, J_\nu^-(0) \right] \right| P_Z \rangle = \langle P_Z | O_{\mu\nu}^n(0) | P_Z \rangle \quad (3.106)$$

Contributions to $L_{\mu\nu}^n$ come only from pieces of the spin averaged matrix elements which grow like $|\vec{P}|^{n+1}$. The corresponding pieces of $O_{\mu\nu}^n$ are parts of $(n+1)^{\text{th}}$ rank Lorentz tensors which can be taken to be symmetric in their indices. The only possibility is

$$\sim \bar{\psi}(0) \gamma_{\alpha_1} \partial_{\alpha_2} \partial_{\alpha_3} \dots \partial_{\alpha_{n+1}} \psi(0) \quad (3.107)$$

We can, therefore, put $g_S = g_P = M_{\text{quark}} = 0$ in calculating $O_{\mu\nu}^n$. We have therefore "derived" the parton model since the moments of the structure functions are given by the same one body operators as in free field theory.

The remaining results (3.95), (3.96), and (3.97) are recovered^(L20) in the case $g_V = 0$ by studying the explicit form of the $n = 1$ sum rules for F_i^γ and F_i^+ which may be written

$$\int \frac{F_2^\gamma d\omega}{\omega^2} = \lim_{P_0 \rightarrow \infty} \frac{1}{2P_0^2} \langle P_Z | \bar{\psi}(0) (i\gamma_Z \partial_Z + g_V \gamma_Z B_Z) \left(\frac{2B}{3} + \frac{Y}{6} + \frac{I_3}{3} \right) \psi(0) | P_Z \rangle \quad (3.108)$$

$$\int (F_2^\nu + F_2^{\bar{\nu}}) \frac{d\omega}{\omega^2} = \lim_{P_0 \rightarrow \infty} \frac{1}{2P_0^2} \langle P_Z | \bar{\psi}(0) (i\gamma_Z \partial_Z + g_V \gamma_Z B_Z) (4B + 2Y) \psi(0) | P_Z \rangle$$

where B and Y are the usual 3×3 baryon and hypercharge matrices ($Q^2 = 2B/3 + Y/6 + I_3/3$). Note that B, B-Y and $2B+Y \pm 2I_3$ are positive diagonal matrices and their contributions to F_2 are positive semidefinite^(L18) (this was used in getting

the inequalities in (3.95) and (3.96)--it corresponds to the parton result that the contribution of each type of quark is positive). If $g_V = 0$:

$$\begin{aligned} \lim_{P_0 \rightarrow \infty} \frac{1}{2P_0^2} \langle P_Z | \bar{\psi}(0) i \gamma_Z \partial_Z B \psi(0) | P_Z \rangle &= \lim_{P_0 \rightarrow \infty} \frac{1}{6P_0^2} \langle P_Z | \theta_{ZZ} - \theta_{ZZ}^g - \mathcal{L} | P_Z \rangle \\ &= \frac{1}{3} (1 - \epsilon), \quad 0 \leq \epsilon \leq 1 \end{aligned} \quad (3.109)$$

$$\epsilon = \lim_{P_0 \rightarrow \infty} \frac{1}{2P_0^2} \langle P_Z | \theta_{ZZ}^g | P_Z \rangle$$

where $\theta_{\mu\nu}$ is the energy momentum tensor, $\theta_{\mu\nu}^g$ being the energy momentum tensor of a free gluon. Equations (3.109) and (3.108) can be combined to give (3.95), (3.96), and (3.97). When $g_V \neq 0$, (3.109) still holds with $i\partial_Z \rightarrow i\partial_Z + g_V B_Z$, but we have not been able to show that $\epsilon \geq 0$ in this case.

In order to get a more detailed feeling for what might reasonably be expected in neutrino experiments we now temporarily abandon the conservative attitude of only making algebraic abstractions from the parton model and take it more seriously. If the proton's momentum were equally distributed among the partons on average we would obtain

$$\langle x \rangle = \left\langle \frac{1}{N} \right\rangle \quad (3.110)$$

where N is the number of partons. Even if (3.110) is not exact, it is reasonable to suppose that the more partons are present the smaller the fraction of the momentum that each carries on average so that small x probes large N and vice versa.* Since some of the constituents in the neutron and proton must be different we expect (e.g.) that $F_2^{\gamma P} \neq F_2^{\gamma n}$, $F_2^{\nu P} \neq F_2^{\nu n}$ for $x \simeq 1$ but presumably they become

*Gourdin^(G13) has enumerated the consequences of (3.110) in the case that no further assumptions are made. Our discussion is more qualitative. Similar conclusions have been reached by other authors (see, e.g., L1) on the basis of superficially rather different assumptions.

equal as $x \rightarrow 0$ if configurations with large N play any role (otherwise the $F_2 \rightarrow 0$ in any case). This is just the prediction of the Regge model in which the Pomeron dominates in this limit.

Another Regge-like conclusion is reached if we consider the quantity

$$\frac{-(F_3^{\nu p} + F_3^{\nu n})x}{(F_2^{\nu p} + F_2^{\nu n})} = \frac{u_p(x) + u_n(x) - u_{\bar{p}}(x) - u_{\bar{n}}(x)}{u_p(x) + u_n(x) + u_{\bar{p}}(x) + u_{\bar{n}}(x)} \quad (3.111)$$

which is, in some sense, a measure of the average baryon number of the constituents. We expect it to be near one for $x \approx 1$ (N small) but go to zero as $x \rightarrow 0$ ($N \rightarrow \infty$).

Next we note that the cross section (3.75) depends on the integrals $\int F_2 dx$, $\int x F_1 dx$, and $\int x F_3 dx$. Assuming that $F_{1,2}^{\nu}$ are much the same as $F_{1,2}^{\gamma}$ and using the argument above for F_3 , we find that these integrals receive most ($\sim 70\%$) of their contribution from $x > 0.1$, $\omega < 10$ (unless quite unexpected behavior occurs in the unexplored small x region). Therefore, the total cross section is dominated by configurations with small N in the parton model, which suggests $\sigma^{\nu n} > \sigma^{\nu p} > \sigma^{\bar{\nu} p} > \sigma^{\bar{\nu} n}$ (although it is certainly possible to construct parton models which do not have this property).

Slightly more quantitatively, let us assume that F_3 is negative as suggested by Eq. (3.111) (this immediately gives $\sigma^{\nu} > \sigma^{\bar{\nu}}$). Equations (3.77) and (3.99)

*E.g., using the curves given by Kuti and Weisskopf^(K16) it is easy to see that the wave function discussed by them and by Bjorken^(B26) would give

$$\frac{\sigma^{\nu(p+n)}}{\sigma^{\bar{\nu}(p+n)}} \approx 2.0, \quad \frac{\sigma^{\nu n}}{\sigma^{\nu p}} \approx 1.7 .$$

Landshoff and Polkinghorne find 2.3 and 1.8 for these quantities in their closely related model.^(L1)

then give:

$$-x F_3^+ \leq F_2^+ \leq \frac{18}{5} (F_2^{\gamma p} + F_2^{\gamma n}) \quad (3.112)$$

The left-hand inequality is saturated when there are no antiquarks (3.111) and the right-hand one when there are no λ 's. Both conditions might be fulfilled for $x \approx 1$ (small N). Supposing that the inequalities are saturated for $x > x_c$ and using the Regge-inspired parameterization $F_3^+ = F_3^+(x_c) \left(2 \sqrt{\frac{x}{x_c}} - 1 \right)$ for $x < x_c$, the F_3^+ sum rule (3.93) then gives $x_c = 0.032$ ($\omega_c = 31$).^{*} This indicates that unless asymptotic (Regge) behavior sets in at rather small x , the inequalities in(3.112) may be approximately saturated for most x and perhaps:

$$- \int x F_3^+ dx \simeq \int F_2^+ dx \quad (3.113)$$

which would give $\sigma^{\nu p + \nu n} \simeq 3(\sigma^{\bar{\nu} p + \bar{\nu} n})$.^{**}

Before discussing the neutrino data, we shall assemble the relevant results for F_i^γ and put them into the appropriate sum rules. The sum rules involve integrals up to $\omega = \infty$ whereas the SLAC data goes up to $\omega \sim 12$ (data are available

^{*}We took $\int_{1/12}^1 (F_2^{\gamma p} + F_2^{\gamma n}) dx = 1.03$, $F_2^{\gamma p} + F_2^{\gamma n} = 0.6$ for $x < 1/12$. Many people favor a lower asymptotic value which would decrease x_c .

^{**}It is often erroneously stated in the literature that the model of Drell, Levy and Yan^(D9) leads to this prediction. Actually this model gives $d\sigma^\nu = 3 d\sigma^{\bar{\nu}}$ for $x \ll 1$, which is not a region of importance for the total cross section. Regge (diffractive) behavior is $d\sigma^\nu = d\sigma^{\bar{\nu}}$ for $x \ll 1$ but again this may not be reflected in the total cross section.

for higher ω but the value of Q^2 is very small); we are, therefore, forced to extrapolate to $\omega=\infty$ for which purpose we use Regge theory.* We adopt the values** (B35)

$$\int_1^{\infty} F_2^{\gamma p} \frac{d\omega}{\omega^2} = 0.16 \pm 0.02 \quad \int_1^{\infty} F_2^{\gamma n} \frac{d\omega}{\omega^2} = 0.12 \pm 0.02 \quad (3.114)$$

$$\int \frac{d\omega}{\omega} (F_2^{\gamma p} - F_2^{\gamma n}) = 0.19 \pm 0.08 \quad \int \frac{d\omega}{\omega^2} (F_2^{\gamma p} - F_2^{\gamma n}) = 0.04 \pm 0.02$$

and assume $2F_1^{\gamma} = \omega F_2^{\gamma}$ so that the sum rules give

$$\int \frac{d\omega}{\omega^2} (F_2^{\nu p} + F_2^{\nu n}) \leq 1.01 \pm 0.14 \quad \int \frac{d\omega}{\omega^3} (F_3^{\nu p} - F_3^{\nu n}) = 0.24 \pm 0.12 \quad (3.115)$$

for the most accessible integrals. The fact that ϵ must be ≥ 0 in Eq. (3.97) gives a lower bound on the first of these integrals but it is not very restrictive.

*i. e., the parameterization $F_2 \sim \omega^{\alpha-1}$, etc., as $\omega \rightarrow \infty$. Mathematically there need not be any connection between the behavior of the scaling functions in this limit and the Regge limit $\nu \rightarrow \infty$ at fixed Q^2 . However, if we suppose that F_2 depends only on ω for $Q^2 > Q_0^2$ and that Regge behavior occurs when $\nu \rightarrow \infty$, Q^2 fixed ($Q^2 > Q_0^2$), then the connection follows.

**The neutron data is preliminary. It may be subject to subtle corrections (due to the fact that it is extracted from e-d experiments) which would tend to decrease $F_2^{\gamma p} - F_2^{\gamma n}$ (W5) (see Section 3.10D).

D. Experimental Results

We shall only discuss the results of the CERN heavy liquid bubble chamber experiments here although some information is available from cosmic ray experiments (see M6 and also C15 for some more recent results). The most striking result is that the total cross section (Fig. 37) apparently rises linearly with energy in agreement with Bjorken's prediction. In the range 2 - 14 GeV, the propane data can be fitted by^(B47)

$$\sigma/\text{nucleon} = (0.52 \pm 0.13) \frac{G^2 M E}{\pi} \quad (3.116)$$

We now turn to a more detailed discussion following the recent analysis of the combined propane and Freon data by Myatt and Perkins^(M11) (see B47 for an earlier analysis of the propane data alone). Figure 38 shows that $q_{\text{av}}^2 = \text{const } E_\nu$ at large E_ν which is a test of scale invariance which has the advantage of being independent of a knowledge of the neutrino flux (obviously if no scale is defined, $\langle q^2 \rangle \sim S \sim M E_\nu$). The mean value of q^2 is also plotted in M11 for fixed ν integrated over E_ν . The result is consistent with a straight line and can be fitted by

$$\frac{\bar{q}^2}{M^2} = (0.50 \pm 0.04) \left(\frac{\nu}{M^2} + 0.53 \pm 0.10 \right) \quad (3.117)$$

Scaling predicts $\bar{q}^2 \propto \nu$ at large ν provided ωF_2 , F_1 and F_3 have the same ω behavior; additional evidence that this is the case will be quoted below.

Following Bloom and Gilman, one might make the further assumption that scaling occurs in an average sense in the variable

$$\omega' = \frac{2M\nu + M^2}{-q^2}$$

even in the non-asymptotic region. This would give $\bar{q}^2 = \text{const} \left(\nu + \frac{M^2}{2} \right)$ in

agreement with (3.117).^{*} This encouraged Myatt and Perkins to base their subsequent analysis on the proposition that scaling in ω' does indeed occur in the non-asymptotic region and to use all the events with $E_\nu > 1$ GeV.

We feel that this may be dangerous. The work of Bloom and Gilman^(B34) shows that (average) scaling obtains at much lower missing mass (encompassing part of the resonance region) in ω' than in ω but not at lower Q^2 .^(B35) In view of the results in Fig. 38, it seems that an analysis based on scaling is unlikely to work very well for events with $E_\nu < 4$ GeV and may be quite misleading for events with $E_\nu < 2$ GeV.

Myatt and Perkins^(M11) give q^2 distributions for various ranges of ν , and also $x' = \frac{1}{\omega'}$ distributions for various ranges of $y = \frac{\nu}{M E}$. These curves can be fitted quite nicely by the empirical formula $(1 - x'^2)^3$ in all cases, which indicates that F_2 , $x' F_1$ and $x' F_3$ must all have much the same x' dependence.

Before the relative magnitudes of $F_{1,2,3}$ were estimated, the data was weighted to simulate the results for an equal number of protons and neutrons using the estimate for $\frac{\sigma^{\nu n}}{\sigma^{\nu p}}$ below (actually this weighting has a negligible effect). The y distributions of the weighted data are shown in Fig. 39 for various ranges of E_ν . The results of fits for the ratios

$$A = \frac{\int \frac{2 F_1 d\omega}{\omega^3}}{\int \frac{F_2 d\omega}{\omega^2}} \qquad B = \frac{\int \frac{F_3 d\omega}{\omega^3}}{\int \frac{F_2 d\omega}{\omega^2}} \qquad (3.118)$$

^{*} $\omega' \min = \frac{2\nu + M^2}{2\nu} > 1$ which, strictly speaking, invalidates this conclusion except at large ν . However, the structure functions fall rapidly for $\omega' < 2$ so that this implicit ν dependence should not be important.

are shown in Fig. 40. The heavily hatched area contains the physically allowed region lying within one standard deviation of the best fit. We feel that this should not be taken too seriously. Forty-four percent of the events which contribute to Fig. 40 have $E_\nu < 2$ GeV and hence (Fig. 38) $\bar{q}^{-2} < 0.5$ GeV². Sticking to events with $E_\nu > 4$ GeV ($\bar{q}^{-2} > 1$ GeV²), the data in Fig. 39 is clearly compatible with B in the range 0 to -1 if A = 1. The best fit to all the data with $E_\nu > 1$ gave

$$\int (F_2^{\nu P} + F_2^{\nu}) \frac{d\omega}{\omega} = 1.54 \pm 0.28. \quad (3.119)$$

Much the same result was obtained by taking only the events in $0 < y < 0.2$ for the different ranges of E_ν and neglecting F_1 and F_3 , which make a negligible contribution in this range of y ; this procedure is subject to the criticism that small y selects small Q^2 (even at $E_\nu = 4$ GeV, events with $y < 0.2$ have $\bar{Q}^2 < 0.7$ GeV² according to 3.117).

The quantity $P = \sigma^{\nu n} / \sigma^{\nu P}$ was estimated as follows. After rejecting events containing more than one identified nucleon--thus indicating certain nuclear breakup--it was observed that, in the remainder (some 40% of the total), the net charge Q of all the secondaries was predominantly 0 or +1e. The relative numbers of these reflect the relative total cross sections on (bound) neutrons and protons, respectively, provided charge-transfer processes are not important; this receives support from the observation that only 3% of such "clean" events in propane, and 11% in Freon, had the "wrong" charge ($Q = -1, +2$ or $+3e$). For $E > 2$ GeV, P was approximately constant, with P (propane) = 1.8 ± 0.3 and P (Freon) = 1.1 ± 0.3 . Thus, the gross average value $P = \sigma^{\nu n} / \sigma^{\nu P} = 1.5 \pm 0.3$ was taken for the high-energy region.

Let us now summarize the main experimental results:

1. The linear rise of σ and the fact that $\bar{q}^{-2} = \text{const } E_\nu$ support the scaling hypothesis.
2. The data are compatible with $2 F_1 = \omega F_2$ ($\sigma_S = 0$) which is also suggested by electroproduction data.
3. The data suggest that B (Eq. 3.118) is negative which implies $\sigma^{\nu p} + \sigma^{\nu n} > \sigma^{\bar{\nu} p} + \sigma^{\bar{\nu} n}$. B could even be close to the minimum allowed value of -1, which would give $\sigma^{\nu p} + \sigma^{\nu n} = 3(\sigma^{\bar{\nu} p} + \sigma^{\bar{\nu} n})$. The available data on $\sigma^{\bar{\nu}}$ is meager and imprecise but suggests $\sigma^{\nu} > 2\sigma^{\bar{\nu}}$. (Y4)
4. Using (3.80), the total cross section (3.116) gives:

$$3.24 \pm 0.81 \gtrsim \int (F_2^{\nu p} + F_2^{\nu n}) \frac{d\omega}{\omega} \gtrsim 1.08 \pm 0.27 \quad (3.120)$$

where we have applied a 4% correction to (3.116) assuming $\frac{\sigma^{\nu n}}{\sigma^{\nu p}} = 1.5$.

If we assume $2 F_1 = \omega F_2$ and $B \lesssim 0$, the upper limit in (3.120) becomes 1.62 ± 0.41 . (We note that the total cross section measurement, (3.116), includes all events with $E_\nu > 2$ GeV. If we are more conservative and only take events with $E_\nu > 4$ GeV, so that $\bar{Q}^2 > 1 \text{ GeV}^2$, then straight lines drawn through the extreme ends of the vertical error bars in Fig. 37

and not constrained to go through the origin give a slope in the range

$$0.25 \frac{G^2 M E}{\pi} \text{ to } 0.98 \frac{G^2 M E}{\pi} .)$$

5. The data require $\sigma^{\nu n} > \sigma^{\nu p}$.
6. Present data do not allow us to draw any firm conclusions about $\Delta Y = 1$ reactions. (M10, Y4)

We note that these results are compatible with the quark model predictions discussed in the previous section. A comparison of Eq. (3.120) with (3.115)

requires that the inequalities are nearly saturated and that B must be negative (ignoring the errors, we would conclude that $B \simeq -1$), which is consistent with the independent experimental evidence that $B < 0$. Comparing (3.120) with (3.97), we get

$$\epsilon \simeq 0.52 \pm 0.38, \quad (3.121)$$

i. e., the present data require gluons as well as quarks (the errors are rather large so that it may be useful to invert the argument for comparison with future experiments: we find that if $\epsilon = 0$, the SLAC data require $\frac{\sigma^{\nu p} + \sigma^{\nu n}}{2} \simeq (0.17 \pm 0.12) \frac{G^2 M E}{\pi}$). No stringent tests of the model are possible at present but the agreement may not be completely trivial as is indicated by the fact that, taken literally, the data are already sufficient to eliminate the Sakata and Fermi-Yang models which give (see the discussion following (3.90))

$$\int (F_2^{\nu p} + F_2^{\nu n}) \frac{d\omega}{\omega^2} = 0.56 \pm 0.08$$

in disagreement with (3.120).

We do not believe that the quark model is necessarily correct. We have presented it in such detail because it seems to be the best model available and it illustrates the fact that high-energy experiments which can test the sum rules may provide fundamental information about the structure of nucleons if scaling is not a chimera. In particular, we note that the F_3 sum rule (3.93), which is the most easily tested experimentally, provides a strong test of the quark model commutators since it depends on the quarks having baryon number $1/3$.

3.7. Detailed Descriptions of Highly Inelastic Reactions

We now turn to more detailed descriptions of the events which make up the linearly rising cross section discussed in the last section. These events must come mainly from channels other than those which we have discussed in detail

so far, which are all expected to have constant cross sections for energies above a few GeV.

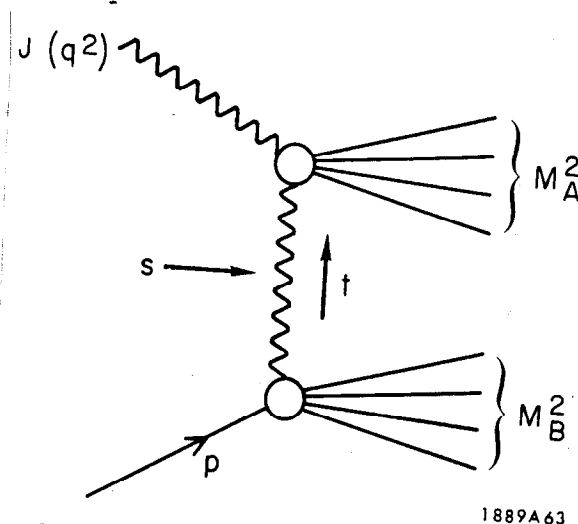
It is useful to distinguish two regions:

1. The diffractive region: ν/Q^2 large ($\nu > 3M^2 + 5Q^2$ might be a reasonable boundary). (N7, S15)
2. The large Q^2 region (in the scaling region but outside the diffractive region; $\omega < 10?$).

A. The Diffractive Region

As $\nu \rightarrow \infty$ with q^2 fixed and small it seems reasonable to treat the current, which is the effective projectile, as a particle of mass q^2 and use ideas borrowed from hadronic physics. For example, in this limit we expect the multiplicity to grow as $\bar{n} = c \log \nu$ and that Regge theory should apply. We do not think it appropriate to review work based on this idea in detail here but we will describe some of the results for illustration. A plausible guess is that this picture also applies as $\nu \rightarrow \infty$ with q^2 fixed and large (see (B26) for a different conjecture).

We shall consider in particular two-body final states or the situation in which all the internal variables of two groups of particles have been integrated over except their invariant masses.



1889A63

We might expect a diffraction picture to apply when $s(\nu)$ is much greater than Q^2 , t and $\frac{M_A^2 M_B^2}{M^2}$. In this picture the dominant channels are those in which no internal quantum numbers are exchanged in the t channel so that A has baryon number zero and $I=1$ (assuming $\Delta S=0$). If A is an eigenstate of G parity, it is produced predominantly by the vector (axial) current if $G = + (-)$ and the effect of $V-A$ interference terms should vanish as $s \rightarrow \infty$. Such general features have been discussed by Piketty and Stodolsky^(P16) and by Pais and Treiman.^(P3, P4, P7)

More specifically the cross section depends on five variables which may be taken to be E , ν , q^2 , ϕ (Eq. 2.10) and $t = (p - p_B)^2$ (M_A^2 and M_B^2 held fixed). The fourfold differential cross section has the form (2.10) with $f_i = f_i(\nu, q^2, t)$. This may be rewritten as^(P7):

$$\frac{d^4 \sigma}{dq^2 d\nu dt d\phi} = \frac{G^2}{E^2} \sum_{i=1}^9 \omega_i(\nu, q^2, t) x_i$$

$$\begin{aligned} x_1 &= 1 & x_6 &= \frac{1}{y} (1-y) \\ x_2 &= \sigma'^2 & x_7 &= \sigma' \cos \phi \\ x_3 &= \frac{1}{y} (1-y) \sigma' \cos \phi & x_8 &= \frac{1}{y} (2-y) \sigma \sin \phi \\ x_4 &= \sigma'^2 \cos 2\phi & x_9 &= \sigma'^2 \sin 2\phi \\ x_5 &= \sigma' \sin \phi \end{aligned} \tag{3.122}$$

$$y = \frac{\nu}{ME}, \quad \sigma' = \sqrt{\frac{4E(E-\nu)+q^2}{4\nu}} + 0(m^2)$$

Pais and Treiman^(P7) studied the ω_i in the case that B is a single nucleon. They found that ω_1 to ω_5 are due to VV and AA terms in the hadronic tensor but ω_6 to ω_9 are due to $V-A$ interference terms. ω_5 is due to leptonic VA interference

terms; it vanishes if all the hadronic form factors have the same phase. If A has a definite G parity, diffraction models, therefore, predict that ω_6 to ω_9 are unimportant at large ν/M^2 . The remaining ω_i behave like $\nu^{2\alpha_p(t)-1}$ as $\nu \rightarrow \infty$. If A is a single particle, the dominant amplitudes all have a common phase in the Regge model so that ω_5 vanishes. In particular channels Regge models give further strong constraints, e. g., if $A = \pi^+$, $\omega_4 = 2\omega_1$. It has been postulated that s channel helicity is conserved in the diffractive region which gives, (E3,P5) e. g., in the case $A = \pi^+$: $\omega_1 = \omega_3 = \omega_4 = \omega_5 = 0$ --a prediction which is easy to test (we note that it is likely to fail since evidence has recently been presented that s channel helicity is not conserved in the related process $\pi^- p \rightarrow A 1^- p$). (A21)

B. The Large Q^2 Region

A unique feature of neutrino and electron scattering is the ability to vary the "mass" of the current which is the effective projectile. At present the only information about the large Q^2 events comes from the CERN heavy liquid bubble chamber experiments (M10) (apart from one experiment on ρ electroproduction at large Q^2). (A19) In those experiments the final hadronic states showed characteristics similar to those familiar in strong interaction processes. Thus the average momentum transfer to the nucleon itself was small ($\leq 0.5 \text{ GeV}^2$), as can be deduced from Fig. 41, if we assume that protons and neutrons emerge from inelastic collisions with approximately equal probability. The pion multiplicity as a function of ν is shown in Fig. 42. The secondary pions were observed to have small transverse momenta (relative to the neutrino beam direction which is essentially coincident with \vec{q}) and energies generally below 1 GeV. (M10)

One of the difficulties in treating the large Q^2 region theoretically is that we like to believe that $\frac{\sigma_s}{\sigma_{R,L}}$ is small and that this implies that the constituents with which the current interacts have spin 1/2. These constituents are, therefore, not

the same as the particles seen in the final state, which are presumably mostly pions. Models which successfully describe high-energy multiparticle hadronic reactions, such as the multiperipheral model, are therefore not directly applicable, and we are reduced to unconvincing intuitive arguments. However, we will review a spectrum of possibilities since this subject is beginning to attract great attention and it may be useful to consider what distributions might be plotted.

We consider first the average multiplicity n . Each channel contributes a positive semidefinite amount to νW_2 . In order that $\nu W_2(\omega, s) \xrightarrow{s \rightarrow \infty} F_2(\omega)$, we are faced essentially with two possibilities.

1. As $s \rightarrow \infty$ the contribution of each channel $\rightarrow 0$ for $s \gg$ threshold.

The new channels which open up conspire to keep F_2 constant and $n(\omega, s)$ is an increasing function of s at fixed ω . Two conjectures:

- (a) On the basis of phase space, perhaps n depends only on s .

An appealing guess with the expected behavior as $\nu \rightarrow \infty$ at fixed Q^2 is $n \sim \log s$.

- (b) Perhaps n increases with Q^2 at fixed s , maybe very slowly.

This is suggested by models in which resonance production dominates; in a geometrical picture, resonances of increasingly large spin can be excited in this limit because

$$l \sim |\vec{q}|_{\text{c.m.}} \quad R \sim \sqrt{\frac{(s - M^2 + Q^2)^2}{4s} + 2M^2 Q^2} \quad R \text{ (writing the}$$

interaction radius as $R = R_{\text{proton}} + R_{\gamma}(Q^2)$, with $R_{\text{proton}} \simeq R_{\gamma}(0)$, a decreasing R_{γ} need not matter). In such models it can be argued that the decay multiplicity increases with the spin.

2. Individual channels scale. In this case we are invited to believe that the new channels which open up continuously as s increases do not play an important role once we are in the scaling region in order that νW_2 does not increase. Perhaps $n(\omega, s) = f(\omega)$,* where $f(\omega)$ increases with ω because of phase space (if the channels which scale have small multiplicity, this could explain the fact that scaling occurs for quite small $s \gtrsim 6 \text{ GeV}^2$). (S16, L6) This result would be true in parton models if the effects of "dressing" the "bare" partons and of final state interactions could really be neglected; thus, e. g., Drell, Levy and Yan find^(D9) $n \sim \log \omega$ for large ω in their model.

For the momentum distributions a popular and intuitively appealing view is that the final particles are divided into two groups, A and B. (D9, B25, B26) In the laboratory system any final hadron in Group B emerges within a cone of width $|\vec{P}_{\perp \text{ max}}| \approx 400 \text{ MeV}$ along the momentum transfer direction \vec{q} and with a finite fraction of the energy ν ; hadrons in Group A are "left behind" with low energy and momentum $\langle \vec{P} \rangle \lesssim 400 \text{ MeV}$. This is suggested by the parton model in which one parton is "struck out" and subsequently dressed to give Group B. The remaining partons give rise to Group A. For the longitudinal momentum distribution

*This is by no means inevitable even if each channel scales; e. g., if $\nu W_2 = c \sum_n \frac{1}{n} \theta(\sqrt{s} - n\mu) \sim c \int_1^{\sqrt{s}/\mu} \frac{dn}{n} = c$, we find $\bar{n} \sim \int_1^{\sqrt{s}/\mu} \frac{dn}{n} = \frac{1}{2} \log\left(\frac{s}{\mu^2}\right)$. (I am indebted to Luca Caneschi for this example.) T. D. Lee has presented some of the arguments above in a more quantitative way.^(L6) In his model, each channel scales, $\bar{n} \sim \log s$, but the multiplicity for hard pions is a function of ω only.

Drell and Yan have derived the scaling law^(D10)

$$\frac{d\sigma}{dx} = \frac{1}{x} f(x, \omega), \quad x = \frac{P_L}{\nu} \quad (3.123)$$

for the particles in group B in their model.

Finally we turn to the relative distributions of various species. Again there is no unanimity. For example, some people have conjectured that as Q^2 increases and shorter distances are probed, SU(3) should become more exact and, e.g., the K/π ratio should increase. On the other hand, in models in which resonances intervene SU(3) should be just as bad as in other processes. This is exemplified by a model which we shall briefly consider in order to illustrate the sort of distribution which might be interesting. Suppose that partons are quarks; then the quark ejected along \bar{q} may lose its energy by successive meson emission until it can merge with the remaining nucleonic debris to form a particle of integral baryon number.^(B26) If we assume that the first (leading) meson emitted is a pseudoscalar, it is easy to construct a table which gives the relative probability of it being a π^+ , π^- , etc. For example, a few entries are:

	π^+	π^-	π^0	K^+	K^-
γp	8/9 (5/9)	1/9 (5/9)	1/2 (5/9)	8/9 (5/9)	0 (5/9)
νp	1 (2)	0 (0)	1/2 (1)	1 (1)	0 (0)
$\bar{\nu} p$	0 (0)	2 (2)	1 (1)	0 (0)	0 (1)

where the first numbers hold if the proton ~ 3 quarks (for small ω perhaps) and the numbers in parentheses if the proton $\sim Q\bar{Q}$ sea (large ω). If we also allow 1^- mesons (ρ , K^* , etc.) to be emitted, the picture is changed; e.g., the fact that because of SU(3) breaking in the masses $\rho \longrightarrow \pi\pi$ but $\rho \not\longrightarrow \bar{K}K$ decreases the K/π ratio and ρ^0 's reduce the π^+/π^- ratio.

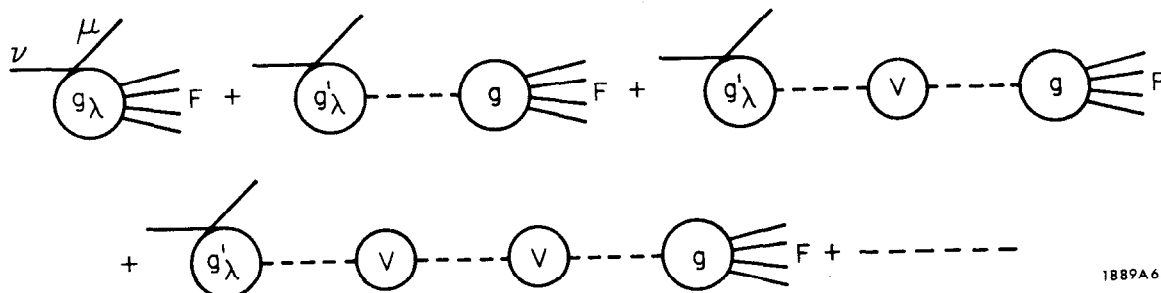
In this quark model, the baryon number remains roughly at rest in the laboratory. In contrast, in Drell's model^(D9) the baryon is found in the jet along \vec{q} in the limit $\omega \rightarrow \infty$ (baryon exchange!). Again we are truly ignorant and it is this that makes the subject interesting.

3.8. Tests of PCAC

Here we shall consider attempts to check Adler's theorem (2.22) and the related shadow effect which we discussed in Section 2.2B. In Fig. 43 we show the forward neutrino cross section calculated using (2.22) for orientation.

A. The Shadow Effect

We begin by recalling an argument of Bell's^(B7) which shows very simply how shadowing can occur in reactions on nuclei. In infinite nuclear matter, the amplitude for producing a final state F is given by adding the diagrams:



where g and g' represent the appropriate amplitudes or currents and V indicates that the meson ----- may interact coherently with the optical potential any number of times before causing the reaction. At low energies it seems reasonable to neglect the coherent propagation of mesons other than the pion (we consider their effect in Section 3.10D) so that the diagrams add to give:

$$M = j^\lambda \left(g_\lambda + g'_\lambda \frac{1}{q^2 - M_\pi^2 - V} g \right) \quad (3.124)$$

For $q^2 \simeq 0$, the various terms are related by generalized Goldberger-Treiman relations (PCAC), thus:

$$q^\lambda g_\lambda = C g, \quad q^\lambda g'_\lambda = C V$$

When $q^2 = 0$, Adler's theorem gives $j^\lambda \propto q^\lambda$ (neglecting m^2) so that

$$M(q^2=0) \propto \frac{M_\pi^2}{M_\pi^2 + V(0)} C g . \quad (3.125)$$

Relative to the amplitude for a single nucleon target, there is a suppression-- "shadow"--factor $\frac{M_\pi^2}{M_\pi^2 + V(0)}$. Some idea of the importance of the effect may be gained from Fig. 44 which shows the double differential cross section in the forward direction $q^2 \simeq 0$ obtained using the static isobar model described in Section 3.5B for $E_\nu = 4 M_p$. The "shadowed" curve was obtained by multiplying by the shadow factor corresponding to a simple forward scattering amplitude approximation for the optical potential V.

In finite nuclear matter the coherent pion wave (χ) can be treated using the optical model equation^(B7):

$$\left(\nabla^2 + q_0^2 - M_\pi^2 - V \right) \chi = \vec{u} \cdot \vec{j} e^{i\vec{q} \cdot \vec{x}} \quad (3.126)$$

where \vec{u} is the transition potential (corresponding to g'_λ above) and j_0 has been eliminated using $q \cdot j = 0$ (m^2). In practice, the optical potential should be obtained from phenomenological studies of pion-nucleus scattering. However, it is clear from Fig. 43 that at the neutrino energies available at CERN, with which we are mainly concerned here, the production of the $N^*(1238)$ is of major importance. Optical model studies are not well developed at these energies. We are, therefore, reduced to studying the case of a plane wave propagating in an infinite medium^(B10) although this may be rather remote from the actual case of rather long wave length pions in finite nuclei.

To interpret the experiments, we must construct a model valid away from $q^2 = 0$. First we note that in an infinite homogeneous medium only the longitudinal current (ℓ_3 along \vec{q}) can generate a coherent pion wave (by rotational invariance). The transverse component gives rise to an unshadowed background whose relative importance depends on $\frac{|\vec{\ell}_t|}{|\ell_3|}$. The explicit form of the lepton current in the laboratory is:

$$\ell_\mu = 4 \sqrt{k_0 k'_0} e^{-i\phi/2} \cos \theta/2 (1, -i \tan \theta/2 e^{i\phi}, -\tan \theta/2 e^{i\phi}, 1) \quad (3.127)$$

where θ and ϕ are the Euler angles which take \vec{k} into \vec{k}' ($\psi = 0$). Hence

$$\lim_{\substack{E \rightarrow \infty \\ \nu, q^2 \text{ fixed} \\ (q^2 \text{ small})}} \frac{|\vec{\ell}_t|}{|\ell_3|} \approx \frac{E - \nu}{\nu} \theta \approx \sqrt{\frac{q^2}{q_3^2}}. \quad (3.128)$$

For N^* production, for which $\nu \simeq 300$ MeV when q^2 is small, this ratio will be substantial if E is a few GeV unless θ is minute. (B8)

The shadow effect depends on the second term in:

$$M = \frac{(q^2 - M_\pi^2)}{(q^2 - M_\pi^2 - V)} j^\lambda g_\lambda + \frac{j^\lambda (g'_\lambda - g_\lambda V)}{(q^2 - M_\pi^2 - V)} \quad (3.129)$$

vanishing at $q^2 = 0$, due to PCAC. Away from $q^2 = 0$ we no longer know how to treat the second term in general. However, in the particular case of the static model, a longitudinal current is equivalent to an incident pion for all q^2 (cf Eqs. (3.52) and (3.53)). Therefore, we might use the static model assuming that the transverse component is unshadowed and the longitudinal component is damped by a factor

$$\left| \frac{q^2 - M_\pi^2}{q^2 - M_\pi^2 - V} \right|. \quad (B10)$$

In this model the differential cross section on a free nucleon for $q^2 \approx 0$ has the form^(B10) (cf Eq. 3.57):

$$\frac{d\sigma}{dq^2} \propto 1 \quad \begin{array}{l} \text{(longitudinal} \\ \text{axial)} \end{array} + \underbrace{\frac{1.74q^2}{q_3^2} + \frac{5.2q^2}{ME} + \frac{3.84q^2}{M^2}}_{\text{transverse}} \quad \begin{array}{l} \text{(axial} \\ \text{interference} \\ \text{vector)} \end{array} \quad (3.130)$$

$$\propto 1 + \frac{16.3q^2}{M^2} + \frac{5.2q^2}{ME} \quad \text{(at the } N^* \text{)} .$$

The transverse and the longitudinal terms, therefore, become comparable for $\theta \approx \frac{12.7 M}{E}$ degrees. In Fig. 45 we show the exact results obtained in the static model integrated over the CERN neutrino spectrum with the experimental cuts used in the CERN "shadow" experiment.

The transverse and longitudinal contributions become comparable at such small angles because $\left| \frac{\ell_t}{\ell_3} \right|$ grows rapidly with θ . This growth is especially rapid in the CERN experiment because $E - \nu > 1.2$ GeV. Since $\left. \frac{d\sigma}{d(\cos \theta)} \right|_{\theta=0} \sim E(E - \nu)$, the appropriate value of E in Eq. (3.128) is quite large. We conclude that at low energies the shadow effect will only become pronounced at very small angles.

We note that, in contrast to the shadow effect with incident photons, the neutrino shadow involves the coherent propagation of charged mesons. These mesons and the outgoing lepton will be influenced by the nuclear Coulomb field. It might be feared that the effect could be large in heavy nuclei. This question has been investigated by Nachtman and it seems that the effect is likely to be small. (N2)

B. Experimental Results

In an experiment performed at CERN slabs of various materials were placed as targets between spark chambers. (B38, H4) The neutrino beam traversed the apparatus and the numbers of muons produced in given angular ranges by different materials were compared. For the smallest angle sample the result was:

$$R_{\text{expt}} = \frac{\sigma_{\nu}(\text{Pb})/208}{\sigma_{\nu}(\text{C})/12} = 0.92 \pm 0.15 \quad (\theta < 5^\circ)$$

Unfortunately it was experimentally impossible to distinguish elastic events (which are not shadowed). Using the Fermi gas model for the elastic events and the static model for the inelastic with the cuts used in the experiment ($\theta < 5^\circ$, $E' > 1.2 \text{ GeV}$), we found (B10):

$$\begin{aligned} R &= 1.15 \quad (\text{no shadowing}) \\ &= 0.96 \quad (\text{with shadowing}) \end{aligned}$$

where we did not change $\sigma_{\pi}(\text{C})$ in the second line but kept $\sigma_{\pi}(\text{Pb}) < \frac{2\pi R^2}{A}$ -- both these assumptions are probably unrealistic and tend to exaggerate the decrease of R (without shadowing we found that the percentage of elastic events was 40% in C and 53% in Pb). In our model (B10) we see that the shadowed term is compensated by the elastic interaction (which grows faster than A) and masked by unshadowed terms which grow rapidly away from the forward direction.

The CERN bubble chamber group attempted to check (2.22) directly (B37; see M7 for a detailed discussion) for which purpose a subsidiary π^{\pm} propane experiment was performed at Saclay. Events were selected with $\theta < 13^\circ$ and $W^2 > 1.2 \text{ GeV}^2$, to exclude quasi-elastic events. This left 55 neutrino events and the tests were inconclusive. Since the events were dominated by N^* production,

the angular cutoff was in any case much too large to make meaningful tests according to the static model.

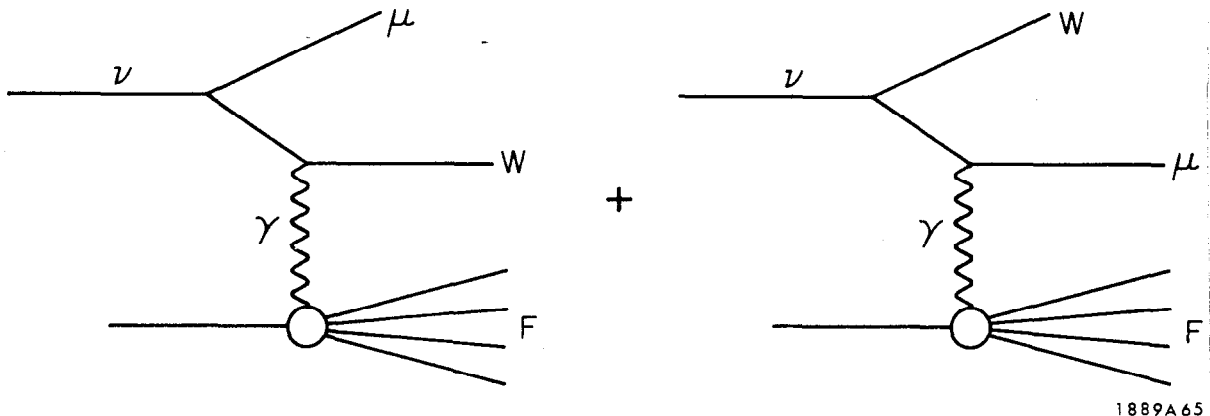
We see that Adler's theorem and its consequences have not yet been subjected to stringent tests which will probably require rather refined measurements.

3.9. W production

In this section we shall discuss W production by neutrinos. At the end we discuss the detection of the W and its branching ratios and we list other means of establishing its existence.

A. Production Cross Section

Assuming that the W does not interact strongly with hadrons, the leading diagrams for W production are:



The cross sections corresponding to these diagrams can be calculated exactly provided we assume that the W has a constant form factor, which is plausible if it has no strong interactions. The only unknown parameters in the calculation are M_W and the anomalous magnetic moment K (it is traditional to assume that the W has no electric quadrupole moment).

Many authors have discussed these processes. Earlier calculations^(L7, S12, B12, V3, W8, U1) treated the case where the target is a nucleus of charge Z which

recoils coherently, giving a factor Z^2 in the cross section per nucleus, and the case of incoherent scattering from nuclei without meson production. The SLAC inelastic electron scattering data suggests that events in which the nucleon breaks up may also be important, however. This is because, except in the limit $E \rightarrow \infty$, there is a minimum momentum transfer to the nucleon $\left(\sim (M_W^2/2E)^2 \text{ as } E \rightarrow \infty \right)$ and the inelastic form factors fall off less rapidly with q^2 than the elastic form factors.

Here we shall discuss the results of Brown and Smith^(B43) who have recently carried out extensive calculations at NAL energies. As the latest workers in this field, they enjoyed the fruits of previous labors with which they made comparison whenever possible. Reasonable agreement was found with all previous calculations of the "elastic" process except those of Berkov et al.^(B13) For the "inelastic" process the results agreed with the work of Chen^(C13) and reasonably well with calculations by Reiff^(R3) but not with those by Folomeshkin.^(F9)

We refer to B43 for details of the calculations, which are straightforward in principle (although very hard in practice), and for the complete results, of which we only give a small sample. Taking:

$$G_E(\text{proton}) = \frac{G_M(\text{proton})}{2.79} = -\frac{G_M(\text{neutron})}{1.91} = \frac{1}{\left(1 - \frac{q^2}{0.71 \text{ GeV}^2}\right)^2} \quad (3.131)$$

$$G_E(\text{neutron}) = 0$$

the total cross section in Fig. 46 was obtained for "elastic" scattering from p and n targets with $M_W = 7 \text{ GeV}$ and various values of K (see also Table 9).

Cross sections were calculated for a proton target which is broken up, using a simple fit to the inelastic electromagnetic form factors. Results are shown in Fig. 47 and Table 9.

With nuclear targets three processes occur:

- coherent scattering
- incoherent scattering without meson production
- incoherent scattering with meson production

For coherent scattering, a nuclear form factor corresponding to the charge density

$$\rho(r) = \frac{C}{1 + e^{(r-R)/b}}$$

$$R = 1.07 A^{1/3} \times 10^{-13} \text{ cm}$$

$$b = 0.568 \times 10^{-13} \text{ cm}$$

$$\int \rho(r) d^3r = Z$$
(3.132)

was adopted and $M_{\text{nucleus}} = \infty$ was used in the kinematics. Some results are shown in Fig. 48 and Table 9.

In the second process it is important to take into account the exclusion principle which restricts the final states available. This was done according to the prescription of Bell and Veltman^(B12) and Fermi motion was included using the method of von Gehlen.^(V3) Results are given in Table 9. Despite the extra factor Z^2 the coherent cross sections are much smaller than the incoherent at nonasymptotic energies because the minimum momentum transfer is substantial and the nuclear form factor falls off rapidly.

The various contributions considered so far can be fairly plausibly combined in the form

$$\sigma = Z \sigma'_p + (A - Z) \sigma'_n + \sigma_{\text{coh}} \text{ (nucleus)}$$
(3.133)

where $\sigma'_{p(n)}$ is the cross section given in Table 9 for "elastic" scattering off a bound proton (neutron) with the exclusion principle and Fermi motion included.

Processes of the third type (incoherent scattering with meson production) were not taken into account and would, in fact, be very difficult to treat correctly; presumably the ratio of their contribution to that of the incoherent quasi-elastic process is roughly the same as the ratio of "inelastic" to "elastic" interactions with a nucleon target so that they are not very important in the cases of interest.

Brown, Hobbs and Smith^(B44) have calculated the angle and energy distributions and the polarizations of the μ^- and W^+ in $\nu A \rightarrow \mu^- W^+ + \dots$ (we refer to their paper for references to earlier work on this subject). In the "elastic" case the rapidly decreasing nucleon form factors strongly favor small momentum transfers t to the nucleon and hence small $(\mu^- W^+)$ invariant mass. At t_{\min} , $\frac{E_{\mu}}{E_W} = \frac{M_{\mu}}{M_W}$ so that it is easy to understand why in general the μ^- takes a small fraction of the neutrino's energy--as illustrated in Fig. 49. The W^+ spectrum is extremely strongly peaked in the forward direction because of the importance of small t . Since at t_{\min} the W^+ and the μ^- travel in the same direction in the laboratory, we can also understand why the μ^- generally tends to continue forward--as shown in Fig. 50. The W^+ polarization is predominantly left-handed, as originally pointed out by Bell and Veltman for lower energies. These results are not altered qualitatively if the "inelastic" channels in which the nucleon breaks up are included.

B. Branching Ratios and the Detection of W's

An important parameter for the interpretation of experiments on W production is the branching ratio

$$B = \frac{\Gamma(W \rightarrow \mu \nu) + \Gamma(W \rightarrow e \nu)}{\Gamma(W \rightarrow \text{hadrons})} \quad (3.134)$$

The value of B has been considered by many authors but no very model independent results have been obtained. $\Gamma(W \rightarrow \text{hadrons})$ depends on the spectral functions ρ_V and ρ_A of the vector and axial vector currents at $q^2 = M_W^2$. ρ_V can be obtained

from $\sigma(e^+ e^- \rightarrow I = 1 \text{ states})$ by an isospin rotation if the isotriplet current hypothesis is assumed. Pais and Treiman^(P8) have recently suggested a way to obtain ρ_A from $e^+ e^-$ annihilation experiments using PCAC and current algebra but the extrapolation required is probably too enormous to be reliable (in principle it can be checked by another prediction). $e^+ e^-$ experiments have not yet been performed at the energies of interest here.

We shall give a guess for B based on the notions of asymptotic chiral symmetry:

$$\lim_{E \rightarrow \infty} \frac{\rho_V}{\rho_A} \rightarrow 1 \quad (3.135)$$

and asymptotic SU(3)

$$\lim_{E \rightarrow \infty} \frac{\sigma(e^+ e^- \rightarrow I = 1 \text{ states})}{\sigma(e^+ e^- \rightarrow I = 0 \text{ states})} = 3 \quad (3.136)$$

Assuming

$$\lim_{E \rightarrow \infty} \sigma(e^+ e^- \rightarrow \text{hadrons}) = C/E^2 \quad (3.137)$$

in accordance with currently fashionable ideas (and noting that if σ falls off more rapidly then $B \rightarrow \infty$ as $M_W \rightarrow \infty$), we find for large M_W :

$$B = 4/3 C \quad (3.138)$$

C being unknown at present, we give the free quark values $C = 2/3$, $B = 2$ for orientation purposes. However, it turns out that the signature for W production is quite clear whatever the value of B.

When the W decays to $\mu \nu$ the signature is the presence of two oppositely charged muons one of which (from W decay) has large transverse momentum $\sim M_W/2$. The characteristics of other processes which yield dimuons were

given in Table 3. It seems that W production will be easy to detect unless B is small.

When the W decays into hadrons, the process simulates an ordinary inelastic neutrino reaction. However, the calculations of Brown, Hobbs and Smith, discussed above, indicate that the μ^- takes a small fraction of E_ν (i.e., ν is large) and tends to be emitted in the forward direction (i.e., Q^2 is small). On the basis of these calculations, Cline et al. ^(C23) estimated that most of such "quasi-deep inelastic" events are contained in the region

$$x = Q^2/2\nu \leq 3 \times 10^{-2}, y = \nu/ME > 0.85$$

which is quite unlike the distribution in genuine inelastic hadron production. This is illustrated in Fig. 51. It is apparent that it should be easy to detect W production by observing the hadronic decays if B is small.

C. Other Means of Establishing the Existence of W's

Before tabulating other means of W production for comparison, we should emphasize that all the present discussion applies to the conventional case of a spin-1 W without strong interactions. If spin-0 W's also exist the decay schemes could be quite different (see Section 1.5C; production cross sections in the model of Lee and Wick have been calculated by Reiff. ^(R4))

Other possible means of producing W's, or detecting their existence, are

1. With incident muons. However, it turns out that the cross section is much less than with incident neutrinos and is further substantially reduced in the realistic case that the (polarized) μ 's from $\pi_{\mu 2}/K_{\mu 2}$ decay are used. (B3, B43, R3)
2. In the process $e^+ e^- \longrightarrow W^+ W^-$. If W's are point-like, the cross section is substantial for large E but threshold is unlikely to be reached with the coming generation of storage rings.

3. In the process $pp \rightarrow W + \dots$ (a "semiweak" process). If the W decays leptonically, the signature of this process is the production of a lepton with large transverse momentum. The apparatus must, therefore, be able to distinguish these single leptons from pairs of leptons produced with large transverse momentum in the process $pp \rightarrow \gamma (\rightarrow l^+ l^-) + \dots$ ^(Y3)
- Because of the intimate connection between the production of a W and a photon with $q^2 = M_W^2$ in most models, the W production cross section can be calculated approximately from the dimuon cross section ^(Y3) and this allows limits to be set on M_W if W's are not observed (assuming a value for the branching ratio B). When the W decays hadronically, the resulting high transverse momentum hadrons are uncharacteristic of hadronic events but they could be produced by virtual photons or other mechanisms (see B48). Present data on dimuon production, scaled using the model of Drell and Yan, ^(D11) suggests that the W production cross section at (e.g.) 500 GeV will be $> 10^{-36} \text{ cm}^2$ for $M_W < 28 \text{ GeV}$ in which case experiments at the CERN-ISR and NAL will shortly set greatly improved limits on M_W . (Other scaling models give even larger cross sections.) ^(A17)
4. Deviations from linearity in $\sigma_{\text{total}}^\nu(E)$, if scaling is correct (see Eq. 3.81). In fact, if $M_W = 20 \text{ GeV}$, the cross section at 100 GeV is reduced to $\sim 20\%$ below the value obtained by extrapolation from lower energies. This may therefore provide a very sensitive means of detecting W's. *

*In their analysis of the Case-Wits-Irvine experiment (on muons produced deep underground by cosmic ray neutrinos) Reines et al. ^(C15) found:

- (1) If $\sigma(\nu p) = \sigma(\nu n) = \sigma(\bar{\nu} p) = \sigma(\bar{\nu} n)$, then $45 \text{ GeV} > M_W > 2.9 \text{ GeV}$.
- (2) If $\sigma(\nu p) = \sigma(\nu n) = 3 \sigma(\bar{\nu} p) = 3 \sigma(\bar{\nu} n)$, then $M_W > 2.3 \text{ GeV}$.

The upper limit comes from assuming scale invariance and analyzing possible deviations from linearity in the extrapolated CERN cross section. The lower limits come from the absence of evidence for W production. (The limits are at the one standard deviation level.)

3.10. Miscellaneous Topics

A. Experimental Anomalies (possible "lepton hadron resonances")

Yoshiki plotted the number of quasi-elastic events in the CERN bubble chamber experiments against the muon-proton invariant mass.^(B45) The results are shown in Fig. 52. The enhancement at a mass of about 1.9 GeV is about three standard deviations from the background attributed to the conventional quasi-elastic process and it appeared at the same position in both the Freon and propane runs. This bump is too small to be the one which (as Kinoshita pointed out^(K9)) would occur if the theory of Tanikawa and Watanabe were correct (Section 1.5D). Furthermore, the angular distribution (Fig. 52) excludes spin 0, which is required in that theory. de Rujula and Zia^(D5) have made a thorough analysis of the consequences of the assumption that the effect is not statistical and can be attributed to a new lepton-baryon resonance. They find that the existence of such an object is not excluded by other experiments ($g-2$, $K_L \rightarrow \mu^+ \mu^-$, etc.) and that it would be hard to detect in other processes. Future experiments will certainly establish whether the phenomenon is a real one.

Another anomalous enhancement in the CERN neutrino data was pointed out by Ramm^(R1) who plotted the $(\mu^- \pi^+)$ and $(\mu^+ \pi^-)$ mass distributions. Some of his results are shown in Fig. 53. The $(\mu^\pm \gamma)$ mass distribution seems to be enhanced in the same energy range.^(R2) Such an enhancement is also seen in $\mu \gamma$ mass distributions obtained in inelastic muon scattering experiments.^(L15) Ramm also claims there is evidence for an anomaly in $\mu \pi$ mass distributions in K_{l3} decays at this energy.^(R1) He concludes that there may exist a resonance with mass M^{+-0} in the range $0.422 \text{ GeV} < M^{+-0} < 0.437 \text{ GeV}$ and a lifetime in the range $10^{-12} - 10^{-22}$ sec (however, doubts have been expressed about the identification of this effect as a resonance.)^(V2) Further data will provide clarification of this very interesting possibility.

These possible anomalies remind us once again that quite unexpected phenomena may be uncovered by high energy neutrino experiments and that it is certainly worth plotting peculiar distributions to look for them (a point we tried to stress in Chapter 1).*

B. Y* Production by Neutrinos

The phenomenological description of N* production in Section 3.5 clearly applies for all members of the $J = 3/2^+$ decuplet. The only other such processes which occur in the conventional theory are $\bar{\nu}n \rightarrow \mu^+ Y^{*-}$ and $\bar{\nu}p \rightarrow \mu^+ Y^{*0}$ for which the $\Delta I = 1/2$ rule gives a ratio of 2:1 (Eq. 2.12). These processes are related to N* production by antineutrinos in the limit of exact SU(3) symmetry. Some results obtained by Wachsmuth^(W9) using the model of Albright and Liu are shown in Fig. 54.

C. Neutrino Production of Higher Resonances

Production of resonances other than the N*(1238) has been considered by Bottino et al.^(B49) and by Zucker.^(Z1)

D. Nuclear Effects in Inelastic Reactions

We consider two effects:

1. The kinematical effect discussed by West.^(W5) This effect, which must exist in principle, occurs because of the Fermi motion. The inelastic threshold increases when the target nucleon is moving away from the incoming beam and this depletes the cross section relative to the result which would be obtained if the nucleus were a collection of stationary nucleons. The effect "scales," i. e., it does not vanish when $\nu \rightarrow \infty$ with ω fixed. Its importance depends sensitively on the choice of wave function. We note that the concept of wave function makes no sense at

*See the paper by Mikamo, Mizutani and Mori^(M8) for a review of possible anomalies in cosmic ray muon data.

the momenta which must play a role if the effect is appreciable, i. e., it can only be reliably calculated in models in which it is negligible! However, it is very unlikely to reduce the cross section per nucleon by more than 5% relative to $(Z \sigma_p + (A - Z) \sigma_n)/A$.^(W6) The main importance of the effect is its influence on the deduction of $\sigma_p - \sigma_n$ from σ_p and σ_d if $\sigma_p - \sigma_n$ is small.

2. Shadowing. We already discussed the PCAC shadow effect extensively in Section 3.8. Now we return to the question of shadowing due to the coherent propagation of mesons other than the pion. Consider the vector current in models in which vector dominance is exact so that the second term in the analogue of (3.129) vanishes for all q^2 . In this case, in infinite nuclear matter:

$$j^\lambda V_\lambda = \frac{(q^2 - M_\rho^2)}{(q^2 - M_\rho^2 - V)} j^\lambda \nu_\lambda .$$

In the forward scattering approximation

$$V = -i \sqrt{q_0^2 - M_\rho^2} \rho \sigma_{\rho N} \simeq -i \frac{M_\rho^2 \sqrt{q_0^2 - M_\rho^2}}{6 \text{ GeV}} \quad (\text{where } \rho \text{ is}$$

the nuclear density). For $|q^2| \ll M_\rho^2$ the shadow factor

$$\left| \frac{q^2 - M_\rho^2}{q^2 - M_\rho^2 - V} \right|$$

is approximately one for q_0 small compared to 6 GeV. This was the basis for our assertion in Section 3.8 that coherent propagation of mesons other than the pion can be neglected at low energies.

At high energies the coherent propagation of ρ , A_1 , etc., must be taken into account. Shadowing depends on:

- (1) A cancellation in the second term in the analogue of (3.129). Experience with vector dominance in electroproduction suggests that it becomes an increasingly bad approximation as Q^2 increases. In this case the cancellation gets worse and the shadowing decreases as Q^2 increases.
- (2) The shadow factor

$$\left| \frac{q^2 - M_m^2}{q^2 - M_m^2 - V} \right| \quad \text{being appreciably different from}$$

one. Unless V is an unexpectedly strong function of Q^2 , the shadow factor will become closer to one as Q^2 increases (essentially this is due to a reduction of the coherence length).

For these reasons we expect the shadow effect to be unimportant at large Q^2 . The region where it is important might correspond roughly to the diffraction region discussed in Section 3.7.

E. Event Rates Expected at NAL

In order to indicate the prospects for neutrino physics in the next few years, we finish by giving, in Tables 10 - 11, some event rates expected at NAL which were kindly supplied by C. Baltay (see Fig. 1 for a very rough guide to the experimental programs at other laboratories). The cross sections assumed are given in Table 12. The counter experiments will probably observe up to 5 times the number of events but it is only the inclusive process (σ_T and $d^2\sigma/dq^2 d\nu$) and the processes in Table 11 which can easily be studied with these techniques.

Acknowledgements

I am grateful to many colleagues at CERN and SLAC for enlightening discussions about neutrino physics during the last two years. S. L. Adler, C.H. Albright, S.M. Berman, M.M. Block, J.D. Bjorken, S.D. Drell, A. Pais, D. H. Perkins, J. Prentki, J. Smith and P.A. Zucker made useful comments on various portions of the manuscript. I wish to thank particularly J.S. Bell, A. de Rújula and R.L. Jaffe who read the entire first draft and made numerous suggestions for improvements in the physics and presentation.